Novel polyhydroxyalkanoate bead-based vaccines against *Pseudomonas aeruginosa* infection

A thesis presented in partial fulfilment of the
requirements for the degree of

Master of Science
In
Biological Sciences

at Massey University, Palmerston North,
New Zealand

Zennia Jean Gonzaga
2018

Abstract

Pseudomonas aeruginosa infections are increasingly problematic due to their multiple antibiotic resistances. To date, there is no commercial vaccine against *P. aeruginosa* infection. This study used polyhydroxyalkanoate (PHA) beads as a delivery platform for selected *P. aeruginosa* antigens to produce novel particulate vaccines against *P. aeruginosa*. Genetic engineering was used to modify the PHA synthase (PhaC), the enzyme that catalyses PHA bead formation, to produce functionalised PHA beads displaying the antigens. The highly conserved PopB antigen, recently revealed as an effective stimulator of Th17 immunity was displayed on the bead surface together with and without the previously selected antigens Ag (epitopes derived from outer membrane proteins OprI, OprF and AlgE). The PHA beads were produced in two production strains: (1) the pathogen *P. aeruginosa* itself, with the benefit of co-purifying host cell proteins (HCPs) expanding the antigen repertoire that could boost the immune response, and (2) *E. coli* strain ClearColi^{TM}, a defined mutant incapable of lipopolysaccharide synthesis enabling production of endotoxin free PHA beads. Vaccination of mice with antigen-coated PHA beads (only PopB or with additional Ag) showed increased production of IL-17, a reflection of induction of a Th17 immunity. Furthermore, Th1 and Th2 mediated immunity were detected from the IgG analysis of the immunised mice with the PHA bead vaccines. Significant enhancement of Th1 immune response using the PHA bead platform was observed compared to the antigen-only counterparts. Challenge of immunised mice with pathogenic *P. aeruginosa* showed that PopB-displaying PHA beads from *P. aeruginosa* and Ag-displaying PHA beads from *E. coli* induced partially protective immunity. The promising PHA bead candidate vaccines can be conjugated with other antigens such as the exopolysaccharide Psl for induction of improved immune response towards protective immunity.

Exopolysaccharide Psl is a mannose rich polymer produced by *P. aeruginosa* in both mucoid and nonmucoid phenotypes. Psl has been revealed to play an essential role in *P. aeruginosa* pathogenicity such as biofilm formation. Previous studies had provided evidence that CdrA binds directly to Psl, functioning as a Psl cross-linker and possibly tethering Psl to the cell surface. Psl is commercially not available, hence the aim of this study was to develop a Psl production strain. This study created a *cdrA* knockout mutant that produces free Psl which may be a potential vaccine antigen against *P.*

aeruginosa infections. An isogenic knockout of *cdrA* was obtained by homologous recombination and this mutant overproduced Psl released from the cell surface. In future studies, this strain will be used to produce Psl to serve as antigen in vaccine formulations.

Acknowledgements

"Success is not final, failure is not fatal: it is the courage to continue that counts".
-Winston Churchill-

This milestone of my career would not have been possible without the help of many people. I would like to thank my supervisor, Professor Bernd Rehm for the opportunity to work under his supervision, and for his unending guidance and encouragement. I am grateful to my co-supervisor, Dr. Zoe Jordens for all of her help, her very useful comments and feedback, and her patience in editing my thesis. I appreciate the help of Jason Lee, Yajie Wang and Jinping Du for guiding me with my experiments. I would also like to thank all my colleagues at Rehm's laboratory, Shuxiong, Majela, Jin, Kampachiro, First, Jason Smith, Patri, Shirin and Fata for the great camaraderie and advice.

I would like to thank New Zealand Aid Scholarship for funding my postgraduate study and the International Student Support team who are very accommodating and helpful throughout my entire stay. My research would have not been possible without the funding provided by Massey University and the MacDiarmid Institute for Advanced Materials and Nanotechnology. My thanks also to the Harvard medical group in the United States for conducting the animal trials and providing me with the data of the immunological analysis and bacterial challenge experiments.

I would like to extend my gratitude to all of my professors, friends, classmates and everyone that has been a part of my New Zealand journey. You have reinforced my interest in biological science at the molecular level and made being away from home significantly easier.

Special thanks to my very optimistic and loving big buddy, Rich Marks for all the support and motivating me when I needed it, as well as to the other buddies. To my family, Nanay, Tatay and Joan for the love and care that they have and are giving me every step of the way. Above all, the almighty God.

Table of Contents

List of abbreviations

A full list of abbreviations used:

°C	Degree Celsius
APC	Antigen presenting cell
Ag	OprI, OprF and AlgE *P. aeruginosa* antigens
AGE	Agarose gel electrophoresis
Ag-PhaC	Ag-PHA_{SCL} synthase
Ag-$PhaC1_{Pa}$	Ag-PHA_{MCL} synthase
Amp	Ampicillin
APS	Ammonium persulfate
BL21	*E. coli* production strain
BSA	Bovine serum albumin
Cb	Carbenicillin
CDW	Cellular dry weight
Cm	Chloramphenicol
Δ	Delta (deleted)
DMSO	Dimethyl sulfoxide
DNA	Deoxyribonucleic acid
dNTPs	Deoxyribonucleotide triphosphates
ELISA	Enzyme-linked immunosorbent assay
EtOH	Ethanol
EDTA	Ethylenediaminetetraacetic acid
g	Gravity/gram
Gm	Gentamicin
GTP	Guanosine triphosphate
HCPs	Host cell proteins
HRP	Horseradish peroxidase
IgG	Immunoglobulin G
IPTG	Isopropyl â-D-1-thiogalactopyranoside
kDa	Kilo Daltons
λ	Lambda (wavelength or type of phage)
λ-DNA	Phage Lambda DNA
LacZ	β-galactosidase

LB	Luria-Bertani (broth)
L	Litre
M	Molarity
ml	Millilitre
mM	Millimolar
MOPS	Morpholinopropane sulfonic acid
MS	Mass spectrometry
OD	Optical density
PCR	Polymerase chain reaction
PhaA	β-ketothiolase
PAO1	*P. aeruginosa* production strain
PHAs	Polyhydroxyalkanoic acids
PHA_{SCL}	Short chain length PHAs
PHA_{MCL}	Medium chain length PHAs
PhaB	Acetoacetyl-CoA reductase
PhaC	PHA_{SCL} synthase
PhaC-PopB	PHA_{SCL} synthase-PopB
PhaC-PopBAg	PHA_{SCL} synthase-PopBAg
$PhaC1_{Pa}$	PHA_{MCL} synthase
$PhaC1_{Pa}$-PopB	PHA_{MC} synthase-PopB
PhaE	Type III PHA synthase subunit
PhaP	Phasin
PhaR	Phasin regulatory protein
PHB	Poly(3-hydroxybutyric acid)
PIA	Pseudomonas isolation agar
PopBAg	Single fusion of PopB, OprI, OprF, and AlgE *P. aeruginosa* antigens
REs	Restriction endonucleases
SDS	Sodium dodecyl sulfate
SDS-PAGE	Sodium dodecyl sulfate gel electrophoresis
TBE	Tris-Borate-EDTA buffer
Tc	Tetracycline
TE	Tris-EDTA buffer

TEM	Transmission and Electron Microscopy
TEMED	Tetramethylethylenediamine
Tet	Tetracycline
TLR	Toll-like receptors
Tm	Primer melting temperature
Tris	Trishydroxymethylaminomethane
v/v	Volume per volume
w/v	Weight per volume
X-Gal	5-bromo-4-chloro-3-indolyl-beta-D-galactopyranoside
XL1-Blue	*E. coli* cloning strain

List of Figures

List of Tables

Chapter 1: Introduction

Polyhydroxyalkanoates (PHAs) are biopolyesters produced naturally as spherical intracellular inclusions by many bacteria, serving as their carbon source and energy storage when these are in excess (Grage et al., 2009; Rehm, 2003). In the presence of suitable substrate, PHA synthase (PhaC) is the key enzyme for PHA biosynthesis and PHA bead assembly, and catalyses the polymerisation of (*R*)-3-hydroxyacyl-CoA thioesters monomers into polyester, while releasing coenzyme A (CoA) (Qi & Rehm, 2001; Rehm, 2007). PhaC remains covalently attached on the surface of PHA beads and can be modified by genetic engineering (Grage et al., 2009). For instance, several studies have successfully engineered PhaC and other PHA surface-associated proteins to display specific proteins of interest on the surface of the beads (Blatchford et al., 2012; Parlane et al., 2011). PHA beads can serve as biobeads to display proteins due to properties such as non-toxicity, biocompatibility, biodegradability (Grage et al., 2009). These properties make these beads suitable for several industrial and medical applications.

Pseudomonas aeruginosa is a ubiquitous opportunistic human pathogen that is a major cause of nosocomial infections leading to life-threatening conditions. The systemic infections from *P. aeruginosa* can lead to a mortality rate of 38% to 70% (Douglas et al., 2001). *P. aeruginosa* continues to be a major problem due to its extraordinary resistance to a range of antibiotics (Tenover, 2006). Hence, alternative strategies are required, with efforts been made to develop an effective vaccine against *P. aeruginosa*. Most candidate vaccines developed to-date use a conventional approach that only offers limited protective capacity (Wu et al., 2012). However, given that (i) a PHA bead-antigen display system has been successfully used to mediate protective immunity in animal trials against hepatitis C (Martínez-Donato et al., 2016; Mifune et al., 2009) and tuberculosis (Parlane et al., 2014; Parlane et al., 2009), and (ii) there is no commercial vaccine available against *P. aeruginosa* – in this research we endeavoured to generate a novel vaccine against this important pathogen using the new PHA bead display technology.

This chapter reviews PHAs (Section 1.1), PHA synthase (Section 1.2), PHA bead formation (Section 1.3) and protein immobilization on the surface of the PHA beads (Section 1.4). The disease caused by *P. aeruginosa* (Section 1.5) and the host immune

response against *P. aeruginosa* (Section 1.6) are also briefly reviewed. Finally, the aims and objectives of this study in developing particulate vaccines against *P. aeruginosa* infections are described (Section 1.7).

1.1 Polyhydroxyalkanoate

Polyhydroxyalkanoates (PHAs) are naturally occurring biopolyesters synthesized by a wide range of bacteria and archaea (Rehm, 2007). Production of PHAs happens when there is an imbalance in nutrient conditions, that is, when carbon source is available in excess and other nutrients are limiting (Campisano et al., 2008; Grage et al., 2009). PHAs are synthesized and deposited as spherical water-insoluble inclusions in the cytoplasm comprising an amorphous hydrophobic polyester core surrounded by a phospholipid monolayer and attached or embedded proteins, including PHA synthases, depolymerases and phasins, and other structural proteins (Grage et al., 2009; Rehm, 2003, 2007). These PHA inclusions serve as carbon and energy storage (Rehm, 2003). Poly-3-hydroxybutyric acid (PHB), a form of PHA synthesised from 3-hydroxybutyrate (3-HB), was the first bacterial PHA polymer identified by Lemoigne in 1926 from *Bacillus megaterium* (Lemoigne, 1926). Furthermore, PHB is the most commonly found and isolated form of PHA from bacteria (Campisano et al., 2008; Keshavarz & Roy, 2010; Rehm, 2010). Since their discovery, PHAs have been extensively studied. Bacteria are capable of accumulating more than 80% of their cellular dry weight (CDW) in PHA (Gerngross & Martin, 1995), and generally produce 5 to 10 PHA beads per cell ranging from 100 to 500 nm in diameter depending on the organism (Grage et al., 2009; Koller et al., 2010; Madison & Huisman, 1999).

PHAs exhibit a range of properties which make them particularly useful to a wide range of applications in the industrial and medical fields. These properties include their biodegradability and thermoplastic nature, the latter of which is significantly impacted by the length and composition of their hydroxyl fatty acids. There are over 150 different hydroxyalkanoic acids known to be found in PHAs (Rehm, 2003, 2007, 2010). PHAs are generally classified according to their chemical structure: (1) short chain length PHAs (PHA_{SCL}) comprising of 3 to 5 carbon atoms, and (2) medium chain length PHAs (PHA_{MCL}) containing 6 to 14 carbon atoms (Figure 1) (Rehm, 2003, 2007). PHA_{SCL} have high melting temperatures and high levels of crystallinity,

and hence are relatively hard and brittle. On the other hand, PHA_{MCL} have low melting temperatures and crystallinity, and are more elastic.

Figure 1. Characteristics of the two major classes of biopolyesters, PHA_{SCL} and PHA_{MCL}. (A) Chemical structures, (B) properties and comparison of material properties with polypropylene (PP). T_m is the melting temperature and T_g is the glass transition temperature. (Reproduced from Rehm, 2007).

In addition to the biodegradability and thermoplastic properties of PHAs, their biocompatibility, production from renewable resources, elastomeric, and modifiable physical and thermal properties have made them very useful in industrial and medical fields (Grage et al., 2009; Rehm, 2003, 2006). Unlike the traditional petrochemical-based plastics (such as polypropylene), PHA is produced from renewable carbon resources such as glucose (Liu et al., 1998). PHAs have similar properties to common polymers (e.g. polypropylene and polystyrene) used in various plastics and they can be subjected to heat processing using current plastic manufacturing processes (Sudesh & Iwata, 2008). Moreover, PHAs are desirable in many environments due to their biodegradability. Hence, PHAs are favourable alternatives in the packaging industry (Keshavarz & Roy, 2010). Furthermore, PHAs are composed of chiral hydroxyl acids

that can be used as building blocks to synthesize chemicals such as vitamins and antibiotics (Ruth et al., 2007). The biocompatibility of PHAs makes them suitable for medical uses because PHAs are well tolerated in the mammalian systems and do not induce undesirable immune responses (Hazer & Steinbüchel, 2007; Legat et al., 2010). In addition, PHAs biocompatibility and elastomeric properties are favourable for use in medical applications such as implants in bone scaffolding (Hazer & Steinbüchel, 2007). Recombinant DNA technology has been extensively used to produce various PHAs and their use as biological beads displaying proteins of interest. Currently, several proteins have been successfully immobilised on the surface of PHA beads, but none are commercially available (Blatchford et al., 2012; Grage et al., 2009; Peternel & Komel, 2011). The key to these applications is the genetic engineering of the proteins to be attached or embedded on the surface of PHA beads, such as PHA synthases.

1.2 PHA synthases

PHA synthases are the key enzymes for PHA biosynthesis and PHA bead formation in the presence of suitable substrate. These enzymes catalyse the polymerisation of (*R*)-3-hydroxyacyl-CoA thioester monomers to produce PHAs with the release of CoA (Grage et al., 2009; Rehm, 2003). There are four major classes of PHA synthases based on the primary structures, subunit composition, and substrate specificity (Table 1) (Rehm, 2003, 2007). Class I and II PHA synthases are composed of a single type subunit (PhaC) with molecular weight between 61 kDa to 73 kDa (Qi & Rehm, 2001). The Class I PHA synthases from *Cupriavidus necator* (also known as *Ralstonia eutropha*) preferentially use short-chain length (SCL) CoA thioesters of (*R*)-3-hydroxy fatty acids (Rehm, 2003). Class II PHA synthases are found in *Pseudomonas* species and preferentially utilise medium chain length (MCL) CoA thioesters of (*R*)-3-hydroxy fatty acids (Rehm, 2003; Ren et al., 2000). In contrast to the previous two classes, Class III and IV synthases are composed of two subunits, both have 40 kDa PhaC as the first subunit, with the second subunits being 40 kDa PhaE and 20 kDa PhaR, respectively (Qi & Rehm, 2001).

Table 1. The four classes of PHA synthases. (Reproduced from Rehm, 2007).

Assessment of the amino acid sequence regions of the 88 PHA synthases from various bacteria revealed six conserved blocks with a highly variable N-terminal region (Rehm, 2003, 2007). Analysis of the truncated *C. necator* Class I PHA synthase showed the N-terminal region to be dispensable (Rehm, 2003). In contrast, the C-terminal region is highly conserved, signifying its importance for enzyme activity (Peters & Rehm, 2005; Rehm et al., 2002). Furthermore, eight amino acids were identical in all known 88 PHA synthases suggesting significant function of these residues. Predominantly, the C-terminus of the Class I and II PHA synthases appears to be hydrophobic suggesting that this area functions as a binding domain to mediate contact between the PHA synthase and the hydrophobic polyester core (Rehm et al., 2002). In contrast, no hydrophobic C-terminal region has been recognised in the PhaC subunits of Class III and IV PHA synthases. However, the second subunits, PhaE and PhaR of class III and IV PHA synthase classes, respectively, possess a hydrophobic C-terminus which might facilitate the binding of the synthases to the hydrophobic polyester core (Jahns & Rehm, 2009; Rehm, 2003).

1.3 Formation of PHA beads

PHA biosynthesis is initiated by provision of (*R*)-3-hydroxyacyl-CoA thioesters substrate to a PHA synthase in the cytoplasm (Philip et al., 2007; Rehm, 2007; Rehm et al., 2002). The PHAs are characterised into two main classes, PHA_{SCL} and PHA_{MCL} (Rehm, 2003, 2007), as described in Section 1.1. The PHA_{SCL} and PHA_{MCL} are primarily categorised based on substrate specificity of the PHA synthases (Rehm, 2007). There has been extensive research on the biosynthesis of Class I and II PHA synthases produced by *C. necator* and *P. aeruginosa*, respectively (Grage et al., 2009; Keshavarz & Roy, 2010; Rasiah & Rehm, 2009; Rehm, 2007). PHA bead formation is a self-assembly process that starts at cytoplasmic regions in bacteria (Peters & Rehm, 2005; Rehm, 2003, 2007).

1.3.1 Biosynthesis of PHA beads

The three key enzymes important in PHA biosynthesis are: PHA synthase (PhaC), β-ketothiolase (PhaA) and acetoacetyl-CoA reductase (PhaB), encoded by *phaC*, *phaA* and *phaB* genes, respectively (Qi & Rehm, 2001; Rehm, 2007; Taguchi & Doi, 2004). Class I and II PHA synthases are encoded by *phaC* while Class III and IV synthases involve expression from both *phaC* and *phaE/phaR* genes (Table 1) (Rehm, 2007). In bacterial genomes, the genes essential in the PHA biosynthesis are clustered together. For example, in *C. necator*, the *phaA, B* and *C* genes are situated in *phaCAB* operon (Grage et al., 2009; Rehm, 2007; Rehm et al., 2002), and the *phaC* gene is constitutively expressed but at low levels (Rehm, 2007). Synthesis of the substrate (*R*)-3-hydroxyacyl-CoA thioesters are catalysed by enzymes PhaA and PhaB, and polymerised by the PhaC dimer (PhaC and PhaE/PhaR for Class III and IV PHA synthases) which is the active synthase forming the PHAs (Peoples & Sinskey, 1989).

The biosynthesis of PHA_{SCL} and PHA_{MCL} are highly dependent on the class of PHA synthase and the carbon source. PHB is an example of a PHA_{SCL} usually found in *C. necator* that uses Class I PHA synthase (Campisano et al., 2008) while *P. aeruginosa* has been shown to require a Class II PHA synthase and produce PHA_{MCL} (Figure 2) (Rehm, 2003; Ren et al., 2000).

Figure 2. Metabolic routes for PHA biosynthesis composed of short-chain length and medium-chain length 3-hydroxy fatty acids. Polyester synthase is the same as PHA synthase (PhaC). β-ketothiolase (PhaA) and acetoacetyl-CoA reductase (PhaB). (Reproduced from Rehm, 2007).

PHA_{SCL} biosynthesis. PhaA catalyses the condensation of two acetyl-CoA molecules from the glycolysis pathway, generating acetoacetyl-CoA and subsequently reduced to (*R*)-3-hydroxybutyrl-CoA by the NADPH-dependent acetoacetyl-CoA reductase PhaB (Peoples & Sinskey, 1989). The PHA synthase then uses (*R*)-3-hydroxybutyrl-CoA to produce PHB.

PHA_{MCL} biosynthesis. Fatty acid *de novo* synthesis and/or fatty acid β-oxidation pathways are involved in the synthesis of PHA_{MCL}, producing various intermediates. Fatty acid *de novo* synthesis pathway produce (*R*)-3-hydroxydecanoyl-ACP while fatty acid β-oxidation pathway can lead to 3-ketoacyl-CoA and Enoyl-CoA that act as precursor molecules and eventually leading to (*R*)-3-hydroxyacyl-CoA thioesters (the substrates of PhaC). Finally, the substrates are polymerised by PHA synthase to produce PHA_{MCL} (Grage et al., 2009; Rehm, 2007).

1.3.2 Self-assembly mechanisms of PHA beads

In vitro synthesis of PHAs and self-assembly of spherical PHA beads was first shown by Gerngross and Martin (Gerngross & Martin, 1995). Utilizing purified PHA synthases and substrates, *in vitro* study demonstrated the ability of PHA synthases to execute self-assembly of PHAs into PHA beads (Gerngross & Martin, 1995). Though the exact mechanism of PHA bead assembly remains unknown, to date two models have been proposed: the micelle model, and the budding model (Figure 3).

Figure 3. Models of PHA bead formation. (A) Micelle model of bead formation (demonstrating the *in vitro* formation in the absence of phospholipids). (B) Budding model of bead formation (displaying bead formation at the cell membrane). (Reproduced from Rehm, 2007).

Micelle model. This model is based on the amphipathic nature of PHA synthase and the formation of the micelle-like structure through the assembly of hydrophobic PHA chains once polymerisation occurs (Stubbe & Tian, 2003). The PHA synthase remains covalently attached to the growing PHA chain (Rehm et al., 2002). This model is supported by the *in vitro* formation of PHA beads that lack cytoplasmic membrane components (Rehm, 2007).

Budding model. The budding model considers the occurrence of the lipid membrane that has been detected at the surface of isolated PHA beads (Mayer & Hoppert, 1997). This model suggests that the soluble PHA synthases are associated with the inner cell

membrane (Thomson et al., 2010), while the polymerisation reaction and PHA bead assembly occurs between the phospholipid bilayer (Rehm, 2007). Ultimately, the formed PHA bead buds off from the membrane into the cytoplasm (Grage et al., 2009; Rehm, 2007). Recent evidence supports the budding model of PHA bead formation. For instance, the time course studies have revealed that PHA beads are in close proximity to the cell membrane during the early stages of bead formation and are not randomly distributed in the cytosol (Tian et al., 2005).

1.4 Immobilization of proteins on PHA beads

Purifying proteins from a complex mixture is tedious and challenging. Several important factors need to be taken into consideration for protein purification including not irreversibly altering the protein structure and/or denaturing the biological activity of the protein (Grage et al., 2009). Protein immobilization, which is used to fuse the protein of interest to a solid support, can be carried out to purify proteins efficiently. Previous studies have shown increased protein stability and activity upon immobilization (Steinmann et al., 2010). Affinity-based purification is a popular way of purifying the protein of interest which relies on a specific interaction between the protein and immobilization matrix (Arnau et al., 2006). Fusion of a purification tag such as polyHis to the target protein is necessary for the interaction. However, this may be disadvantageous as the purification tag may change the intrinsic properties of the target protein (Waugh, 2005). Enzymatic cleaving of the affinity tag from the protein of interest after purification may solve this problem (Esposito & Chatterjee, 2006). However, in some cases an affinity tag could reduce the solubility of the target protein, causing the formation of insoluble aggregates (Waugh, 2005). Hence, optimisation of the affinity-based purification processes for protein of interest may be very expensive and labour extensive (Grage et al., 2009).

Protein immobilization using polymers is an alternative. Generally, the production of functionalized polymers requires three basic steps: (1) production and purification of the polymer, (2) production and purification of the protein (or other active ingredient), and (3) assembly of the two components, usually via chemical crosslinking or emulsification (Hanefeld et al., 2009). However, each step (and process within it) can be costly, prone to variability, and requires the removal of toxic compounds. Hence, another technique wherein the target protein and bio-bead (immobilization matrix) are

produced in the same cell, and the protein is immobilized intracellularly and displayed on the surface of the bead would be beneficial. In particular, the beads displaying the protein of interest can be easily purified by centrifugation of the disrupted cells (Steinmann et al., 2010).

The surface associated proteins of the PHA beads such as PHA synthase can be genetically modified for target protein production, and cost effective production makes it a suitable technique for protein immobilization and purification (Grage et al., 2009; Parlane et al., 2011). Recently, a method was established exploiting the natural process of PHA bead formation to produce functionalized bio-beads (Draper & Rehm, 2012). Genetic engineering to produce fusions of the PHA-associated proteins and the target proteins led to the development of PHA beads displaying the target protein on their surface. Synthesising the functionalised particles *in vivo* has the main advantage of being a one-step process as the PHA beads and the functionalised proteins are produced and cross-linked in the same cell. For example, Banki et al. (2005) developed a protein purification technique involving PHA bead production intracellularly with intein-mediated self-splicing. The target protein was attached to the C-terminus of PhaP (serves as the affinity tag), and displayed on the surface of the PHA beads produced from recombinant *E. coli* cells. As the target protein was fused to the surface of the beads by the affinity tag PhaP, protein immobilisation was achieved in a single step and no further cross-linking was needed (Banki et al., 2005). Subsequently, PHA bead purification was achieved by cell lysis and centrifugation, and the target protein was separated by intein cleavage. The same purification technique was applied to several other proteins including maltose binding protein, chloramphenicol acetyltranferase and β-galactosidase (LacZ) (Banki et al., 2005). PHA beads are a cheaper alternative than the conventional methods, and the one step process is beneficial for large scale industrialised protein production, immobilization and purification (Grage et al., 2009).

1.4.1 Applications of PHA beads as bio-beads

PHA beads can serve as bio-beads and have several applications. Examples include diagnostics, imaging, protein purification, vaccine development and many others (Figure 4). This is due to their size, lack of toxicity, biocompatibility, biodegradability, and modifiable physical and thermal properties (Grage et al., 2009; Steinmann et al.,

2010). The PHA beads can be a tool in industrial applications. For example, PHA beads displaying the target proteins organophosphohydrolase (OpdA) and amylase can be utilised for bioremediation and food productions, respectively (Blatchford et al., 2012; Rasiah & Rehm, 2009).

Figure 4. Applications of functionalized PHA beads. (Reproduced from Draper & Rehm, 2012).

One interesting feature of PHA beads is their small size, ranging from 100 to 500 nm in diameter (Grage et al., 2009; Steinmann et al., 2010). This allows them to have a wide range of applications in molecular biology, biotechnology and medicine, including drug and gene delivery, separation of biological molecules and cells, fluorescent labelling, and tissue engineering (Salata, 2004). Furthermore, PHA beads are well tolerated by mammalian systems and are unlikely to generate unwanted immune responses (Hazer & Steinbüchel, 2007; Legat et al., 2010). Hence, PHA beads are applicable in vaccine development and PHA bead-displaying protein antigens have shown immunogenicity *in vivo*, and induced Th1 and Th2 immune responses (Parlane et al., 2011; Parlane et al., 2012; Parlane et al., 2009).

1.5 *Pseudomonas aeruginosa* as a pathogen

P. aeruginosa is a Gram-negative opportunistic pathogen which can live in wide range of environments, from its natural habitat in soil and water, to plants and animals. The ability of *P. aeruginosa* to tolerate extreme environments including hostile conditions and its inherent resistance to many antibiotics has contributed to it being a major cause of hospital-acquired infections worldwide (Lavoie et al., 2011) *P. aeruginosa* caused infection that was independently related to a greater risk of hospital death in the extended prevalence of infection in intensive care report (EPIC II) (Vincent et al., 2009). *P. aeruginosa* rarely causes infection in healthy hosts with a strong immune system, but can cause acute and chronic infections in susceptible people with a weakened immune system, such as patients with severe burns, HIV and cystic fibrosis (CF) (Priebe & Goldberg, 2014). The infections can result in life-threatening conditions that can be difficult to treat. Furthermore, *P. aeruginosa* is the major cause of chronic infection in CF patients and is the main cause of mortality of these individuals (Doering, 2010). The SOAP (subjective, objective, assessment, plan) study is a clinical documentation conducted in European countries which showed that among the bacterial infections in intensive care units, only *Pseudomonas* infection was associated with increased mortality (Vincent et al., 2006).

P. aeruginosa is the most common cause of respiratory infection in CF patients and greatly impacts their overall survival (Gibson et al., 2003; Koch, 2002). CF is a hereditary recessive disorder caused by mutations in the cystic fibrosis transmembrane conductance regulator (*CFTR*) gene. Furthermore, this disorder can cause defective ion transport of water, chloride and sodium from the basolateral to the secretary epithelia leading to the production of thick mucus which is favourable for *P. aeruginosa* colonization. Generally, the bacteria causing *P. aeruginosa* infections are of non-mucoid phenotype and subsequently convert into mucoid phenotype due to the overproduction of alginate, this occurs under stress conditions, such as host immune responses and/or presence of antibiotics (Ma et al., 2012; Ramsey & Wozniak, 2005). As a result, this mucoid phenotype forms biofilms that contain extracellular polysaccharides (alginate, Psl, and Pel), proteins and extracellular DNA. The biofilm protects *P. aeruginosa* from the host's immune response (phagocytosis) and lessens antibiotics' susceptibility via prevention of effective diffusion (Flemming & Wingender, 2010). Colonization of the lungs of CF patients by *P. aeruginosa* occurs

in early life and the change from non-mucoid to a mucoid phenotype can take from months to years (Mishra et al., 2012). Failure of the immune system to clear the infections leads to chronic infections that can be lifelong and result in weakened pulmonary function (Ramsey & Wozniak, 2005).

1.5.1 Antibiotic resistance of *P. aeruginosa*

Treatment of infections caused by *P. aeruginosa* has been an escalating problem due to multiple antibiotic resistances of the bacteria. *P. aeruginosa* can evade a range of antibiotics due to its natural resistance and the ability to use various mechanisms, therefore increasing the mortality rate of infections that it causes (Tenover, 2006). Recently, the World Health Organisation published *P. aeruginosa* as a critical priority and among the twelve pathogens that pose the greatest threat to human health (World Health Organisation, 2017). This was due to the resistance of *P. aeruginosa* to carbapenem, the last resort antibiotic for highly resistant bacteria. These findings signify the increasing and alarming threat of *P. aeruginosa*. In addition, despite the advances in the field of microbiology and antimicrobial treatment, *P. aeruginosa* infection continues to be a major struggle.

1.5.2 Vaccine development

The relentless problem of *P. aeruginosa* infection and its challenging antibiotic resistance suggest an urgent need for a vaccine. Vaccine development against *P. aeruginosa* infections has been ongoing for decades, with many vaccines being developed and undergoing trials and testing. However, at present there is no efficient and commercially available vaccine against *P. aeruginosa* despite the alarming occurrence of diseases due to unsuccessful antibiotic treatments.

1.5.2.1 Traditional vaccines

Traditional vaccines have been based on the live-attenuated organisms, killed or inactivated pathogens, or inactivated bacterial toxins (Kallerup & Foged, 2015). Whole cell based live attenuated vaccines can elicit strong, long-lived cellular and antibody responses due to their intrinsic immune stimulatory capability. However, there is a serious disadvantage of using the approach of live systems as it has been linked to adverse effects that were mild in some cases but can be severe and lead to death in other circumstances (Huang et al., 2004). Safety is the main issue of using

this approach, due to the possibility of the microbe reverting back to a virulent disease-causing form. There were circumstances wherein the attenuated strains instigated disease in individuals with impaired immune systems such as with HIV (O'Hagan & Rappuoli, 2004). These issues limit the use of this traditional approach and make it undesirable to use live attenuated pathogens in the development of new vaccines.

Several vaccines prepared using the traditional approach have successfully contributed to the prevention and control of many infectious diseases. However, despite their success, traditional approaches to vaccine design have not produced effective vaccines to control and prevent all infectious diseases such as chronic pulmonary infection caused by *P. aeruginosa*. Evidently, there is no commercially available vaccine against *P. aeruginosa* despite the high levels of mortality and morbidity worldwide. Dependence of most *P. aeruginosa* candidate vaccines on conventional defence mechanisms such as antibody-mediated toxin inhibition and antibody-mediated opsonophagocytic killing appear to be inadequate due to the limited protective capacity of these vaccines (Wu et al., 2012). Therefore, there is a need for alternative vaccine design and development approaches for the prevention of *P. aeruginosa*.

1.5.2.2 Modern vaccines

New strategies for vaccine development are emerging and leaning towards subunit vaccine technology. In contrast to the live-attenuated or killed vaccines, subunit vaccines comprise specific antigens and/or epitopes recognised to stimulate the immune system (Arnon, 2006). Furthermore, using only defined antigens subunit vaccines lower the chance of adverse reactions, thereby increasing safety. The antigens can either be protein that can directly interact with T cells, or polysaccharide, which are T cell independent and bind directly to B cell receptors (Baxter, 2007). However, identification of the protective antigens takes a lot of time and effort. Fortunately, advances in technology resulted in development of the reverse vaccinology approach. Reverse vaccinology uses bioinformatics to identify the genes coding for possible antigenic determinants as vaccine candidates, thereby speeding up the development of vaccines (Nossal, 2011). In addition, Recombinant DNA technologies allow the use of purified recombinant proteins (Milacic et al., 2012) and development of cost-effective multicomponent subunit vaccines (Skeiky & Sadoff,

2006). Also, development of conjugate vaccines such as protein-polysaccharide conjugate vaccines, in which conjugation results in the formation of covalent bonds between protein and polysaccharide, has an enormous impact in vaccine development (Pollard et al., 2009). Effects of conjugation can alter the immune response towards a T cell dependent response for both protein and polysaccharide. This is beneficial particularly for the polysaccharide component as this T cell dependent response leads to the generation of memory cells (Baxter, 2007).

Designing multicomponent subunit vaccines can increase immunogenicity and consequently protection. The type of immune response has been shown to be influenced by the activation of specific toll-like receptors (TLRs) or multiple TLRs, leading to the regulation of Th1/Th2 immune response, and results in either cell mediated or humoral response (Dadley-Moore, 2006; Querec et al., 2006). Novel vaccines that contain multiple antigens/epitopes that enable the activation of multiple TLRs could result in longer lasting, stronger and specific immune response. However, the different components may result in an antagonistic effect such as the delayed viral clearance reported from combinations of epitopes of influenza virus (Crowe et al., 2006). Hence, modern vaccines depend on the identification of appropriate antigens and epitopes with great potential to stimulate the appropriate immune response. In order to acquire the greatest immune response, importance is given to what and how to present the antigens to the immune system (Hilleman, 2000). Therefore, the use of specific antigenic epitopes, in conjunction with novel adjuvants and/or delivery systems, could lead to safer vaccines with enhanced efficacy – which are described below.

Adjuvants. Adjuvants are used to enhance the immune response but have no antigenic properties themselves. Most modern vaccines are based on subunit or recombinant proteins and need the addition of adjuvant to function better (Singh & O'Hagan, 1999). Small particulate delivery systems such as PHA beads and virus-like particles (VLPs) can also be categorised as adjuvants due to their ability to modify the immune response by simulating properties of pathogens such as charge, size and hydrophobicity (Milacic et al., 2012). The only adjuvants that the US Food & Drug Administration have approved for the use in humans are aluminium compounds such as aluminium hydroxide (alum), aluminium phosphate, and MF59 (Singh & O'Hagan, 1999).

However, alum has several limitations including not being effective for all antigens, it mostly activates Th2 antibody response which is not effective for defence against intracellular pathogens, and development of local adverse reactions (Lindblad, 2004). Other experimental adjuvants are available but the main issue is toxicity (Aguilar & Rodriguez, 2007). Furthermore, adjuvants are greatly reliant on formulation and individual application.

Delivery systems. There is an interest in vaccine delivery systems due to their ability to enhance the uptake of antigens by antigen presenting cells (APCs), thereby improving the immune response. Enhancement of cellular immune response was observed when small particles displaying antigens were used as a vaccine (Parlane et al., 2011). Examples of particulate delivery systems for antigens are polylactide co-glycolide (PLG) microparticles, virus-like particles (VLPs), liposomes, immune stimulating complexes (ISCOMs), chitosan, and biological polyesters such as PHAs. The capability of particulate delivery systems to mimic numerous properties of pathogens is one of their advantages (Bachmann & Jennings, 2010; Parlane et al., 2011). In addition, particulate delivery systems offer the benefits of targeting APCs, controlled antigen release, antigen display and co-incorporation of immunostimulants. Particulate antigen delivery systems also act as adjuvants (O'Hagan et al., 1991; Singh et al., 2006).

1.5.2.3 PHA beads as vaccines and their production hosts

There has been increasing interest in the development of PHA beads based vaccines due to the biodegradability, biocompatibility, and small particulate size of PHA beads making them attractive as vaccine delivery agents. There are two major advantages of using PHA beads compared to other particulate systems: (1) the production process is one-step, and (2) the vaccine candidates are covalently attached and displayed on the surface of PHA beads in a uniform orientation (Grage et al., 2009; Parlane et al., 2009); thereby eliminating crosslinking or encapsulation steps.

Several production hosts for PHA beads isolation have been explored. *E. coli* strains have been typically used due to the ease of production, high yield of PHA beads and high antigen production on the surface of the beads. PHA beads displaying mycobacterial antigens, antigen-85A (Ag85A) and early secretory antigenic target

(ESAT-6) (Parlane et al., 2012; Parlane et al., 2009), and PHA beads displaying hepatitis C core antigen (HCc) (Parlane et al., 2011), were produced in *E. coli* and shown to be safe and effective vaccines in mice trials. However, the Gram negative *E. coli* strains used are known to contain LPS endotoxins which could contaminate the beads (Cotten et al., 1994; Parlane et al., 2012); limiting their use in humans. LPS are comprised of a hydrophilic polysaccharide moiety (core oligosaccharide, O-antigen) that are covalently connected to a hydrophobic lipid moiety (Lipid A) (Magalhães et al., 2007). Lipid A is accountable for the majority of endotoxins' biological activity. The endotoxins produce a variety of pathophysiological effects such as fever, systemic inflammation, shock and in worst case, death (Magalhães et al., 2007). Hence, other organisms have been explored as possible production hosts that do not contain LPS such as the Gram-positive *Lactococcus lactis* (Parlane et al., 2011; Parlane et al., 2012). However, PHA production in Gram-positive bacteria is still low compared to Gram negative bacteria. Furthermore, *L. lactis* is considerably more difficult to lyse efficiently due to its inherently resistant cell wall, size and shape. A revolutionary development was made with ClearColi^{TM}, an *E. coli* strain that contains genetically modified LPS resulting in endotoxin-free products (Mamat et al., 2013). Recent studies successfully used the *E. coli* strain ClearColi^{TM} to produce PHA beads displaying the pneumococcal surface adhesin A (PsaA) antigen on the surface of the bead and showed a specific Th2 immune response upon mice vaccination (González-Miro et al., 2017). On the other hand, a *P. aeruginosa* production strain was utilized by Lee et al. (2017) to display the *Pseudomonas* antigens on the PHA beads with the advantage of other proteins from the target bacteria (host derived proteins); thereby expanding the antigenic repertoire of the developed vaccine.

1.5.3 Potential antigens for protection against *P. aeruginosa*

Several research institutes have designed vaccines targeting cellular and virulence related factors of *P. aeruginosa* (Table 2). A brief overview of potential vaccine targets against *P. aeruginosa* is described in this section.

Table 2. Promising antigens for *P. aeruginosa* vaccine. (Reproduced from Sharma et al., 2011).

Antigens	Advantages	Limitations	Stage of development
Lipopolysaccharides (LPS)	Generation of high levels of opsonic antibodies	High heterogeneity, Low immunogenicity, Pyrogenic and toxic	I-III phase
Mucoid Exopolysaccharide (MEP)	Low heterogeneity	For CF use only	I phase
Outer membrane proteins	Highly conserved and immunogenic Anti-OprF inhibits quorum-sensing through IFNγ binding to *P. aeruginosa*	No significant drawback	I/II phase
Flagella	Moderate heterogeneity, Adjuvant effect through TLR5	Loss of flagella in CF variants	I-III phase
Pilin	High immunogenicity	High heterogeneity, Hidden receptor binding site	Preclinical
PcrV, Exotoxin A and proteases	Neutralizes cytotoxic effects and pathology	Less effective in bacterial clearance	Preclinical
Killed	Presentation of multiple antigens to immune system	Toxicity	I phase
Live attenuated (*P. aeruginosa* ΔaroA)	Efficient activation of mucosal immunity	Residual virulence	Preclinical
Attenuated *Salmonella enterica* delivered O-antigen or OprF-OprI	Efficient activation of mucosal immunity	Residual virulence	I/II phase
Ad vector delivered OprI	High immunogenicity and adjuvant properties	Pre-existing anti-Ad immunity	Preclinical

Lipopolysaccharides (LPS). Early vaccine studies were focused on cell wall components such as LPS. *P. aeruginosa* strains containing LPS antigen have 20 serotypes, with each serotype possessing subtype strains with variations summing up to more than 30 subtypes (Knirel, 1990). Pseudogen, a heptavalent O antigen vaccine composed of seven serotypes of LPS, was effective in preventing *P. aeruginosa* infections in adult patients with burn wounds and cancer (Young et al., 1973). An octavalent O-polysachharide conjugate vaccine, Aerugen was developed and had initial positive results producing high levels of O-polysaccharide specific antibodies but phase III study failed to confirm the positive preliminary results. Although positive results were observed in animal models, the protection was limited to the strains used to isolate the vaccine antigen. This suggests serotype dependency of LPS-based vaccines, and that development of at least 30 valent vaccine is needed to be effective against almost all relevant strains. Due to the toxicity and inherent pyrogenic properties of LPS-based vaccines, these vaccines were not clinically acceptable (Döring et al., 2007).

Flagella. Flagellin is the main protein component of *P. aeruginosa* flagella which is divided into two serotypes A and B, and are highly conserved protein filaments (Rosok et al., 1990). Hence, a successful vaccine needs to be bivalent for broad protection. Animal trials have demonstrated that bivalent flagella based vaccines in CF patients was safe, immunogenic and lowered the infection risk with *P. aeruginosa* (Döring et al., 2007). A more recent study showed that antibodies directed against flagella as a whole was superior in protective immunity than flagellin alone (Campodonico et al., 2010). A vaccine developed against the flagella may be promising due to its high immunogenicity and cross-reactivity. However, a limitation of the flagella vaccine is the reduced or loss in production of flagella detected in mucoid phenotype of *P. aeruginosa* isolates from CF patients, therefore making a flagellin-based vaccine ineffective against established mucoid infections (Tart et al., 2006). Loss of the flagella is believed to be an adaptive response mechanism to evade detection by host defences (Wolfgang et al., 2004).

Pili. *P. aeruginosa* express pili on their surface which they use for mediating interactions with other bacteria, host and the environment. Furthermore, pili assist in biofilm formation and motility. Purified pili protein exhibited efficacy upon mice

vaccination (Ohama et al., 2006). However, obstacles for development of pilin-based vaccines are serological heterogeneity and hidden conserved binding sites.

Outer membrane proteins (OMPs). The OMPs earned considerable interest as vaccine candidates and revealed great potential in vaccine development. Several studies have focused on the use of the major OMP F (OprF) and outer membrane lipoprotein I (OprI) antigens due to their high conservation and serotype-independent characteristics (Baumann et al., 2004; Westritschnig et al., 2014). Furthermore, previous immunization studies with OprF and OprI had shown broad protection against all *P. aeruginosa* serotypes (Doring & Pier, 2008; Martin et al., 1993). Several studies in different animal models exhibited promising results particularly high long-lived antibody titers (Holder, 2004). Recent vaccine developments focused on the use of immunogenic epitopes of OprF fused with or without OprI, and explored combination with different delivery vectors such as adenoviral vectors and pulsed dendritic cells (Matthews, 2010; Peluso et al., 2010). OprI, shown to be a natural adjuvant has been observed to induce long lived $CD4^+$ Th1 immune response resulting in activation and maturation of APCs (Revets et al., 2005). Moreover, vaccination studies using OprI suggested regulation of conversion from cluster of differentiation 4^+ ($CD4^+$) Th2 into $CD4^+$ Th1 mediated immune response (Revets et al., 2005), which is suggested to be more protective (Moser et al., 2002). Specific antigenic epitopes of OprI and OprF have been combined and revealed to have synergistic effects against *P. aeruginosa* (Von Specht et al., 2000).

Another potential target for vaccine development, OMP alginate pore (AlgE) is a protein found on the cell surface of *P. aeruginosa*. AlgE is present on mucoid variants of *P. aeruginosa*, is vital for alginate transport, and is associated with the infection status of CF patients (Rehm et al., 1994). The alginate itself is a poor inducer of antibodies but AlgE may provide an alternative target and was reported to be highly immunogenic.

Type III secretion system (T3SS). *P. aeruginosa* uses a T3SS apparatus as a virulence factor to directly inject cytotoxic effector proteins into the host cells (Hauser, 2009). Components of the T3SS have been targeted in vaccine development. PopB is a promising vaccine antigen candidate which is an important component of

the T3SS (Engel & Balachandran, 2009; Roy-Burman et al., 2001; Vance et al., 2005). The T3SS apparatus has a translocon composed of highly conserved proteins PopB and PopD that are stabilised by PcrH chaperone (Discola et al., 2014). Importantly, the membrane protein PopB is highly conserved and a major translocator protein in *P. aeruginosa*. PopB was identified by Wu et al. (2012) using reverse vaccinology and from the screening of antigens stimulating Th-17 using the splenocytes of the mice vaccinated with live-attenuated *P. aeruginosa* vaccine. Immunised mice with PopB stimulated IL-17 production and elicited Th17 immune responses that resulted in lung and spleen clearance from *P. aeruginosa* in the challenge experiment. Furthermore, IL-17 was shown to have a key role in LPS serotype-independent protection against *P. aeruginosa* and was linked to rapid recruitment of neutrophils (Priebe et al., 2008). The CF patients infected with *P. aeruginosa* produced a humoral immune response to PopB antigen (Rao et al., 2009). Hence, the use of the PopB antigen appears to be a promising vaccine candidate harnessing a novel mechanism of immunity against *P. aeruginosa.* Moreover, the Th17 immune response is anticipated to work synergistically with opsonophagocytic antibodies (Wu et al., 2012).

Another component of T3SS is PcrV, situated on the bacterial surface and vital for the translocation of the effector proteins. PcrV- based vaccines have shown protection in murine lung infection models and burn mouse models (Sharma et al., 2011).

Exopolysaccharides (EPS). Overproduction of mucoid exopolysaccharide (MEP; also known as alginate) is associated with the mucoid phenotype of *P. aeruginosa*, particularly observed with chronic infections in the respiratory tract of CF patients. Alginate is composed of linear polymer of D-mannuronic acid and its C5' epimer L-guluronic acid (Franklin et al., 2011). D-mannuronic acid hydroxyl residue can be altered by O-acetylation. Alginate is present in mucoid variants but not in non-mucoid strains of *P. aeruginosa,* but is an important constituent in biofilm architecture (Ramsey & Wozniak, 2005). Alginate is highly conserved, making it a target for vaccine development. However, alginate has been found to be a poor stimulator of protective antibodies. Conjugation of alginate with carrier proteins can improve the immunogenicity (Doring & Pier, 2008).

An alternative target is the EPS Psl which is a major virulence factor of *P. aeruginosa*. Psl consists of repeating pentasaccharide units of D-mannose, D-glucose and L-rhamnose. Psl staining revealed that Psl surrounds the surface of the bacteria in a helical fashion (Franklin et al., 2011). Psl can be present in both non-mucoid and mucoid strains conferring protection from host defences e.g. phagocytic immune cells and reactive oxidative species (Byrd et al., 2009). Psl deficient *P. aeruginosa* have been shown to be more efficiently phagocytized and killed by neutrophils and macrophages in comparison to wild-type and Psl overexpression variants (Mishra et al., 2012). In biofilm formation, Psl plays a vital role in initial reversible surface attachment of the non-mucoid variants of *P. aeruginosa* (Ma et al., 2009). Previous studies have shown that CdrA directly binds to Psl polysaccharide promoting biofilm formation (Borlee et al., 2010). In addition, the structural integrity of the biofilm is highly influenced by CdrA which is dependent in the presence of Psl. Hence, Psl and CdrA are essential components of the EPS matrix to enhance biofilm stability making them good targets for vaccine development particularly for CF patients.

1.6 Host immune response to *P. aeruginosa*

Understanding the host immune response and the defence mechanisms of bacteria are pre-requisite towards development of effective vaccines against *P. aeruginosa*. The immune systems of mammals are divided into two parts: (1) the innate immune system which includes nonspecific recognition of foreign organisms by pathogen associated molecular patterns but in which immunological memory is not created, and (2) adaptive immunity which is antigen specific utilizing antigen presentation by APCs and which generates immunological memory. Utilising the innate immune response is a vital approach to control *P. aeruginosa* infection as it initiates and guides the correct adaptive immune response. The adaptive immune response is activated when the innate immune response insufficiently controls the infection. There are two types of adaptive responses: (1) the cell-mediated immune response which is controlled by activated T cells, and (2) the humoral immune response which is controlled by activated B cells and antibodies.

P. aeruginosa has the capability to alter the expression of the recognition factors, such as flagella leading to varying response of the host's immune system to different bacterial strains or at different times. Mucosal, humoral, opsonizing immunity and T-

cell responses are excellent ways to fight *P. aeruginosa* infections (Sharma et al., 2011). Selected mechanisms have been reviewed by Priebe and Goldberg (Figure 5) such as the humoral immune response comprising opsonophagocytosis through the involvement of antibodies to LPS, alginate, flagella and OprI; as well as interfering the binding of OprF to IFN-γ acting as anti-virulence antibody; and the T3SS disruption shown to be essential for PcrV (Priebe & Goldberg, 2014). In addition, T cell defence mechanisms include IL-17 secretion by PopB and live attenuated vaccines; IFN-γ secretion by OprF; and GM-CSF via live attenuated vaccines. T cell mechanisms and opsonophagocytosis can act hand in hand to boost protection against *P. aeruginosa* (Priebe & Goldberg, 2014).

Figure 5. Promising vaccines' protective mechanisms against *P. aeruginosa.* **(**Reproduced from Priebe & Goldberg, 2014).

Cytokines are a diverse group of proteins that play an important role in regulation of immunological mechanisms. There are changes in cytokine levels upon association with disease (Courtney et al., 2004). Previous studies described the mouse $CD4^+$T cell clones can be either T-helper 1 (Th1) or T-helper 2 (Th2) immune responders. Th1 response is associated with low antibody response and IFN-γ production, while Th2

response is characterized by the production of IL-4 and IL-5 and high antibody response (Abbas et al., 1996). CF patients were investigated and a correlation of Th2 immune response with chronic lung infection was found, thereby suggesting the superior protective action of Th1 immune response compared to Th2 (Jensen et al., 2010). Moreover, this result is aligned with Moser and colleagues (2000) findings that the cell mediated response of $CD4^+$ Th1 type is extra protective (Moser et al., 2000). On the other hand, Th17 immunity is a distinct lineage that has been characterized by IL-17 production (Harrington et al., 2005; Steinman, 2007). IL-17 has been shown to have an essential role in the host defence mechanism of the lung against bacterial infections (Kolls et al., 2003; Ye et al., 2001).

1.7 Aim and objectives of this study

The main aim of this study was to develop a particulate vaccine to fight against *P. aeruginosa* infections by manipulating the bead production process and to produce antigen displaying PHA beads. This research was divided into three parts:

- Plasmid construction, PHA_{MCL} bead production by *P. aeruginosa* cells, mice vaccination, and immunological analysis.
- Plasmid construction, PHA_{SCL} bead production and soluble protein isolation from *E. coli* cells, mice vaccination, and immunological analysis.
- Generation and characterisation of *cdrA* knockout mutant for Psl production as a potential vaccine candidate for future studies.

Section I: Development and production of antigen-displaying PHA beads in *P. aeruginosa* and evaluation of protection in mice.

Recent studies by Lee et al. (2017) used *P. aeruginosa* PAO1 Δ*phaC1ZC2* Δ*alg8* Δ*pelF* (PAO1 ΔCΔ8ΔF) strain to manipulate the bead production process (Figure 6). This PHA negative mutant PAO1 Δ*phaC1ZC2* was used to enable the production of PHA_{MCL} beads facilitated exclusively by an introduced PHA synthase (the wild-type non-engineered $PhaC1_{Pa}$) with the attached fusion protein antigens (engineered to integrate the selected vaccine candidate antigens). Specific genes essential for the production of *alg8* and the glucose-rich Pel polysaccharide (*pelF*) were deleted to promote PHA_{MCL} assembly through evasion of competing biosynthesis pathways (Lee et al., 2017). The overview of the generation of PAO1 ΔCΔ8ΔF is described below.

The PAO1 Δ*phaC1ZC2* Δ*alg8* Δ*pelF* Δ*pslA* (PAO1 ΔCΔ8ΔFΔP) mutant, defective in Psl polysaccharide was used to produce the wild-type $PhaC1_{Pa}$ beads. PAO1 ΔCΔ8ΔF was used to produce the remaining beads.

A

B

C

Figure 6. A schematic overview of the generation of *P. aeruginosa* knockout mutant PAO1 ΔCΔ8ΔF. Site-directed homologous recombination was used to delete major genes to facilitate the production of PHA_{MCL} beads. (A) The *alg8* gene was deleted. (B) The *pelf* gene was deleted. (C) The resultant triple mutant strain, unable to produce PHA, alginate and pel polysaccharide. (Reproduced from Lee et al., 2017).

The OprI, OprF and AlgE from *P. aeruginosa* were used as the candidate antigens and immobilized on the surface of PHA bead. Selected antigenic epitopes of the $OprI_{21-83}$ and $OprF_{329-342}$ were derived from earlier studies showing that they elicited a protective immune response in animal trials (Baumann et al., 2004; Cui et al., 2015; Gilleland & Gilleland, 1995; Hughes et al., 1992; Rawling et al., 1995; Von Specht et al., 2000). Two epitopes of AlgE, HLRRPGEEV (L5) and NLTTRIATGKQ (L6) corresponding to amino acids 233-241 and 287-303, respectively, were selected by B-cell epitope prediction method EPCES (Liang et al., 2009). Three repeats of the OprF epitope and one copy of OprI and AlgE (L5 and L6) epitopes were combined into a

single fusion designated as OprI/F-AlgE (Ag). Bioengineering of *P. aeruginosa* expressing the candidate antigens $PhaC1_{Pa}$ (wild-type control), Ag-$PhaC1_{Pa}$ (antigens fused to the N-terminus of $PhaC1_{Pa}$) and $PhaC1_{Pa}$-Ag (antigens fused to the C-terminus of $PhaC1_{Pa}$) had produced PHA_{MCL} beads-displaying functionalised proteins (Lee et al., 2017). The bead formation indicated that the functionality of PHA synthase to polymerize PHA bead formation was retained. The Ag-$PhaC1_{Pa}$ beads were significantly larger compared to the $PhaC1_{Pa}$-Ag beads, suggesting that fusion site is important for PHA bead accumulation. Moreover, there was higher production of Ag-$PhaC1_{Pa}$ fusion protein and this elicited a dominant Th1 immune response in a mice vaccination study (Lee et al., 2017), justifying the use of Ag-$PhaC1_{Pa}$ combination in this study.

This research is particularly interested in displaying PopB on the surface of PHA_{MCL} beads. PopB is a highly conserved virulence factor of *P. aeruginosa* and has been shown to be an effective stimulator of Th17 immunity (Wu et al., 2012). Furthermore, mice immunized with purified PopB were protected from lethal pneumonia, and stimulated antibody independent and IL-17 dependent responses (Wu et al., 2012). Hence, PopB may provide a novel mechanism of immunity, thereby making PopB a promising vaccine candidate against *P. aeruginosa*. Truncated $PopB_{171\text{-}390}$ was fused with $PhaC1_{Pa}$ and Ag-$PhaC1_{Pa}$.

The main aim of this part of the study was to produce functionalized PHA_{MCL} beads displaying PopB alone, and a combination of PopB and Ag from *P. aeruginosa* PAO1 ΔCΔ8ΔF production strain. Section I tested two hypotheses: (1) the constructed plasmids would produce PHA_{MCL} beads displaying the selected antigens; (2) the addition of PopB antigen on the surface of the beads would induce a greater Th17 immune response, characterised by increased IL-17 production; and (3) the PHA_{MCL} beads displaying antigen(s) would protect the vaccinated mice from bacterial challenge. The objectives of section I are described below:

- To construct five plasmids containing single genes and combinations of *PopB* and *Ag* genes, and use this to transform XL1-Blue *E. coli* for expression and *P. aeruginosa* for PHA_{MCL} bead production.
- To isolate antigen-displaying PHA_{MCL} beads from the *P. aeruginosa*.

- To characterise and assess the PHA_{MCL} beads by fluorescence microscopy, transmission electron microscopy (TEM) and gas chromatography-mass spectrometry (GC-MS).
- To characterise and evaluate the fusion proteins displayed on the surface of the beads by sodium dodecyl sulphate polyacrylamide gel electrophoresis (SDS-PAGE) and mass spectrometry (MS).
- To assess the candidate particulate vaccines and identify the one with the highest immune response by mice vaccination, cytokine and antibody analysis.
- To determine the protective efficacy of the candidate particulate vaccines by bacterial challenge.

Section II: Development of antigen-displaying PHA_{SCL} beads in *E. coli* strain ClearColi^{TM} and evaluation of protection in mice.

An alternative production strain was explored due to the low yields of PHA_{MCL} beads displaying PopBAg fusion from *P. aeruginosa* and very low levels of PopBAg fusion protein production on the bead surface. Recombinant *E. coli* strains as a host has advantages of faster growth, overexpression of proteins, higher PHA bead yield and obtaining PHA beads displaying proteins of high level of purity. However, *E. coli* strains contain LPS endotoxins that contaminate *E.coli* products and limit applications for humans as they require additional costly and delicate processes (Cotten et al., 1994; Parlane et al., 2012). A breakthrough study had developed *E. coli* strain ClearColi^{TM} with the advantage of the absence of endotoxin production due to the modification of LPS; thereby providing a safer alternative for development of human vaccines.

This part of the study created the corresponding plasmids to that were developed in section I. The primary focus of this study was to produce functionalized PHA_{SCL} beads displaying Ag alone, PopB alone, and a combination of PopB and Ag from the *E. coli* ClearColi^{TM} production strain. In addition, isolation of soluble versions of Ag and PopBAg would serve as positive controls in mice vaccination experiments. Section II tested three hypotheses: (1) the constructed plasmids would produce PHA_{SCL} beads displaying the selected antigens in *E. coli* strain ClearColi^{TM}; (2) the proteins displayed would be purer than those from *P. aeruginosa* (without the host derived

proteins); (3) the addition of PopB antigen on the surface of the beads would induce a greater TH17 mediated response, characterised by increased IL-17 production; and (4) the PHA_{SCL} beads displaying antigen(s) would protect the vaccinated mice from bacterial challenge. The objectives of section II are described below:

- To construct three plasmids containing single and combinations of *PopB* and *Ag* genes for PHA_{SCL} bead production and one plasmid for soluble protein isolation. The plasmids would be used to transform XL1-Blue *E. coli* for expression, and *E. coli* ClearColi^{TM} for PHA_{SCL} bead and soluble protein isolation.
- To isolate and purify the PHA_{SCL} beads displaying antigens and soluble proteins from the *E. coli* ClearColi^{TM} production strain.
- To characterise and assess the PHA_{SCL} beads by fluorescence microscopy, TEM and GC-MS.
- To characterise and evaluate the fusion proteins displayed on the surface of the beads and the soluble proteins by SDS-PAGE and MS.
- To assess the candidate particulate vaccines and identify the one with the highest immune response by mice vaccination, cytokine and antibody analysis, and bacterial challenge.
- To determine the protective efficacy of the candidate particulate vaccines by bacterial challenge.

Section III: Generation of CdrA knockout mutant for free Psl production.

The *P. aeruginosa* PAO1 ΔCΔ8ΔF mutant (Figure 6) was used to generate PAO1 Δ*phaC1ZC2* Δ*alg8* Δ*pelF* Δ*cdrA* mutant for the production of free Psl polysaccharide. For future studies, isolation of the Psl from the PAO1 ΔCΔ8ΔFΔ*cdrA* mutant would allow a controlled attachment of purified Psl to PHA beads such as the PHA beads developed from Section I and II of this study by conjugation, as a novel potential vaccine target against *P. aeruginosa*.

The CdrA is cross-linked to Psl polysaccharide after being transported out of the cell by CdrB; therefore CdrA and Psl are two key components of the EPS matrix that enhance biofilm stability. Psl provides protection against *P. aeruginosa* by phagocytosis from host immune cells (Mishra et al., 2012). Furthermore, Psl has the

ability to attach to both living and non-living cells with high affinity (Colvin et al., 2012); making it a good target for vaccine development to inhibit *P. aeruginosa* attachment to host cells and finally reducing the risk of early biofilm formation in chronic infections. However, to date, Psl is not commercially available and there is a need to produce a purified Psl to cater its various applications.

The aim of this section was to generate a *cdrA* knockout mutant and assess Psl production. The hypothesis of section III was that *cdrA* knockout mutant would overproduce free Psl polysaccharide that can be used for future studies. The objectives of this section are described below:

- To generate a *cdrA* knockout from *P. aeruginosa* PAO1 ΔCΔ8ΔF strain by transconjugation that would be used for the production of free Psl polysaccharide.
- To assess the Psl production of the PAO1 ΔCΔ8ΔFΔ*cdrA* (*cdrA* knockout mutant) in comparison to the Psl producing PAO1 ΔCΔ8ΔF as positive control and the non-Psl producing PAO1 ΔCΔ8ΔFΔ*pslA* as negative control using solid surface attachment (SSA) assay and enzyme-linked immunosorbent assay (ELISA).

Chapter 2: Materials and Methods

Unless stated, all reagents were purchased from Sigma-Aldrich, Ajax Finechem, or Merck; centrifugation procedures were carried out at room temperature (22 ± 4°C); and all water (or H_2O) was Milli-Q treated. When required, samples' absorbance was measured using a Biochrom Libra S5 spectrophotometer (Biochrom Ltd, England). Ultracentrifugation was carried out using a Sorvall WX Ultra 80 (Thermo Scientific).

2.1 Bacterial strains, plasmids and primers

2.1.1 Bacterial strains

The bacterial strains used in this study are listed in Table 3 below.

Table 3. Bacterial strains used in this study.

Bacterial strains	Relevant characteristics	References
E. coli		
XL1-Blue	*recA1 endA1 gyrA96 thi-1 hsdR17 supE44 relA1 lac* [F' *proAB lacI*^{q} *lacZ* Δ*M15* Tn*10* (Tet^{r})]	Stratagene
ClearColi^{TM} BL21(DE3)	F– *ompT hsdSB (rB- mB-) gal dcm lon* λ(DE3 [*lacI lac*UV5-T7 gene 1 *ind1 sam7 nin5*]) *msbA148* Δ*gut*QΔ*kds*D Δ*lpxL*Δ*lpxM*Δ*pagP*Δ*lpxP*Δ*eptA*	Lucigen
BL21 (DE3)	F– *ompT hsdSB (rB- mB-) gal dcm* (DE3)	Invitrogen
BL21 Star^{TM} (DE3)	F– *ompT hsdSB (rB- mB-) gal dcm rne131* (DE3)	Invitrogen
BL21 (DE3) (pLysS)	F– *ompT hsdSB (rB- mB-) gal dcm* (DE3) pLysS (Cm^{r})	Invitrogen
BL21 Star^{TM} (DE3) pLysS	F– *ompT hsdSB (rB- mB-) gal dcm rne131* (DE3) pLysS (Cm^{r})	Invitrogen

Shuffle T7 Express	F´ *lac, pro, lacI*^{Q} / *Δ(ara-leu)7697 araD139 fhuA2 lacZ::T7 gene1 Δ(phoA)PvuII phoR ahpC* galE (or U) galK λatt*::pNEB3-r1-*cDsbC* (Spec^{R}, *lacI*^{q}) *ΔtrxB rpsL150*(Str^{R}) *Δgor Δ(malF)3*	NEB
E. coli S17-1	thi-1 proA hsdR17 (Rk-Mk+) recA1; tra gene of plasmid RP4 integrated in chromosome	Simon et al. 1983
P. aeruginosa		
P. aeruginosa PAO1	Prototroph, non-mucoid	ATCC 15692
PAO1 Δ*phaC1ZC2* Δ*alg8* Δ*pelF*	PAO1 Δ*phaC1ZC2* Δ*alg8* derivative with markerless, isogenic *pelF* deletion, triple mutant	Lee et al. 2017
PAO1 Δ*phaC1ZC2* Δ*alg8* Δ*pelF* Δ*pslA*	PAO1 Δ*phaC1ZC2* Δ*alg8* Δ*pelF* derivative with markerless, isogenic *pslA* deletion, quadruple mutant	Jason Lee
PAO1 Δ*phaC1ZC2* Δ*alg8* Δ*pelF* Δ*cdrA*	PAO1 Δ*phaC1ZC2* Δ*alg8* Δ*pelF* derivative, isogenic cdrA deletion, quadruple mutant	This study

Tet^{r}, tetracycline resistance

Cm^{r} chloramphenicol resistance

2.1.2 Plasmids

The plasmids used in this study are listed in Tables 4, 5, 6 and 7 below.

Table 4. Plasmids used in the development of antigen-displaying PHA_{MCL} beads produced in *P. aeruginosa*.

Plasmid name	Relevant characteristics	References
pUC57	Cloning vector, ColE1 origin, Amp^r	Fermentas
pUC57_Ag(N)	pUC57 derivative containing *P. aeruginosa* codon optimized OprI/F-AlgE fusion antigen fragment (L5-L6-OprF(x3)-OprI-Linker (GSGGG) flanked by *Xba*I/*Nde*I sites	Lee et al. 2017
pUC57_XPopBS	pUC57 derivative containing *P. aeruginosa* codon optimized PopB antigen fragment flanked by *Xba*I/*Sal*I sites	This study
pBBR1JO-5	Gm^r, P_{lac}, pBBR1MCS-5 with MCS from pBluescript SK□-	Pham et al. 2004
pBBR1JO-5_PhaC1$_{Pa}$	pBBR1JO-5 derivative containing Shine-Dalgarno-*phaC1* fragment from pBHR71 in *Xba*I/*BamH*I sites of pBBR1JO-5	Lee et al. 2017
pHERD20T-2_PhaC1$_{Pa}$	Shine-Dalgarno-*phaC1$_{Pa}$* fragment from pBBR1JO-5_PhaC1 inserted into *Xba*I/*Hind*III site of pHERD20T-2	Jason Lee
pHERD20T-2_Ag-PhaC1$_{Pa}$	Codon optimized Ag fragment from pUC57_Ag(N) inserted into *Xba*I/*Nde*I sites of pHERD20T-2_PhaC1 upstream of *phaC1$_{Pa}$*	Lee et al. 2017
pHERD20T-2_PopBAg-PhaC1$_{Pa}$	Codon optimized PopB fragment from pUC57 XPopBS inserted into *Sal*I/*Xba*I sites of pHERD20T-2_Ag-PhaC1$_{Pa}$ upstream of *Ag-phaC1$_{Pa}$*	This study

pHERD20T-2_PopB-PhaC1$_{Pa}$	Codon optimized PopB fragment from pHERD20T-2_PopBAg-PhaC1$_{Pa}$ replacing Ag into *Xba*I/*Nde*I sites of pHERD20T-2_Ag-PhaC1$_{Pa}$ upstream of *phaC1$_{Pa}$*	This study
pHERD20T-2_Ag-PhaC1$_{Pa}$-Ag	Codon optimized Ag fragment from pUC57 Ag(N) inserted into *XbaI/Hind*III sites of pHERD20T-2_Ag-PhaC1$_{Pa}$ downstream of *phaC1$_{Pa}$*	Jason Lee
pUC57_Ag(C)	pUC57 derivative containing *P. aeruginosa* codon optimized OprI/F-AlgE fusion antigen fragment (OprI-OprF(x3)-L6-L5) flanked by *Sma*I/*EcoR*I sites	Lee et al. 2017
pBBR1JO-5_PhaC1$_{Pa}$-Ag	Condon optimized OprI/F-AlgE fusion antigen fragment from pUC57 Ag(C) inserted into *Sma*I/*EcoR*I site of pBBR1JO-5_PhaC1$_{Pa}$-gfp replacing GFP	Lee et al. 2017
pHERD20T-2_PhaC1$_{Pa}$-Ag	*phaC1$_{Pa}$*-LSGL-Ag fragment from pBBR1JO-5_PhaC1$_{Pa}$-Ag inserted into *Xba*I/*Hind*III sites of pHERD20T-2	Lee et al. 2017
pHERD20T-2_PhaC1$_{Pa}$-PopB	Codon optimized PopB fragment from pUC57 XPopBS replacing Ag into *Xho*I/*EcoR*I sites of pHERD20T-2_PhaC1$_{Pa}$-Ag	This study
pHERD20T-2_Ag-PhaC1$_{Pa}$-PopB	Codon optimized PopB fragment from pHERD20T-2 PopBAgPhaC1 replacing Ag into *Xho*I/*EcoR*I sites of pHERD20T-2_AgPhaC1$_{Pa}$-Ag	This study
pHERD20T-2_PhaC1$_{Pa}$-PopBAg	Codon optimized PopB fragment from pUC57 XPopBS replacing Ag into *Xho*I/*EcoR*I sites of pHERD20T-2_PhaC1$_{Pa}$-Ag upstream of *phaC1Ag*	This study

Amp^r, ampicillin resistance; Gm^r, gentamicin resistance

Table 5. Plasmids used in the development of antigen-displaying PHA$_{SCL}$ beads produced in *E. coli* strain ClearColi^{TM}.

Plasmid name	Relevant characteristics	References
pUC57_NPopBN	pUC57 derivative containing *E. coli* codon optimized PopB antigen fragment flanked by *Nco*I/*Nde*I sites	This study
pET-14b	Amp^r; T7 promoter	Novagen
pMCS69	Cm^r; T7 promoter; pBBR1MCS derivative containing codon optimised genes *phaA* and *phaB* from *C. necator*	Amara & Rehm, 2003
pET-14b_PhaC	pET-14b derivative containing *phaC* gene fragment	Peters and Rehm 2005
pET-14b_ObodyB7-PhaC (pPoly-N-ObodyB7)	pET-14b_PhaC derivative containing ObodyB7 inserted into *Nde*I/*Spe*I sites	Du and Rehm, unpublished
pET-14b_Ag-PhaC (pPoly-N-Ag)	Codon optimized Ag fragment from pET-16b_His$_{10}$-Ag replacing ObodyB7 into *Nde*I/*Spe*I sites of pET14b_ObodyB7-PhaC	This study
pET-14b_PhaC-RV1626 (pPoly-C-RV1626)	pET-14b_PhaC derivative containing RV1626	Rubio et al. 2016
pET-14b_PhaC-PopB (pPoly-C-PopB)	Codon optimized PopB fragment from pET-16b_His$_{10}$-PopBAg replacing RV1626 into *Xho*I/*BamH*I sites of pET-14b_PhaC-RV1626	This study

pET-14b_PhaC-PopBAg (pPoly-C-PopBAg)	Codon optimized PopBAg fragment from pET-16b_His_{10}-PopBAg replacing RV1626 into *Xho*I/*BamH*I sites of pET-14b_PhaC-RV1626	This study

Amp^r, ampicillin resistance

Cm^r chloramphenicol resistance

Table 6. Plasmids used in the development of soluble proteins produced from *E. coli* strain ClearColi^{TM}.

Plasmid name	Relevant characteristics	References
pET-16b	Amp^r, T7 promoter, His_{10}-tag	Novagen
pET-16b_His_{10}-Ag	pET-16b derivative containing His_{10}-tagged *E. coli* codon optimized OprI/F-AlgE fusion antigen fragment (OprI-OprF(x3)-L6-L5) in *Nde*I/*BamH*I sites of pET-16b	Lee et al. 2017
pET-16b_His_{10}-PopBAg	pET-16b_His_{10}-Ag derivative containing His_{10}-tagged *E. coli* codon optimized PopB fragment from pUC57_NPopN inserted into *Nco*I/*Nde*I sites of pET-16b_His_{10}-Ag upstream of *Ag*	This study

Amp^r, ampicillin resistance

Table 7. Plasmids used in the development of *cdrA* knockout mutant.

Plasmid name	Relevant characteristics	References
pEX18gm	Gm^r, allelic exchange vector containing *sacB* gene for counter-selection	Borlee et al. 2010
pEX4625	pEX18gm derivative containing *cdrA* deletion construct	Borlee et al. 2010

Gm^r, gentamicin resistance

2.1.3 Primers

The primers used in this study are listed in Tables 8, 9, 10 and 11 below. All the primers were synthesised by Sigma-Aldrich, USA or GenScript, USA.

Table 8. Primers used in the generation antigen-displaying PHA$_{MCL}$ beads produced in *P. aeruginosa.*

Primer name	Restriction site	5'-3' Sequence	References
XbaI popB_fwd	*Xba*I	ATCCTCTAGAAGGAGAT ATACTTATGTTTGGTTG GATC	This study
NdeI popB_rev	*Nde*I	ACTCATATGGCCACCGC CACTACCCGCTGCCGGT CGGCTGGACAGGTTG	This study
Primer 5' (XhoI)	*Xho*I	AAAAA CTCGAGTTTGG TTGGATCAGTGCAATAG CTTCGATC	This study
Primer 3' (EcoRI)	*EcoR*I	AAAAAAGAATTCTCAG ATCGCTGCCGGTCGGCT GGACAGGTTG	This study
XhoI-2	*Xho*I	ACAAACTCGAGTTTGGT TGGATCAGTGCAATAGC TTCG	This study
EcoRI-2	*EcoR*I	AAAAAAGAATTCTCACT TGCGGCTCGCCTTCTCC	This study

Table 9. Primers used in the generation of antigen-displaying PHA$_{SCL}$ beads produced in *E. coli* strain ClearColi^{TM}.

Primer name	Restriction site	5'-3' Sequence	References
NdeI_fwdAg	*Nde*I	AAACATATGTCAAGCC ACAGCAAAGAAACTGA AGCC	This study
SpeI_revAg	*Spe*I	AAAAAAACTAGTTACTT CTTCTCCAGGGCGACGC AGG	This study
Xho1_fwdPopB Ag	*Xho*I	AAAAACTCGAGTTCGGT TGGATTAGCGCGATTGC GAGC	This study
BamHI_revPopB Ag	*BamH*I	AAAGGATCCTCATACTT CTTCTCCAGGGCGAC	This study
BamHI_revPopB	*BamH*I	AAAGGATCCTCAAATC GCCGCCGGACG	This study

Table 10. Primers used for generating *cdrA* knockout mutant.

Primer name	Restriction site	5'-3' Sequence	References
cdrAout40_ fwd	N/A	GCTTCTCAGATTTTCGT CATTTAACTGACGAAAT GCAGTG	This study
cdrAoutout32_ rev	N/A	GCGTCCATTGCGAAGGT TTCATCATTCACCTC	This study

Table 11. Sequencing primers used in this study.

Primer name	Restriction site	5'-3' Sequence	References
pHERD20T_fwd	N/A	GCAACTCTCTACTGTTTCTCCATACCCG	Jason Lee
5' phaC1_rev	N/A	ATGCCGATCACCGGATTCAGGTTC	Jason Lee
HisAg_fwd	N/A	AAGGAGATATACCATGGGCCATC	Jason Lee
HisAg_rev	N/A	TCATACTTCTTCTCCAGGGCGACG	Jason Lee
P10	N/A	AATAGATCTGTGCTGGCGGTGGCGATTGATAAACGCGG	Jason Lee
P87	N/A	CAAGGCGATTAAGTTGGGTAACGCC	Jason Lee
P79	N/A	TTGCACTGGCAGCAATGGC	Jason Lee
T7_promoter	N/A	TAATACGACTCACTATAGGG	Allan Wilson Centre
BamHI_revPopBAg	*BamH*I	AAAGGATCCTCATACTTCTTCTCCAGGGCGAC	This study
XhoI_fwdPopBAg	*Xho*I	AAAAACTCGAGTTCGGTTGGATTAGCGCGATTGCGAGC	This study
cdrAout40_fwd	N/A	GCTTCTCAGATTTTCGTCATTTAACTGACGAAATGCAGTG	This study
cdrAoutout32_rev	N/A	GCGTCCATTGCGAAGGTTTCATCATTCACCTC	This study

5’ pET-14b	N/A	GTAGTAGGTTGAGGCC GTTGA	Anika Jahns
N-PhaC_rev	N/A	CGATCTTGACGCCTGC CAGC	Anika Jahns
C-PhaC_fwd	N/A	AGCCACTGGACTAACG ATGC	Anika Jahns
T7_terminator	N/A	GCTAGTTATTGCTCAG CGG	Anika Jahns

2.2 Media

2.2.1 Liquid media

The following liquid media were used in this study. All media were autoclaved at 121 °C for 20 minutes. When required, antibiotics (Section 2.3) and other supplements were sterilised either by autoclaving or filtration (0.22μm filter) before the addition to sterile autoclaved medium, cooled to approximately 50 °C.

2.2.1.1 Luria-Bertani (LB) medium

Luria-Bertani (LB) medium (Invitrogen Corporation, USA) was prepared according to the manufacturer’s instructions, 20 g of dry media was dissolved in 1 litre of H_2O.

2.2.1.2 Luria-Bertani (LB) miller medium

Luria-Bertani (LB) miller medium was prepared similar to the LB medium (Section 2.2.1.1) with the addition of 1% sodium chloride (NaCl) for the growth of osmosensitive *E. coli* strain ClearColi^{TM} (Lucigen, Middleton, WI) (Lee et al., 2017).

2.2.1.3 Mineral salt medium (MSM)

Mineral salt medium (MSM) was prepared as described previously with some modifications suitable for the PHA_{MCL} bead production in *P. aeruginosa* (Peters & Rehm, 2006; Schlegel et al., 1961). NH_4Cl concentration was reduced for nitrogen starvation. The following recipe is for 1 L media.

Chemicals	Amount
Na_2HPO_4	3.57 g
KH_2PO_4	1.5 g
NH_4Cl	0.5 g
H_2O	Volume to 1 Litre

The pH was adjusted to 7.5 with NaOH 10M and autoclaved. After media had cooled down, the following supplements were added:

Supplements	Stock solution	Amount (ml)
$MgSO_4 \cdot 7H_2O$	0.811 M	1
$CaCl_2 \cdot 2H_2O$	0.136 M	1
Fe(III)NH_4-Citrate	0.005 M	1
Gluconate	25% (w/v)	40
Supplement solution SL6	1000x	1

The following outlines the composition of the supplement solution SL6, as described by Schlegel et al. (1961). It is important to note that the chemicals are added in order and allowed to dissolve before adding the next chemical. The stock solution was filtered sterilized using a 0.22 μm filter.

Chemicals	Amount for 1000x stock solution (g)
$ZnSO_4 \cdot 7H_2O$	10
$MnCl_2 \cdot 4H_2O$	3
H_3BO_3	30
$CoCl_2 \cdot 6H_2O$	20
$CuCl_2 \cdot 2H_2O$	1
$NiCl_2 \cdot 6H_2O$	2
$Na_2MO_4 \cdot 2H_2O$	3
H_2O	Volume to 1 Litre

2.2.1.4 Nutrient Broth

Nutrient Broth (Oxoid, England) was prepared according to the manufacturer's instructions; 13 g of the dry media was dissolved in 1 litre of H_2O.

2.2.1.5 *Pseudomonas* isolation (PI) medium

The *Pseudomonas* isolation (PI) medium was prepared as previously described (Remminghorst & Rehm, 2006):

Chemicals	Amount
Gelatin Peptone	20 g
K_2SO_4	10 g
$MgCl_2 \cdot 6H_2O$	1.4 g
Triclosan	25 mg
Glycerol	20 ml
H_2O	Volume to 1 Litre

The pH was adjusted to 7 using NaOH.

2.2.2 Solid media

Unless stated, all the solid media counterpart of the listed liquid media above were prepared by adding agar (Neogen, USA) to 1.5% (w/v) prior to autoclaving. All media were autoclaved at 121 °C for 20 minutes and poured into sterile Petri dishes after cooling to approximately 50 °C. When required, antibiotics (Section 2.3) were added.

2.2.2.1 *Pseudomonas* isolation (PI) agar

The *Pseudomonas* isolation (PI) agar was prepared according to the manufacturer's instructions (Becton, Dickinson and Company, USA), 45 g of dry media was dissolved in 1 litre of H_2O and supplemented with glycerol to 2% (v/v) and agar (Neogen, USA) to 1.5% (w/v). The components were mixed and dissolved with the help of heating in a microwave oven for 3-5 minutes before autoclaving.

2.3 Antibiotic stock solutions and concentrations

Antibiotics solutions were prepared as previously described (Rasiah & Rehm, 2009) and listed in Table 12. The stock solutions were sterilised by filtration through a 0.22 μm filter and stored at -20 °C for further use. When required, autoclaved media were cooled to approximately 50 °C before the addition of antibiotics.

Table 12. Antibiotic stocks and final concentrations.

Antibiotics	Stock solution (mg/mL)	Final concentration (µg/ml)
For *E. coli*		
Ampicillin (Na-salt)	100 in H_2O	100
Chloramphenicol	50 in absolute EtOH	50
Gentamicin (sulphate)	10 in H_2O	10
For *P. aeruginosa*		
Carbenicillin	300 in H_2O	300
Gentamicin (sulphate)	300 in H_2O	300

2.4 Cultivation conditions

E. coli and *P. aeruginosa* were cultivated as previously described by Blatchford et al. (2012) and Lee et al. (2017), respectively. Bacterial strains were grown in Erlenmeyer flasks or falcon tubes containing the desired medium (Section 2.2) and were added with appropriate antibiotics (Section 2.3), a carbon source and supplements. Unless stated, all bacterial strains were cultivated at 37^{o}C with shaking at 200 rpm for 19-48 hours (19 hours for soluble protein isolation and 48 hours for bead production). To maximise aeration, the ratio of the container volume to culture volume was approximately ≥5:1.

2.4.1 PHA formation conditions

2.4.1.1 PHA_{MCL} bead production in *P. aeruginosa*

The PHA_{MCL} bead production conditions in *P. aeruginosa* were as previously described by Lee et al. (2017). The *P. aeruginosa* PAO1 Δ*C*Δ*8*Δ*F* production strain (Section 2.1.1) was transformed by the recombinant expression vectors by electroporation (Section 2.6.2). *P. aeruginosa* PAO1 Δ*C*Δ*8*Δ*F* strains containing the respective recombinant plasmids were grown on MSM (Section 2.2.1.3) under nitrogen limiting conditions and 1% (w/v) final concentration of sodium gluconate as a carbon source to promote PHA bead formation. Antibiotics (Section 2.3) were added at the following concentrations: 300 µg/mL carbenicillin for strains harbouring pHERD20T-2 derivatives; and 300 µg/mL gentamicin for strains harbouring pBBR1MCS-5 derivatives. Three stages of cultures were performed due to the slow

growth of *P. aeruginosa* (Figure 7). Overnight cultures were carried out from the frozen stock and subsequently the inoculation of the middle culture the next day. Finally, the main cultures (0.4-1L) were inoculated from the middle culture with a starting OD_{600} of 0.1 and cultivation was performed at 37 ºC on a TR/Novotron shaker (INFORS HT, Switzerland). Induction of the main cultures was performed by the addition of arabinose at final concentration of 0.5% (w/v) when OD_{600} reached 0.4-0.5 (approximately 4-5 hours). PAO1 Δ*C*Δ*8*Δ*F* strains harbouring pBBR1MCS-5 derivatives were constitutively expressed in *P. aeruginosa* and did not require induction. The cultures were further grown at 37 ºC for 48 hours.

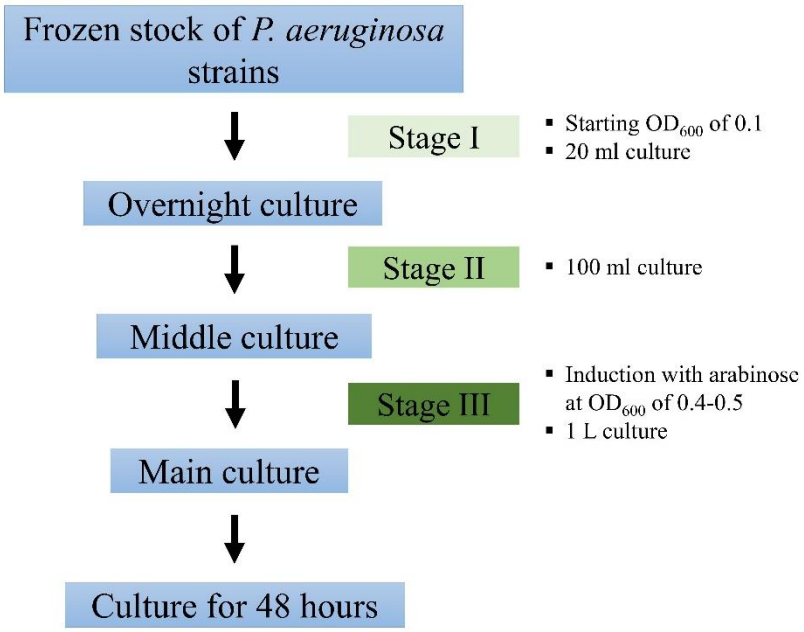

Figure 7. Three stages of cell culture of *P. aeruginosa* strains from frozen stock for PHA_{MCL} bead production.

2.4.1.2 PHA_{SCL} bead production in *E. coli* strain ClearColi™

The PHA_{SCL} bead production conditions in *E. coli* strain were performed as previously described by Parlane et al. (2011). The *E. coli* strain ClearColi™ (Lucigen, Section 2.1.1) harbouring plasmid pMCS69 was transformed with recombinant pET expression vectors. Unlike the *P. aeruginosa* strains, *E. coli* strains had 2 stages of culture (Figure 8). Overnight cultures of the *E. coli* ClearColi™ production strains were inoculated from the frozen stock (Stage I). The main cultures were inoculated with the overnight culture at starting OD_{600} of 0.1 (Stage II) and cultivated at 37 °C in LB miller medium (Section 2.2.1.2) containing 100 µg/ml ampicillin, 50 µg/ml

chloramphenicol and 1% (v/v) glucose. The cultures were added with IPTG at a final concentration of 1 mM when OD_{600} had reached 0.4 – 0.5 (approximately 3-4 hours) to induce gene expression. The cultures were subsequently grown at 25 °C on a TR/Novotron shaker (INFORS HT, Switzerland) for 48 hours.

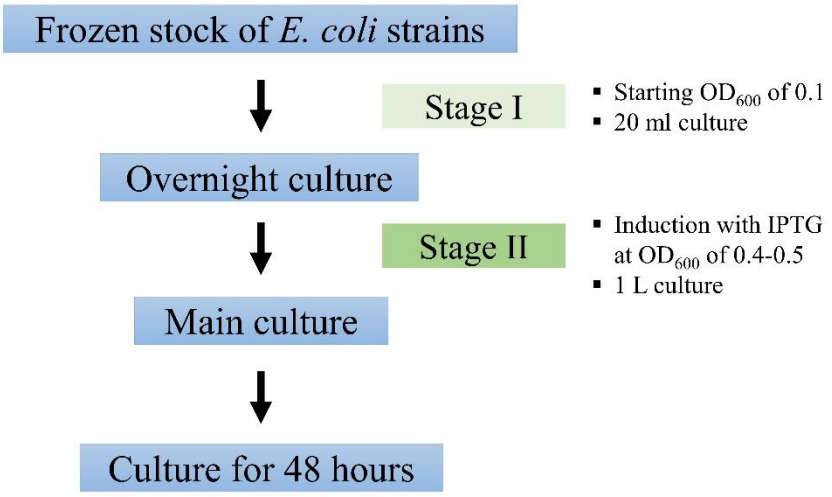

Figure 8. Two stages of cell culture of *E. coli* strains from frozen stock for PHA_{SCL} bead production.

2.4.2 Protein production conditions

The soluble protein production conditions in *E. coli* strains were performed as described previously (Lee et al., 2017). The *E. coli* strains namely, BL21 (DE3), ClearColi™ BL21 (DE3), BL21 Star™ (DE3), BL21 (DE3) pLysS, BL21 Star™ (DE3) pLysS and Shuffle T7 Express (Section 2.1.1) were transformed with the recombinant plasmids based on pET-16b expression vectors. Similar to the cultivation of *E. coli* for PHA bead production, there were two stages of cultivation for the soluble protein isolation from *E. coli* (Figure 8). The main cultures were inoculated with the overnight culture to give a starting OD_{600} starting of 0.1. The cultivation was performed at 37 °C in appropriate media (LB miller for ClearColi™ BL21 (DE3), Section 2.2.1.2; and LB liquid media for the rest of the strains, Section 2.2.1.1), 100 µg/ml ampicillin and 1% (v/v) glucose. Induction of the main culture was performed by the addition of IPTG at a final concentration of 1 mM when OD_{600} had reached 0.3 and cultures were subsequently grown at 25 °C on a TR/Novotron shaker (INFORS HT, Switzerland) for 19 hours.

2.5 Long-term storage and revival of bacterial strains

2.5.1 Storage of bacterial strains

The *E. coli* and *P. aeruginosa* strains were grown overnight for 19-22 hours in LB liquid medium (Section 2.2.1.1) with the addition of appropriate antibiotics at 37 °C with aeration on a thermoline orbital shaker TLM510 (N.S.W, Australia, Section 2.4). To maintain the viability of the strains, 1 ml of overnight culture was mixed with 70 µl of sterile dimethylsulfoxide (DMSO) to give a final concentration of 6.5 % (v/v) in a 2 ml cryovial tube and subsequently stored at -80 °C for future use.

2.5.2 Revival of bacterial strains

The *E. coli* and *P. aeruginosa* strains were revived by removing a small chip of frozen stock using sterile inoculating tip, which was used to inoculate the LB liquid medium (Section 2.2.1.1) containing the appropriate antibiotics. Subsequently, the inoculated medium was incubated overnight for 19-22 hours at 37 °C with aeration on a thermoline orbital shaker TLM510 (N.S.W, Australia; Section 2.4).

2.6 Competent cell preparation and plasmid DNA uptake

2.6.1 Preparation and transformation of competent *E. coli*

2.6.1.1 Preparation of competent *E. coli* cells

The competent *E. coli* cells were prepared as previously outlined with some modifications (Hanahan, 1983). One percent (0.5 ml) of the overnight culture of the relevant *E. coli* strain was used to inoculate 50 ml of LB liquid medium (Section 2.2.1.1), with appropriate antibiotics (Section 2.3) and incubated at 37 ^{o}C until the OD_{600} had reached approximately 0.3. The cell culture was incubated on ice for 15 minutes and bacterial cells subsequently harvested via centrifugation (Heraeus multifuge 1 S-R, Sorvall) at 8,000 x g for 20 minutes in 4 ^{o}C temperature. The cell pellet was re-suspended in 18 ml of RF1 solution and further incubated on ice for 30 minutes. The cells were harvested at 8,000 x g for 20 minutes at 4 ^{o}C and re-suspended in 4 ml of RF2 solution. Lastly, 200 µl aliquots were distributed into sterile 1.7 ml microcentrifuge tubes, flash frozen in liquid nitrogen and stored at -80 ^{o}C for future use. The composition of RF1 and RF2 solutions which were sterilised by filtration using 0.22 µm filters are outlined below:

RF1 solution

Chemicals	Concentration
RbCl	100 mM
$MnCl_2$	50 mM
Potassium acetate	30 mM
$CaCl_2 \cdot 6H_2O$	10 mM

The solution was adjusted to pH 5.8 with acetic acid.

RF2 solution

Chemicals	Concentration
RbCl	10 mM
MOPS	10 mM
$CaCl_2 \cdot 6H_2O$	75 mM
Glycerol	15% (v/v)

The solution was adjusted to pH 5.8 with NaOH.

2.6.1.2 Transformation of *E. coli* cells

The *E. coli* cells were transformed as previously described (Sambrook et al., 1989). The 200 µl aliquots of frozen competent cell (Section 2.6.1.1) were thawed on ice for 20 minutes prior to the addition of 50 to 500 ng of purified plasmid DNA or 10 µl of ligation mix and subsequently incubated on ice for additional 40 minutes permitting the adsorption of plasmid DNA at the surface of the cell. To promote plasmid DNA uptake, competent cells were gently mixed and heat-shocked at 42 °C for 90 seconds, followed by immediate incubation on ice for 5 minutes. For cell regeneration, 800 µl of LB liquid medium (Section 2.2.1.1) was added and the mixtures incubated at 37 °C for 1 hour. In order to select the colonies containing the plasmid of interest, 100 µl of this was spread on solid LB-agar medium (Section 2.2.2) containing appropriate antibiotics (Section 2.3). The agar plates were incubated at 37 °C for 19-21 hours.

2.6.2 Preparation and electroporation of electro-competent *P. aeruginosa*

The electro-competent *P. aeruginosa* were prepared, and electroporation was performed as outlined previously (Choi et al., 2006). The relevant *P. aeruginosa* strains were grown overnight in 20 ml of LB liquid medium (Section 2.2.1.1)

containing appropriate antibiotics (Section 2.3). The overnight culture was equally distributed into four microcentrifuge tubes and the cells were harvested via centrifugation (Heraeus Pico 17, Thermo Scientific) at 15,000 x g for 2 minutes. The cells were washed twice in 300 mM sterile sucrose solution and harvested via centrifugation with the same parameters above. The cells from the four tubes were combined into a single microcentrifuge tube and re-suspended in 100 µl of 600 mM sterile sucrose solution, comprising the electro-competent *P. aeruginosa* cells suspension. Subsequently, the suspension was mixed with 100 µl of H_2O containing the 250-500 ng of plasmid DNA, having a final sucrose concentration of 300 mM. This suspension was transferred to a 2 mm gap Gene Pulser electroporation cuvette (Biorad, USA) and pulse was applied (2.5 kV) using a Biorad Micropulser (Biorad, USA). Immediately, 800 µl of LB liquid medium (Section 2.2.1.1) was added and the culture was then transferred to a sterile 1.7 mL microcentrifuge which was incubated at 37°C for 1.5 hours with shaking at 200 rpm for recovery. Finally, successful transformants were selected by spreading 150 µl of the cell suspensions diluted 2,000-4,000-fold onto solid PIA medium (Section 2.2.2.1) containing appropriate antibiotics (Section 2.3).

2.6.3 Transconjugation of *P. aeruginosa*

The transfer of conjugation-competent-plasmids into *P. aeruginosa* strains was performed as previously described (Friedrich et al., 1981). The donor strain *E. coli* S17-1 (Section 2.1.1) was used to transfer plasmids harbouring the Mob (*oriT*) region into *P. aeruginosa* strains. The relevant plasmid was used to transform the *E. coli* S17-1 donor strain (Section 2.6.1.2). The donor strain and the recipient *P. aeruginosa* strain were cultivated separately in 20 ml of LB liquid medium (Section 2.2.1.1) containing appropriate antibiotics (Section 2.3) to mid log (OD_{600} of 0.6-0.8) and stationary phases (24 hours), respectively. The cultures were harvested separately by centrifugation at 4,000 x g for 20 minutes in 4^{o}C. The harvested cell pellets were suspended in 0.9% (w/v) sterile saline and centrifuged under the same conditions. The cells were re-suspended in 1 ml of the 0.9% (w/v) sterile saline and then 200 µl of the donor and recipient suspensions were mixed together by inversion in sterile 1.7 ml microcentrifuge tubes. The cells were harvested by centrifugation at 15,000 x g for 2 min at 4 ^{o}C, and re-suspended in 200 µl of 0.9% (w/v) sterile saline. The suspension was carefully poured onto a nutrient agar plate (Section 2.2.2) which was gently

transferred to 37 °C incubator after 15-30 minutes and incubated for 22-24 hours. After incubation, the cells were scraped from plates using a sterile spatula into a sterile 1.7 microcentrifuge tube, and re-suspended in 1 ml of 0.9% (w/v) sterile saline. Finally, the successful transconjugants were selected by plating 200 µl of the cell suspension on PIA agar (Section 2.2.2.1) containing the appropriate antibiotics (Section 2.3) and carbon source.

2.7 Molecular Cloning

General protocols for DNA manipulation were performed as previously outlined (Sambrook et al., 1989).

2.7.1 Plasmid isolation and concentration

2.7.1.1 High Pure Plasmid Isolation Kit

The High Pure Plasmid Isolation Kit (Roche, USA) was used for the plasmid isolation from the recombinant *E. coli* and *P. aeruginosa* cell cultures according to the manufacturer's instructions. The relevant bacterial strains containing the plasmid of interest were grown at 37 °C for 16 h in LB medium (Section 2.2.1.1) supplemented with appropriate antibiotics (Section 2.3). Cells were harvested and suspended in the suspension buffer containing RNase (for RNA contamination removal) and disrupted by alkaline lysis using the Lysis Buffer. Afterwards, Binding Buffer containing the chaotropic salt guanidinium chloride was added to the lysed cell suspension in order to denature the proteins (precipitated while entrapping the chromosomal DNA). The suspension was centrifuged at 15,000 x g for 10 min to separate the precipitated proteins and chromosomal DNA from the soluble fraction containing the plasmid DNA. The plasmid DNA was bound to the glass fleece of the High Pure Filter Tube and washed with the Wash Buffers I and II to remove contaminants. Lastly, 50 µl of the Elution Buffer (10 mM Tris-HCl buffer pH 8.5) was used to elute the plasmid DNA which was stored at -20 ^{o}C for future use.

2.7.1.2 Plasmid DNA Clean and Concentration Kit

The Clean and Concentrator Kit (Zymo Research, USA) was used according to the manufacturer's instructions to prepare a suitable plasmid solution for DNA cloning and sequencing. This step is appropriate after plasmid isolation with low concentrations or dirty plasmid preparations.

2.7.1.3 DNA concentration and purity analysis

DNA concentration and purity were assessed by using NanoDrop 1000 Spectrophotometry (ThermoScientific) according to the manufacturer's instructions. The spectrophotometric analysis measured the samples' absorbance ratio at 260/280 nm and 1.8 to 2.0 indicated high purity DNA.

2.7.2 DNA Hydrolysis with restriction endonucleases

The DNA digestion methods carried out in this study followed the laboratory protocols as previously published (Sambrook et al., 1989) with some modifications. Plasmid DNA (Section 2.7.1) and PCR products (Section 2.7.3) were hydrolysed by restriction endonucleases (REs) for cloning, plasmid DNA analysis and verification purposes. All the REs were used according to the manufacturer's instructions (Invitrogen Corporation, Roche or New England Biolabs). For restriction analysis, 10 U of enzyme and 0.1 vol of 10x recommended buffer was used for every 1 μg of DNA. Bovine serum albumin (BSA) was added to reactions to a final concentration of 10 mg/ml when recommended by the manufacturer. For DNA hydrolysis with two REs using compatible buffers (100% activity for both REs), a single reaction was used containing the plasmid DNA, two REs and the compatible buffer. All digestions were performed at 37 °C for 2 hours. DNA fragments were separated using agarose gel electrophoresis (Section 2.7.4) and fragments of interest were recovered from gels for consequent cloning (Section 2.7.5).

2.7.3 Polymerase chain reaction

Polymerase chain reaction (PCR) was employed for the amplification of the target DNA fragments for cloning and diagnostic purposes (Sambrook et al., 1989). The reaction was accomplished through repeating steps of denaturation, annealing and extension. The denaturation step separates the double-stranded DNA into single strands. The annealing step permits the primer to bind to the single stranded DNA template and the DNA polymerase synthesises a new DNA strand complementary to the DNA template for the extension step. For cloning, the high fidelity proofreading Platinum® *Pfx* DNA polymerase (Invitrogen Corporation, USA) was employed. In addition, Taq polymerase (Thermo Fisher Scientific) was used for diagnostic/verification purposes. The reaction mixtures were prepared in 0.2 mL

sterile thin walled PCR tubes (Axygen, USA) with 20 µl total volume for each individual reaction, as outlined in Tables 13 and 14.

Table 13. PCR reaction mixture using Platinum® *Pfx* DNA polymerase.

Reagents	Amount
10x *Pfx* Amplification Buffer	20.0 µl
PCRx Enhancer Solution	22.5 µl
$MgSO_4$ (50 mM)	2.0 µl
DMSO	2.5 µl
Primer 1 (10 pmoles/µl)	3.0 µl
Primer 2 (10 pmoles/µl)	3.0 µl
dNTPs (10 mM each)	3.0 µl
Template DNA	~2.0 ng
Platinum® *Pfx* DNA Polymerase (2.5 U/ µl)	1.0 µl
H_2O	Volume to 100 µl

Table 14. PCR reaction mixture using Taq polymerase (Thermo Fisher Scientific).

Reagents	Amount
10x Taq Amplification Buffer	2.5 µl
$MgCl_2$ (25 mM)	1.5 µl
dNTPs (10 mM each)	0.5 µl
Primer 1 (10 pmoles/µl)	0.5 µl
Primer 2 (10 pmoles/µl)	0.5 µl
Template DNA	~2.0 ng
Taq DNA Polymerase (2.5 U/ µl)	0.2 µl
H_2O	Volume to 20 µl

The PCR reactions were performed in a Biometra personal thermocycler (Whatman Biometra, Germany). Tables 15 shows the PCR reaction program using *Pfx* DNA polymerase and the Taq DNA polymerase (Thermo Fisher Scientific).

Table 15. PCR reaction condition.

Steps	Conditions
1. Initial Denaturation	94 °C for 300 seconds
2. Denaturation	94 °C for 45 seconds
3. Annealing	Optimal annealing temperature* for 30 seconds
4. Extension	68°C (*Pfx*) or 72°C (Taq) for 60 seconds per 1 kbp
5. Cycle	Repeat steps 2 – 4 for 35 cycles
6. Final Extension	68°C (*Pfx*) or 72°C (Taq) for 300 seconds
7. Hold	10°C

*An optimal annealing temperature is dependent on the melting temperature of the primer-DNA hybrid. Generally, the annealing temperature is 5^{o}C below the melting temperature of the primers. If required, optimisation can be done by changing the annealing temperature (± 3-5 ^{o}C).

2.7.4 Agarose gel electrophoresis

Agarose gel electrophoresis (AGE) was performed as previously described (Sambrook et al., 1989) and used for the separation of DNA fragments after PCR (Section 2.7.3) and restriction endonuclease hydrolysis (Section 2.7.2). When required, DNA could be recovered from gels (Section 2.7.5). Generally, agarose gels of 1% and 2% (w/v) were used to resolve DNA fragments above and below 1000 bp, respectively. Agarose (Bioline, USA) was mixed with 1x TBE (Tris/Borate/EDTA) electrophoresis buffer and completely melted in a microwave oven. The solution was allowed to cool down to approximately 50 ^{o}C and poured into a gel chamber with well comb inserted. After solidification, the comb was removed and the gel was placed into an electrophoresis apparatus, and submerged in 1x TBE buffer. DNA samples were supplemented with 6x DNA loading dye prior to being loaded into the wells. The compositions of the 10x TBE buffer and 6x DNA loading dye are shown below:

TBE buffer (10x)

Chemicals	Concentration
Tris-HCl	500 mM
Boric acid	500 mM
EDTA	25 mM

DNA loading dye (6x)	
Chemicals	**Concentration**
Urea	4 M
Sucrose	50% (v/v)
EDTA	50 mM
Bromophenol Blue	0.1%

A suitable molecular size standard (Section 2.7.4.1) was loaded into a separate well of the gel along with the samples. Electrophoresis parameters were dependent on the size of the AGE chamber and the degree of separation required among the DNA fragments. Typically, AGE was run at 100 - 120 V for 45 – 60 minutes. Agarose gels were stained for at least 20 minutes in ethidium bromide solution (2 µg/ml) and de-stained for 1 minute in H_2O. Visualisation of the DNA bands was performed using a UV transilluminator at $\lambda = 254$ nm (Bio-Rad, Gel Doc 2000, USA). For the separation of DNA fragments required for cloning, SYBR safe DNA gel stain (Invitrogen, USA) was used according to manufacturer's instructions instead of ethidium bromide and was visualised using a Safe Imager™ 2.0 Blue-Light Transilluminator (Invitrogen, USA).

2.7.4.1 DNA ladder standards

Two DNA molecular size standards were used in this study to estimate the size of DNA fragments on AGE. Lambda phage DNA (λ-DNA) (Invitrogen, USA) was hydrolysed with the RE *Pst*I (Sambrook et al. 1989, Section 2.7.2) to generate the fragments shown in Table 16. The digested λ-DNA was mixed with 6x loading dye and stored at -20 °C for future use. To determine the smaller sizes of DNA fragments, GeneRuler 100 bp DNA ladder plus (Fermentas, Canada) was used according to the manufacturer's instructions and the sizes are shown in Table 16.

Table 16. DNA ladders: λ/*PstI* and GeneRuler 100 bp ladder plus.

DNA ladders	Sizes (bp)
λ/*PstI*	15, 72, 94, 160, 164, 200, 211, 216, 264, 339, 448, 468, 514, 805, 1093, 1159, 1700, 1986, 2140, 2443, 2449, 2560, 2838, 4507, 4749, 5077, 11490
GeneRuler 100 bp ladder plus	100, 200, 300, 400, 500, 600, 700, 800, 900, 1000, 1200, 1500, 2000, 3000

2.7.5 Recovery of DNA fragment from agarose gels

The DNA fragments separated by AGE stained with SYBR safe DNA gel stain (Section 2.7.4) was recovered using the Zymoclean™ Gel DNA Recovery Kit (Zymo Research, USA) according to the manufacturer's instructions.

2.7.6 DNA ligation

T4 DNA ligase (Invitrogen, USA) was used in the ligation of the desired fragments (Sambrook et al., 1989). DNA fragments and vectors were obtained first by DNA hydrolysis using the appropriate REs (Section 2.7.2), separated by AGE with SBYR safe DNA gel stain (Section 2.7.4), and purified (Section 2.7.1.2). A high insert to vector ratio of ≥ 6:1 was used for high ligation efficiency. Ligation reactions were set up in 1.7 ml microfuge tubes according to manufacturer's instructions and incubated for 16-22 hours at 4 ºC.

2.7.7 DNA sequencing

Confirmation of the recombinant plasmids and PCR products was done using DNA sequencing, provided by Massey Genome Service (Massey University, Palmerston North) utilizing a capillary ABI3730 Genetic Analyser (Applied Biosystems Inc., USA). DNA sequencing reactions were set up in 0.2 ml clean sterile thin walled PCR tubes (Axygen, USA) containing 400-600 ng of the DNA template and 4 pmol/µl of primer in a total volume of 20 µl. The results were provided in ABI format and analysed using Vector NTI version 11 (Invitrogen Corporation, USA).

2.8 PHA bead and protein isolation

PHA bead and protein isolation were accomplished through cell harvesting (Section 2.8.1), cell disruption (Section 2.8.2) and purification and sterilisation (Section 2.8.3).

2.8.1 Cell harvesting

Cell cultures were harvested after 19 hours (soluble protein isolation; Section 2.4.2) or 48 hours (PHA bead isolation; Section 2.4.1) growth by centrifugation at 6,000 x g for 20 minutes at 4 ^{o}C in a Sorvall Rc-5B (DuPont instruments). The cell pellets were washed once by re-suspending with relevant buffer solution (1x PBS buffer, pH 7.4 for soluble protein isolation; 50 mM Tris buffer, pH 8 for PHA bead production in *P. aeruginosa*). The composition of 1x PBS buffer is outlined below:

1x PBS buffer

Chemicals	Concentration
NaCl	135 mM
KCl	2.7 mM
Na_2HPO_4	10 mM
KH_2PO_4	1.76 mM

The pH of the solution was adjusted to 7.4 using HCl.

The washed cell sediments were prepared for cell disruption (Section 2.8.2) by re-suspending as 10% slurry (w/v) in lysis buffer and mixing using homogeniser. The lysis buffer compositions are outlined below:

Function	Chemicals	Concentration	pH
***P. aeruginosa* PHA bead production**	Tris	50 mM	The pH was adjusted to 8 using NaOH.
	Ethylenediaminetetraacetic acid (EDTA)	50 mM	
***E. coli* PHA bead production**	Tris	25 mM	The pH was not adjusted.
	EDTA	5 mM	
	Sodium dodecyl sulfate (SDS)	0.04% w/v	
Soluble protein isolation	$NaH_2PO_4 \cdot 2H_2O$	50 mM	The pH was adjusted to 7.7 using NaOH.
	NaCl	500 mM	
	Imidazole	40 mM	
	Triton X-100	0.03%	

2.8.2 Cell disruption

2.8.2.1 Sonicator

Sonication is a cell disruption method using sound energy. Sonicator (Virsonic 600) was only used for the isolation of the soluble proteins from different *E. coli* strains (Section 2.4.2) in small volumes (50 mL). The 10% (w/v) cell slurry (Section 2.8.1) was subjected to cell lysis by sonicating 10 sec 'on' and 10 sec 'off' for a total of 10-15 minutes 'on' at a power setting of 21 W. This crude cell lysate was centrifuged at 9,500 x g for 1 hour at 4^{o}C and supernatant fraction containing soluble protein was filtered through 0.22 μM pore size filter prior to purification (Section 2.8.3.2).

2.8.2.2 Microfluidizer

Microfluidizer (Alphatech Systems) is a mechanical cell disruption method used when dealing with larger volumes of cultures (1-15 litres). This was used to disrupt cells with high efficiency for soluble protein isolation and PHA bead isolation from *P. aeruginosa* and *E.coli*.

2.8.2.2.1 PHA_{MCL} bead isolation from *P. aeruginosa*

The 10% (w/v) cell suspension (Section 2.8.1) was subjected to 5 passes of mechanical cell disruption at 20,000 psi in microfluidizer. The crude cell lysate was centrifuged at 10,000 x g for 1 hour at 4 ^{o}C. PHA_{MCL} beads from *P. aeruginosa* were soft, hence

needed a higher speed and longer time to harvest than the beads from *E. coli*. The PHA_{MCL} beads were washed twice in Tris buffer (50 mM Tris, pH 8) and purified using caustic wash (Section 2.8.3).

2.8.2.2.2 PHA_{SCL} bead isolation from *E. coli* strain ClearColi™

The 10% (w/v) cell suspension (Section 2.8.1) was subjected to 5 passes of mechanical cell disruption at 20,000 psi in microfluidizer. The crude cell lysate was centrifuged at 6,000 x g for 30 minutes at 4 ^{o}C, a lower speed and shorter time compared to the beads from *P. aeruginosa* to minimise cell debris and obtain purer PHA beads. The PHA_{SCL} beads were washed twice in lysis buffer (Section 2.8.1) and purified using caustic wash (Section 2.8.3).

2.8.2.2.3 Soluble protein isolation

The cell suspension (Section 2.8.1) was subjected to 3 passes of mechanical cell disruption at 20,000 psi. The crude cell lysate was centrifuged at 9,500 x g for 1 hour at 4 ^{o}C. Subsequently, the supernatant fraction containing soluble protein was filtered through 0.22 μM pore size filter and subjected to ultracentrifugation prior to affinity purification (Section 2.8.4).

2.8.3 PHA bead purification and sterilization

Two washes were explored for the isolation of PHA_{SCL} beads from *E.coli* strain ClearColi™: the urea wash buffer and caustic buffer wash. Different concentrations of urea were tested to determine the optimum concentration. Ultimately, the final PHA bead suspensions produced from *P. aeruginosa* and *E. coli* strain ClearColi™ were washed with caustic buffer. The PHA beads were re-suspended as 10% slurry (w/v) in caustic buffer and homogenized briefly until the beads were completely re-suspended (approximately 30 seconds). All the PHA beads were sterilized in 1x PBS (pH 7.4) with 70% Ethanol overnight. Afterwards, the PHA beads were re-suspended in 1x PBS (pH 7.4) and a representative sample of 200 μl from each group was spread onto LB agar. Subsequently, the agar plates were incubated at 37°C overnight to check for the absence of colony-forming units (CFUs) to confirm sterility. The urea and caustic buffers compositions are outlined below:

Urea wash buffer

	Urea concentration		
Chemicals	**2M**	**4M**	**6M**
Tris (100 mM)	0.300 g	0.300 g	0.300 g
EDTA (5 mM)	0.046 g	0.046 g	0.046 g
Urea	3 g	6 g	9 g
Triton X-100 (2% v/v)	0.5 ml	0.5 ml	0.5 ml
H_2O	25 ml	25 ml	25 ml

The pH of the solutions were adjusted to 10, 10.5 and 11 using NaOH.

Caustic wash buffer

Chemicals	Concentration
NaOH	0.1 M
SDS	0.04% w/v

2.8.4 Protein purification and sterilization

Affinity purification of the recombinant His-tagged proteins obtained after ultracentrifugation was performed using the Zymo (Irvine, CA) His-Spin Protein Miniprep Kit following the manufacturer's instructions with some modifications. Four hundred microliters of the filtered cell lysate was mixed with 300 µL of dried His-Affinity Gel while mixing on a tilting platform for 5 minutes at approximately 4 ^{o}C. The column was centrifuged at 17,000 x g for 30 seconds to 1 minute in 4 ^{o}C and sample binding step was repeated until the whole volume had been processed. Each column was washed twice with 250 µL of wash buffer and subsequently eluted with 150 µL of elution buffer. The eluted protein was passed through PD-10 column (Sigma-Aldrich, USA) for buffer exchange with 1x PBS (pH 7.4). The soluble proteins His_{10}-Ag and His_{10}-PopBAg were sterilised by filtration through a 0.22 µM pore size syringe filter. The composition of wash and elution buffers are shown below:

Wash buffer

Chemicals	Concentration
$NaH_2PO_4 \cdot 2H_2O$	50 mM
NaCl	500 mM
Imidazole	50 mM
Triton X-100	0.03%

The pH of the solution was adjusted to 7.7 using NaOH.

Elution buffer

Chemicals	Concentration
$NaH_2PO_4 \cdot 2H_2O$	50 mM
NaCl	500 mM
Imidazole	500 mM

The pH of the solution was adjusted to 7.7 using NaOH.

2.9 Characterisation of PHA beads

2.9.1 Nile-red staining and Fluorescence microscopy

Nile-red staining and fluorescence microscopy were used to detect and analyse the cells producing PHA beads and the isolated PHA beads. Nile-red staining was performed as previously described (Spiekermann et al., 1999). Generally, 1 ml of culture and 200-600 µl of purified PHA beads were harvested by centrifugation (Heraeus Pico 17, Thermo Scientific) at 6,000 x g for 1 minute and the supernatant was carefully removed with a pipette. Ten microliters of Nile-red solution (0.25 mg/ml in DMSO) was added to the remaining pellet and mixed thoroughly. Subsequently, 1 ml of 50 mM potassium phosphate buffer (pH 7.5) was added and incubated at room temperature for 15 min in the dark. After incubation, the suspension was harvested by centrifugation at 6,000 x g for 1 minute and washed once with 1 ml of 50 mM potassium phosphate buffer (pH 7.5). The sediments were then re-suspended in 1 ml (or 200 µl if that was the starting volume) of 50 mM potassium phosphate buffer (pH 7.5), spotted onto a glass slide, and covered with a coverslip. The slide was examined using fluorescence microscope (Olympus, Japan) using filter 4 under 1000x magnification and Magnafire^{TM} 2.1 (Optronics, USA) imaging software was used to capture images digitally.

2.9.2 Gas chromatography-mass spectrometry

Gas chromatography-mass spectrometry (GC-MS) was used to determine the PHA content of cells quantitatively and the purity of the isolated PHA beads (Brandl et al., 1988). Cells and the purified PHA beads (400-1000 µl) were centrifuged (Heraeus Pico 17, Thermo Scientific) at 17,000 x g for 2 minutes and lyophilised using a Freeze dryer (Kinetics Thermal Systems). The lyophilised cells and purified PHA beads ranging from 10-20 mg were suspended in 2 mL chloroform with 105 µg/ml undecane in GC-MS bottles. The samples were subjected to methanolysis by adding 2 mL of 15% (v/v) methanolic sulphuric acid and incubated at 100 ^{o}C in a heated oil bath for 5 hours. After incubation, the tubes containing the methanolyzed samples were allowed to cool down at room temperature and subsequently 2 mL of H_2O was added. The samples were then vortexed thoroughly for 1 minute and left at room temperature for phase separation. The bottom phase containing methyl esters of the corresponding fatty acid constituents was recovered and analysed by GC/MS for 3- hydroxyalkanoate methyl esters. All the sample preparation and processing was done by the author and the GC-MS analysis was conducted at Plant and Food Research (Palmerston North, New Zealand). The PHB standards (2-80 mg, Sigma-Aldrich, USA) were processed along with the PHA bead samples isolated from *E. coli* strain ClearColi^{TM}. Multichain standards were provided by Plant and Food Research for PHA_{MCL} bead samples isolated from *P. aeruginosa*. The reagents used in the sample preparation are outlined below:

Chloroform with 105 µg/ml undecane

Chemicals	Amount
Chloroform	100 ml
Undecane	14.2 µl

15% (v/v) methanolic sulphuric acid

Chemicals	Amount
Methanol	85 ml
Sulphuric acid	15 ml

2.9.3 Transmission Electron Microscopy

All transmission electron microscopy (TEM) data were obtained at the Manawatu Microscopy and Imaging Centre (MMIC, Massey University, Palmerston North, New Zealand). The pelleted samples were sent for TEM processing at MMIC in microcentrifuge tube(s). All the subsequent processing was done by MMIC and the images were taken by the author.

2.10 General methods of protein analysis

2.10.1 Sodium dodecyl sulfate-polyacrylamide gel electrophoresis

SDS-polyacrylamide gel electrophoresis (SDS-PAGE) was performed in a vertical slab gel electrophoresis apparatus for protein characterisation and analysis as previously described (Sambrook et al., 1989). Typically, each SDS-PAGE gel consists of two layers: a lower separating gel layer (10%, w/v, pH 8.9) and an upper stacking gel layer (4%, w/v, pH 6.8). The gel was made between two glass plates (16 cm x 19.5 cm) in a pre-cast cassette (Invitrogen, USA) (8 cm x 8 cm) resulting in a gel thickness of 1.5 mm. This method was run using electrode buffer and prepared as outlined below:

Electrode buffer

Reagent	Amount
5x High molecular weight running buffer (see below)	100 ml
200x Reducing agent (see below)	2.5 ml
H_2O	500 ml

5x High molecular weight running buffer

Chemicals	Concentration	Amount
MOPS	250 mM	52 g
Tris buffer	250 mM	30 g
SDS	0.5%	5 g
EDTA	5 mM	2 g
H_2O		Volume to 1 Litre

200x Reducing agent

Chemicals	Concentration	Amount
Sodium bisulfite	1M	10.4 g
H_2O		Volume to 100 ml

Separating gel preparation

The separating gel was prepared by combining the first three reagents in the table below and was degassed by adding 2-5 mg of Na_2SO_3 to avoid air bubble formation. Polymerisation of the gel was initiated by the addition of ammonium persulfate (APS) (40 %, w/v) and N, N, N‘, N‘-tetramethylethyl-endiamin (TEMED). The mixture was gently poured into the pre-cast cassette (leaving significant space for the stacking gel), immediately layered with isopropanol and allowed to polymerise for 30 minutes to 1 hour. After polymerisation, the isopropanol layer was poured off and the gel was rinsed twice with H_2O. The composition of the separating gel is outlined below:

Separating gel

Chemicals	Amount
3.5x Bis-tris gel buffer (see below)	2.86 ml
30% Bis-Acrylamide	3.33 ml
H_2O	3.81 ml
40% APS	25 µl
TEMED	7 µl

3.5x Bis-tris gel buffer

Chemicals	Concentration	Amount
Bis-tris	1.25 M	65.4 g
H_2O		250 ml

The pH of the solution was adjusted to 6.5-6.8 with HCl.

Stacking gel

Similar to the separating solution, the stacking gel solution was made by combining the first three reagents in the table below, degassed, and 40% (w/v) APS and TEMED

were added to initiate polymerisation. This solution was gently poured on top of the separating gel layer in the pre-cast cassette and a comb was immediately inserted for the formation of the wells. The gel was allowed to set at room temperature for 30 minutes to 1 hour. After polymerisation, the comb was carefully removed and the gel was used directly or stored in damp tissue at 4 ^{o}C for future use. The composition of the stacking gel is outlined below:

Stacking gel

Chemicals	Amount
3.5x Bis-tris gel buffer	1.43 ml
30% Bis-Acrylamide	0.65 ml
H_2O	2.92 ml
40% APS	12.5 µl
TEMED	3.5 µl

2.10.1.1 Protein sample preparation for SDS-PAGE and electrophoresis conditions

Protein samples were prepared for SDS-PAGE by adding 10-20 µl of protein sample in 1.7 ml microfuge tube. Two volumes of protein sample were mixed with 1 volume of 3x SDS-denaturing buffer and incubated on a heating block at 95 °C for 10 min. The denatured protein solution was allowed to cool down at room temperature before it was loaded into the wells of the gel. GangNam-stain^{TM} (iNtRON biotechnology, Korea; Table17), molecular weight standard, and samples for the estimation of the molecular weight of the proteins, were all loaded into separate wells of the gel. Parameters for electrophoresis were 150 V for approximately 45 minutes. The composition of 3x denaturing buffer is given below:

Denaturing buffer (3x)

Chemicals	Amount
SDS	8.0 g
EDTA	37.2 mg
Glycerol	40 ml
B-mercaptoethanol	20 ml
Bromothymol blue	10 mg
Tris-HCl (100 mM, pH 6.8)	Volume to 100 ml

Table 17. Protein marker used in SDS-PAGE.

Protein marker	Molecular weights (kDa)
GangNam stain	9, 14, 18, 22, 30, 41, 53, 70, 100, 130, 170, 235

2.10.1.2 Protein staining and de-staining solution

The SDS-PAGE gel was carefully removed from the cast and stained with approximately 150 ml of Coomassie Brilliant Blue Staining solution in a tilt-shaker (Labnet International, USA) for 15 minutes at 40 rpm. After staining, the gel was washed thoroughly with H_2O and subsequently de-stained with approximately 150 ml of destaining solution while shaking for 1-2 hours or until the protein bands were visible and background colour from the staining solution was removed. GEL-DOC 2000 (Bio-Rad Laboratories, USA) and Image Lab Software (Version 3.0 build 11, Bio-Rad Laboratories, USA) were used to capture the gel images. The compositions of the staining and de-staining solutions are described below:

Coomassie Brilliant Blue Staining solution

Chemicals	Amount
Coomassie blue R-250	4 g
Ethanol	450 ml
Acetic acid	90 ml
H_2O	460 ml

Destaining solution

Chemicals	Amount
Ethanol	660 ml
Acetic acid	200 ml
H_2O	1,140 ml

2.10.2 Densitometry

Fusion protein percentage of the total protein in bead fractions was determined by densitometry. This was performed via gel images analysis of SDS-PAGE (Section 2.10.1) using myImageAnalysis Software (Thermo Scientific). Known concentrations of BSA were used as standards for quantification.

2.10.3 Immunoblot analysis

Confirmation of the fusion proteins on PHA beads isolated from *P. aeruginosa* was performed using immunoblot analysis (Lee et al., 2017). The samples were run on SDS-PAGE (Section 2.10.1), transferred to nitrocellulose membrane (Section 2.10.3.1), subject to relevant primary and secondary antibodies, and visualised by chemiluminescence upon exposure and development of X-ray film (Section 2.10.3.2).

2.10.3.1 Transfer to nitrocellulose membrane

A semi-dry transfer system (iBlot® Gel Transfer Stacks Nitrocellulose and iBlot® Gel Transfer System, Invitrogen Corporation, USA) was used according to the manufacturer's instructions to transfer the proteins from SDS-PAGE gel (Section 2.10.1) to nitrocellulose membrane. The anode (bottom) and cathode (top) consist of copper sheets amalgamated to matrices infused with relevant buffers. The anode matrix contains the 0.2 μm nitrocellulose membrane on which the SDS-PAGE gel was carefully placed. A sheet of filter paper moistened with de-ionised H_2O was place on top of the SDS-PAGE gel and the air bubbles were removed using a roller, followed by the placement of cathode on the top. The sponge was placed on the top of the cathode to ensure application of even pressure. The lid was securely fastened and the transfer programme No. 3 (7 mins) was initiated.

2.10.3.2 Blocking, addition of antibody and visualisation

After the transfer, the nitrocellulose membrane (Section 2.10.3.1) was blocked overnight with 5% (w/v) skim milk in 1x PBS (135 mM NaCl, 2.7 mM KCl, 10 mM Na_2HPO_4 and 1.76 mM KH_2PO_4, pH 7.4) and 1% (w/v) BSA at 4°C. The membrane was washed three times with 1x PBS supplemented with 0.05% v/v Tween-20 (PBST) for 5 minutes each wash and incubated for 1 hour with the primary antibody, rabbit polyclonal anti-PhaC1_529 (epitope used: RSGKTRKAPASLGN; Genscript, USA) at 1:20,000 dilution in PBST supplemented with 1% (w/v) BSA. Subsequently, the membrane was washed another three times with PBST for 5 minutes each wash and incubated with the secondary antibody, anti-Rabbit HRP (Ab6721, Abcam, UK) at 1:25,000 dilution in PBST supplemented with 1% (w/v) BSA for 1 hour. After three washes with PBST, development was carried out by incubating the membrane with 2 ml of Super Signal West Pico Stable Peroxide and 2 ml of Luminol/Enhancer solutions (Thermo Scientific, USA) for 5 minutes. All incubation and wash steps were carried out with gentle agitation and incubations with light sensitive antibodies and substrates were carried out in the dark. For visualisation of bands, the membranes were exposed to BioMax XAR film (Kodak, USA) and images were developed using a developer (Kodak X-Omat-100, USA).

2.10.4 Mass Spectrometry (MS)

Protein bands of interest on SDS-PAGE gels (Section 2.10.1) were excised and protein identification was performed using mass spectrometry (MS). Sample preparation, digestion with trypsin and extracted were done by the author. The extracted protein samples were submitted for MS at Institute of Fundamental Sciences (IFS), Massey University, New Zealand.

2.11 Animal testing of the PHA beads and immunological analyses

Mice vaccination (Section 2.11.1), immunological assays (Section 2.11.2) and bacterial challenge (Section 2.11.3) were performed at Harvard Medical School, Boston's Children Hospital, USA. Christina Merakou did all the laboratory experiments and data collection while the author did the data analysis.

2.11.1 Mice vaccination

Female FVB/NJ mice aged 6 to 7 weeks were purchased from The Jackson Laboratory and were vaccinated three times subcutaneously with 200 µl/injection at 2 week intervals (n = 8 per group). Two separate experiments were carried out: (1) mice vaccination using PHA_{MCL} beads isolated from *P. aeruginosa*, and (2) mice vaccination using PHA_{SCL} beads isolated from *E. coli* strain ClearColi^{TM}. For the first experiment, 7 µg each of $PhaC1_{Pa}$ beads, Ag-$PhaC1_{Pa}$ beads, $PhaC1_{Pa}$-PopB beads, PopB/PcrH (positive control; PcrH is the PopB chaperon), OprF/I (positive control), PopB/PcrH + OprF/I (positive control) were used for mice vaccination. The second experiment comprised the following samples: 3 µg of PhaC, 3 µg of Ag-PhaC, 5 µg of PhaC-PopB, 5 µg of PhaC-PopBAg, 7 µg of His_{10}-Ag, 7 µg of His_{10}-PopBAg, and 30 µg of PopB/PcrH. All samples were prepared with 1.25 mg/ml final concentration of the Alum (A8222, Sigma, MO) adjuvant in 10 mM Tris saline (150 mM NaCl) which also served as negative control. Protein concentration was calculated using densitometry and BSA standards (Section 2.10.2).

2.11.2 Immunological assays

In the first experiment with PHA_{MCL} beads from *P. aeruginosa*, blood collection was performed via tail bleeding, but this was unsuccessful. The tail bleeding technique produced insufficient volumes of blood for analysis. Retro-orbital whole blood collection was performed for the second experiment with mice vaccinated with PHA_{SCL} beads from *E. coli* strain ClearColi^{TM}, and successfully extracted blood for immunological analysis. Serum antibodies were measured using ELISA as previously described (Priebe et al., 2008) (Section 2.12.2). Mouse IL-17 DuoSet ELISA Kit (R&D Systems) was used for the IL-17 cytokine analysis. Mice splenocytes were stimulated with PopB/PcrH, His_{10}-Ag, His_{10}-PopBAg and PhaC beads for IL-17 cytokine measurements. IgG responses were analysed by coating the microtitre plates with PopB/PcrH, His_{10}-Ag and PhaC beads.

2.11.3 Challenge with *P. aeruginosa* N13 strain

Mice were challenged with *P. aeruginosa* N13 strain 3 weeks after the final vaccination. For the preparation of the inocula for the *in vivo* challenge experiments, frozen stocks of the bacteria were streaked and grown at 37 °C overnight on tryptic soy agar (TSA). The bacteria were suspended in PBS and the concentrations of the

bacteria were measured spectrophotometrically and confirmed by plating. Intranasal challenge was done by administering each mouse with 20 µl of the inoculum ($2.6x10^6$ CFUs; 10ul for each nostril). The mice were observed and analysed for survival percentage.

2.11.4 Statistical Analysis

Statistical analyses were performed using the Prism software (GraphPad Software, La Jolla, CA). The survival data were analysed using the Kaplan-Meier method and log-rank. The IgG responses were expressed in half maximal effective concentration (EC50). IgG responses and IL-17 cytokine were analysed by one-way analysis of variance (ANOVA) with statistical significance ($p < 0.05$) indicated by letter based representation of pairwise comparisons between groups using Tukey's post-hoc test.

2.12 Assessment of the *cdrA* knockout mutant

The *cdrA* knockout mutant was generated by transconjugation (Section 2.6.3) and subsequently analysed for Psl production via solid surface attachment assay (Section 2.12.1) and enzyme-linked immunosorbent assay (Section 2.12.2).

2.12.1 Solid surface attachment assay

Solid surface attachment (SSA) assay was performed as previously described with some modifications (Ghafoor et al., 2011). The relevant *P. aeruginosa* strains were grown overnight in LB liquid medium (Section 2.2.1.1) at 37ºC with shaking. The OD_{600} was measured and dilutions of starting OD_{600} equivalent to 0.005, 0.0025 and 0.00125 were prepared by serial dilutions. Ultimately, starting OD_{600} of 0.005 was used for the rest of the experiments. One hundred microliters of the diluted cultures were added to the wells of three UV-sterilised 96-well flat-bottom microtitre plates and each plate was incubated at 37 ºC for 12, 20 or 96 hours without shaking, allowing the production of Psl polysaccharide.

2.12.2 Enzyme-linked immunosorbent assay

After incubation of the microtitre plates containing the cultures (Section 2.12.1), enzyme-linked immunosorbent assay (ELISA) was performed as previously described with some modifications (Parlane et al., 2009) to determine Psl production. The plate was washed three times with 370 µl of 1x PBS (135 mM NaCl, 2.7 mM KCl, 10 mM

Na_2HPO_4 and 1.76 mM KH_2PO_4, pH 7.4) and blocked for 30 minutes in 1x PBS (pH 7.4) with 0.5% BSA at room temperature with gentle shaking. The plate was then washed three times with 370 µl of 1x PBS (pH 7.4) and 100 µl of 100 µg/mL *Hippeastrum hybrid* (HHA)-HRP (Cat# H-8008-1) was added which was used to detect the Psl. The plate was gently shaken at room temperature in the dark for 1 hour. After antibody incubation, the plate was washed three times with 370 µl of 1x PBS (pH 7.4), and 100 µl of OPD substrate (SIGMAFAST OPD tablet set #P9187) was added and incubated in the dark for 30 mins to detect colour change from light yellow to orange. Subsequently, 100 µl of 0.5 N H_2SO_4 was added to stop reaction and the absorbance was measured at 490 nm on an ELx808iu ultra microtiter plate reader (BIO-TEK Instruments Inc., USA) (Jahns et al., 2008). The results were expressed as optical density units at 490 nm.

Chapter 3: Results

3.1 Development of antigen-displaying PHA_{MCL} beads produced in *P. aeruginosa*

To develop a candidate vaccine to prevent *P. aeruginosa* disease, four antigens, namely, OprI, OprF, AlgE and PopB were displayed on the surface of PHA_{MCL} beads which were produced in *P. aeruginosa* PAO1 ΔCΔ8ΔF or PAO1 ΔCΔ8ΔFΔP production strains. To achieve this, the following 8 plasmids were used: (1) pBBR1JO-5_PhaC1$_{Pa}$ (Lee et al., 2017); (2) pHERD20T-2_PhaC1$_{Pa}$; (3) pHERD20T-2_Ag-PhaC1$_{Pa}$ (Lee et al., 2017); (4) pHERD20T-2_PopB-PhaC1$_{Pa}$; (5) pHERD20T-2_PopBAg-PhaC1$_{Pa}$; (6) pHERD20T-2_PhaC1$_{Pa}$-PopB; (7) pHERD20T-2_Ag-PhaC1$_{Pa}$-PopB; and (8) pHERD20T-2_PhaC1$_{Pa}$-PopBAg (Table 4). The first 3 plasmids were constructed by Jason Lee (IFS, Massey, Palmerston North, New Zealand), while the author constructed the remaining 5 plasmids, described in Sections 3.1.1 and 3.1.2.

The hypotheses of this study were that PopB fusion to PhaC1$_{Pa}$ and Ag would retain the catalytic activity of the PhaC1$_{Pa}$ to produce PHA_{MCL} beads. Furthermore, the fusion proteins would be successfully displayed on the PHA_{MCL} beads produced by the *P. aeruginosa* production strain. To test these hypotheses, plasmids were constructed in XL1-Blue *E. coli* and used to transform the *P. aeruginosa* PAO1 ΔCΔ8ΔF or PAO1 ΔCΔ8ΔFΔP strains. The production of PHA_{MCL} beads was assessed and characterized using Nile-red staining and fluorescence microscopy (FM) (Section 2.9.1), transmission electron microscopy (TEM) (Section 2.9.3), and gas chromatography-mass spectrometry (GC-MS) (Section 2.9.2). The fusion proteins were analysed and confirmed using SDS-PAGE (Section 2.10.1), immunoblot analysis (Section 2.10.3) and mass spectrometry (MS) (Section 2.10.4). Densitometry (Section 2.10.2) was used to quantify the fusion protein as a percentage of the total protein in PHA_{MCL} bead fractions.

3.1.1 N-terminal fusion of PopB to PhaC1$_{Pa}$

PopB was independently fused to each N-terminus of pHERD20T-2_PhaC1$_{Pa}$ and pHERD20T-2_Ag-PhaC1$_{Pa}$ creating pHERD20T-2_PopB-PhaC1$_{Pa}$ and pHERD20T-2_PopBAg-PhaC1$_{Pa}$, respectively (Table 4). This approach was made taking into account the better performance of fusion with Ag at the N-terminal of PhaC1$_{Pa}$ (Lee et al., 2017). The pUC57 plasmid containing XPopBS antigen fragment, which was obtained from Genescript Corporation (USA), was hydrolysed (Section 2.7.2) with *Sal*I and *Xba*I restriction enzymes (REs). Separately, pHERD20T-2_Ag-PhaC1$_{Pa}$ (Table 4) was hydrolysed with the same REs, *Sal*I and *Xba*I resulting in a linearized vector backbone fragment. The DNA fragments (PopB and linearized vector pHERD20T-2_Ag-PhaC1$_{Pa}$) were separated from their respective digestion mixtures using AGE with SYBR safe stain (Section 2.7.4), and subsequently recovered and purified by gel purification (Section 2.7.5). Purified fragments were ligated (Section 2.7.6), generating the final plasmid pHERD20T-2_PopBAg-PhaC1$_{Pa}$ containing 4 different antigens from *P. aeruginosa*. Direct cloning (without an intermediate plasmid vector) was done for a simpler and faster approach. The plasmid was used to transform (Section 2.6.1.2) *E. coli* XL1-Blue (Table 3) and spread-plated onto LB agar medium containing carbenicillin (Section 2.3). Single colonies were selected and confirmed for the presence of the insert using plasmid isolation (Section 2.7.1), and *Sal*I and *Xba*I RE digestion (Section 2.7.2). Lastly, final confirmation by DNA sequencing (Section 2.7.7) using pHERD20T_fwd and 5' PhaC1_rev primers was performed at Massey University Genome Service. The strategy of pHERD20T-2_PopBAg-PhaC1$_{Pa}$ construction is presented in Figure 9.

The pHERD20T-2_PopBAg-PhaC1$_{Pa}$ was used as the template to amplify PopB using *Xba*I PopB_fwd and *Nde*I PopB_rev primers. The PCR product, PopB was isolated by AGE (Section 2.7.4), recovered (Section 2.7.5), hydrolysed with *Xba*I and *Nde*I REs, and cleaned and purified (Section 2.7.1.2). The vector pHERD20T-2_Ag-PhaC1$_{Pa}$ (Table 4) was hydrolysed with *Xba*I and *Nde*I REs, and recovered and purified by gel purification (Section 2.7.4). Similar to the above, direct cloning was done to ligate (Section 2.7.6) PopB to the compatible sites of the linearized vector pHERD20T-2_PhaC1$_{Pa}$, resulting in the final pHERD20T-2_PopB-PhaC1$_{Pa}$ plasmid. The plasmid was used to transform *E. coli* XL1-Blue and confirmed by *Xba*I and *Nde*I RE digestion. Further confirmation was done by DNA sequencing using

pHERD20T_fwd and 5' phaC1_rev primers. The strategy of pHERD20T-2_PopB-PhaC1$_{Pa}$ construction is presented in Figure 10.

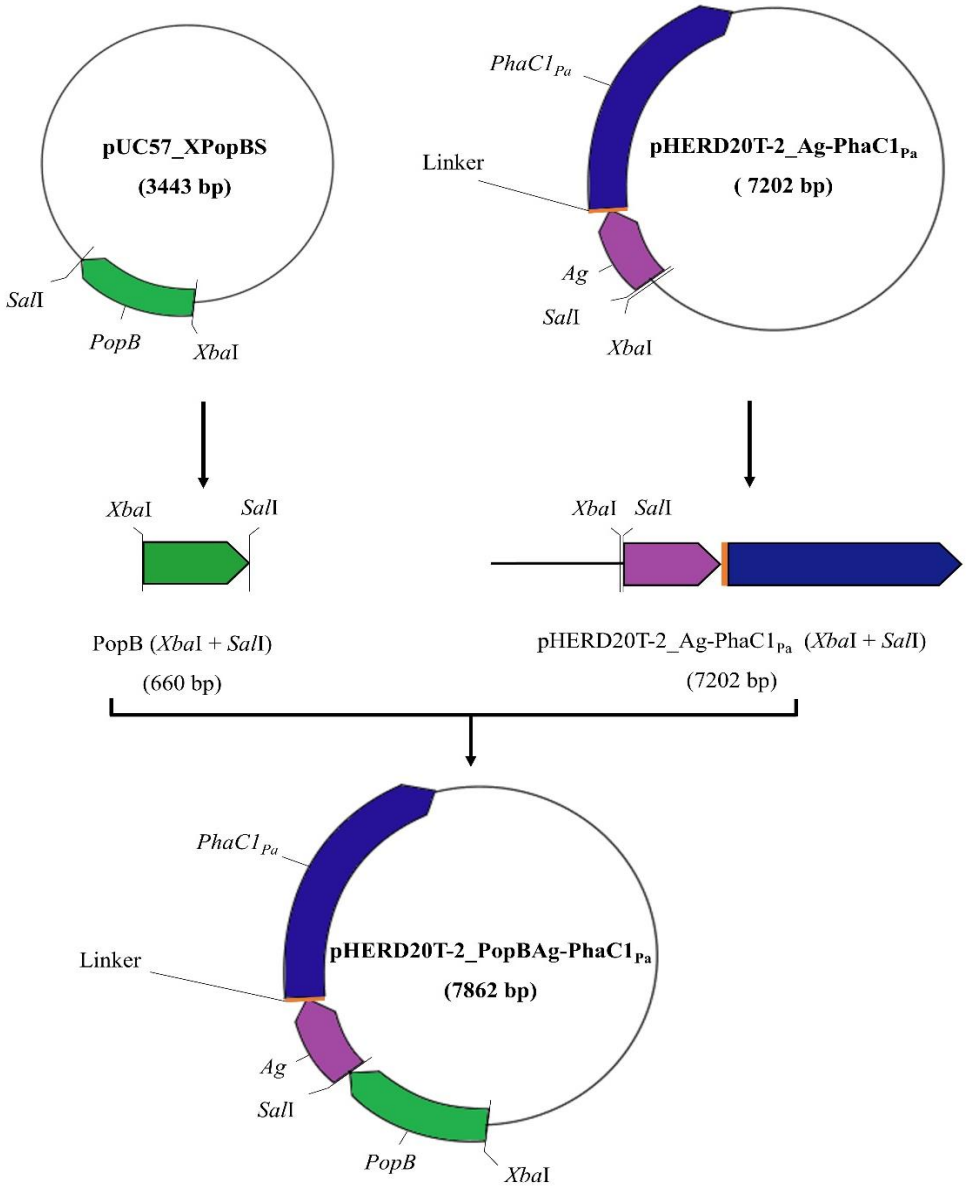

Figure 9. Strategy for the construction of pHERD20T-2_PopBAg-PhaC1$_{Pa}$. The *Pseudomonas* codon optimized *PopB* gene was isolated from pUC57_XPopBS, followed by restriction enzyme digestion using *Xba*I and *Sal*I (Section 2.7.2). The DNA fragment was recovered using agarose gel electrophoresis (Section 2.7.4) and gel purification (Section 2.7.5). The PopB fragment was ligated using T4 DNA ligase (Section 2.7.6) into the linearized vector pHERD20T-2_Ag-PhaC1$_{Pa}$ which was generated by restriction enzyme digest with *Xba*I and *Sal*I, generating the final plasmid pHERD20T-2_PopBAg-PhaC1$_{Pa}$.

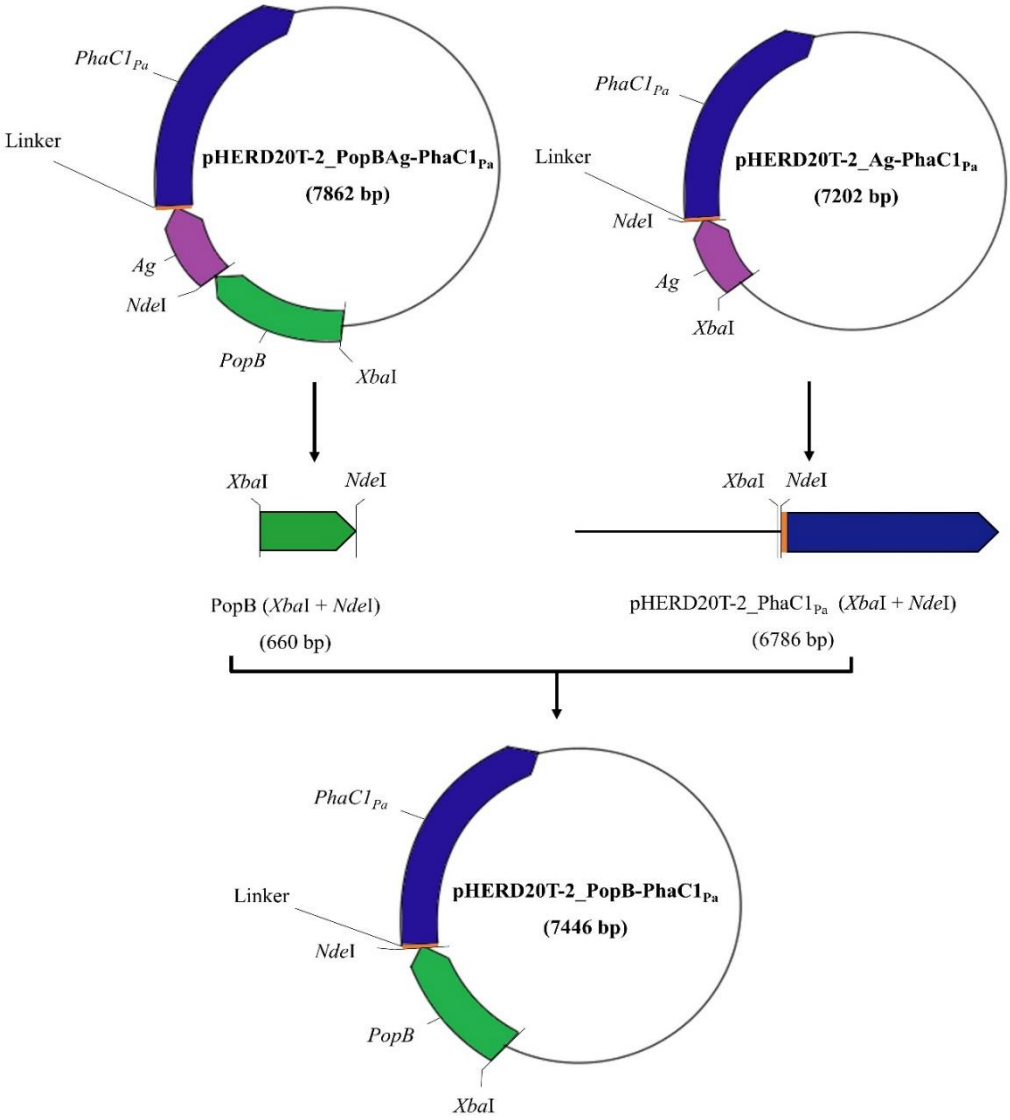

Figure 10. Strategy for the construction of pHERD20T-2_PopB-PhaC1Pa. The PopB fragment was obtained from pHERD20T-2_ PopBAg-PhaC1Pa by PCR amplification (Section 2.7.3) using primers *Xba*I PopB_fwd and *Nde*I PopB_rev, followed by separation of DNA fragments using agarose gel electrophoresis (Section 2.7.4) and gel purification (Section 2.7.5). Subsequently, the recovered PopB fragment was digested by *Xba*I and *Nde*I restriction enzymes (Section 2.7.2) and purified from the digestion mixture (Section 2.7.1.2). The PopB fragment was ligated using T4 DNA ligase (Section 2.7.6) into the linearized vector pHERD20T-2_PhaC1Pa which was generated by restriction enzyme digest with *Xba*I and *Nde*I, generating the final plasmid pHERD20T-2_PopB-PhaC1Pa.

3.1.2 C-terminal fusion of PopB to PhaC1$_{Pa}$

C-terminal fusion of PopB to PhaC1$_{Pa}$ was an alternative approach because the N-terminal fusion of PopB failed to produce PHA$_{MCL}$ beads (Section 2.8) manifested by only brown cell debris being harvested after cell disruption using the Microfluidizer. The strategy of constructing pHERD20T-2_PhaC1$_{Pa}$-PopB and pHERD20T-2_Ag-PhaC1$_{Pa}$-PopB was similar to the molecular sub-cloning of pHERD20T-2_PopB-PhaC1$_{Pa}$ (Section 3.1.1). The pUC57_XPopBS (Table 4) was amplified by PCR (Section 2.7.3) using primers Primer 5' (XhoI) and Primer 3' (EcoRI). The PopB fragment was recovered by AGE (Section 2.7.4) followed by gel purification (Section 2.7.5). Subsequently, PopB fragment was hydrolysed using *Xho*I and *EcoR*I REs (Section 2.7.2) and, separated from the digestion mixture (Section 2.7.1.2). In parallel, the plasmids pHERD20T-2_PhaC1$_{Pa}$-Ag and pHERD20T-2_Ag-PhaC1$_{Pa}$-Ag (Table 4) were digested (Section 2.7.2) with *Xho*I and *EcoR*I REs, resulting in linearized vectors pHERD20T-2_PhaC1$_{Pa}$ and pHERD20T-2_Ag-PhaC1$_{Pa}$ which were isolated via AGE (Section 2.7.4) and gel purified (Section 2.7.5). Subsequently, the PopB gene was ligated (Section 2.7.6) to each of the respective linearized vector fragments, generating the final plasmids pHERD20T-2_PhaC1$_{Pa}$-PopB and pHERD20T-2_Ag-PhaC1$_{Pa}$-PopB. The plasmids were used to transform (Section 2.6.1.2) *E. coli* XL1-Blue (Table 3) and spread plated onto LB-agar media containing carbenicillin (Section 2.3). Single colonies were selected and the successful transformants were verified using *Xho*I and *EcoR*I restriction enzyme digestion (Section 2.7.2) and DNA sequencing (Section 2.7.7) using primers P79 and P87 for pHERD20T-2_PhaC1$_{Pa}$-PopB and P10 and P87 for pHERD20T-2_Ag-PhaC1$_{Pa}$-PopB. The strategy for the construction of pHERD20T-2 PhaC1$_{Pa}$-PopB and pHERD20T-2 Ag-PhaC1$_{Pa}$-PopB are presented in Figures 11 and 12, respectively.

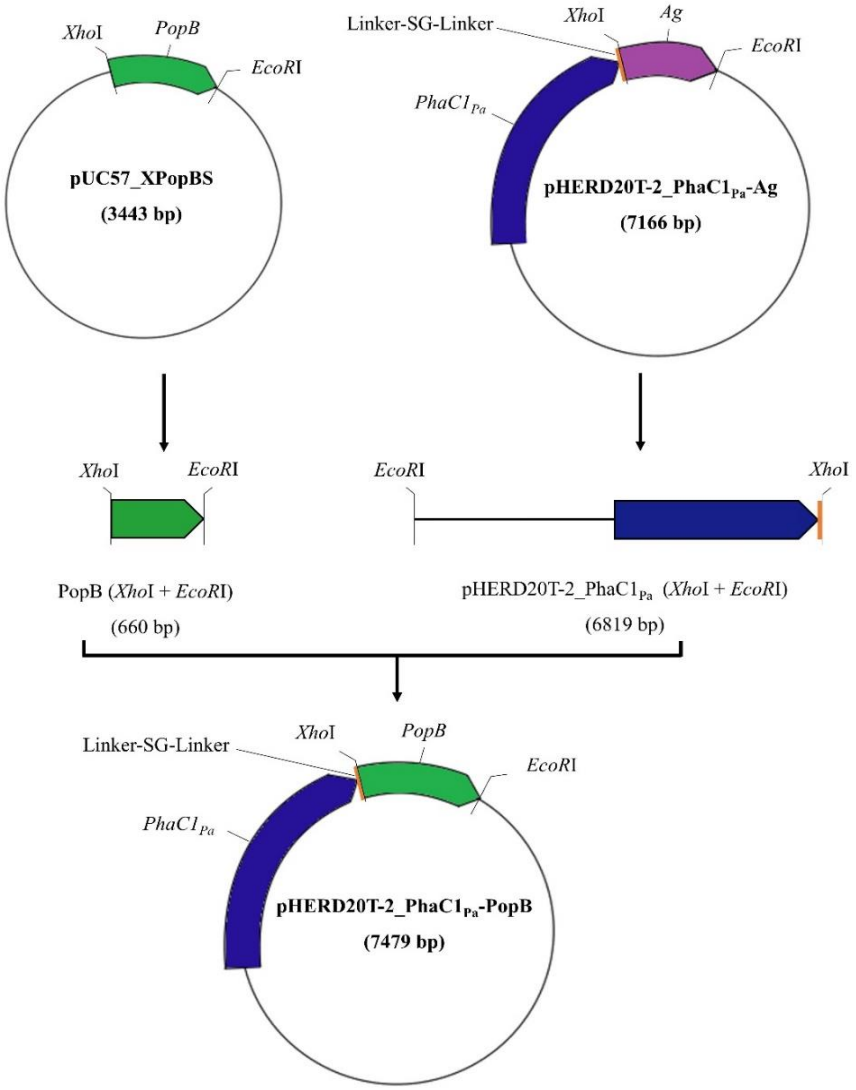

Figure 11. Strategy for the construction of pHERD20T-2_PhaC1$_{Pa}$-PopB. The *Pseudomonas* codon optimized *PopB* gene was isolated from pUC57_XPopBS by PCR amplification using primers Primer 5' (XhoI) and Primer 3' (EcoRI) (Section 2.7.3), followed by recovery of DNA fragments using agarose gel electrophoresis (Section 2.7.4) and gel purification (Section 2.7.5). The recovered PopB fragment was digested using restriction enzymes *Xho*I and *EcoR*I (Section 2.7.2), and purified (Section 2.7.1.2). The PopB fragment was ligated using T4 DNA ligase (Section 2.7.6) into the linearized vector pHERD20T-2_PhaC1$_{Pa}$ which was generated by restriction enzyme digest with *Xho*I and *EcoR*I, generating the final plasmid pHERD20T-2_PhaC1$_{Pa}$-PopB.

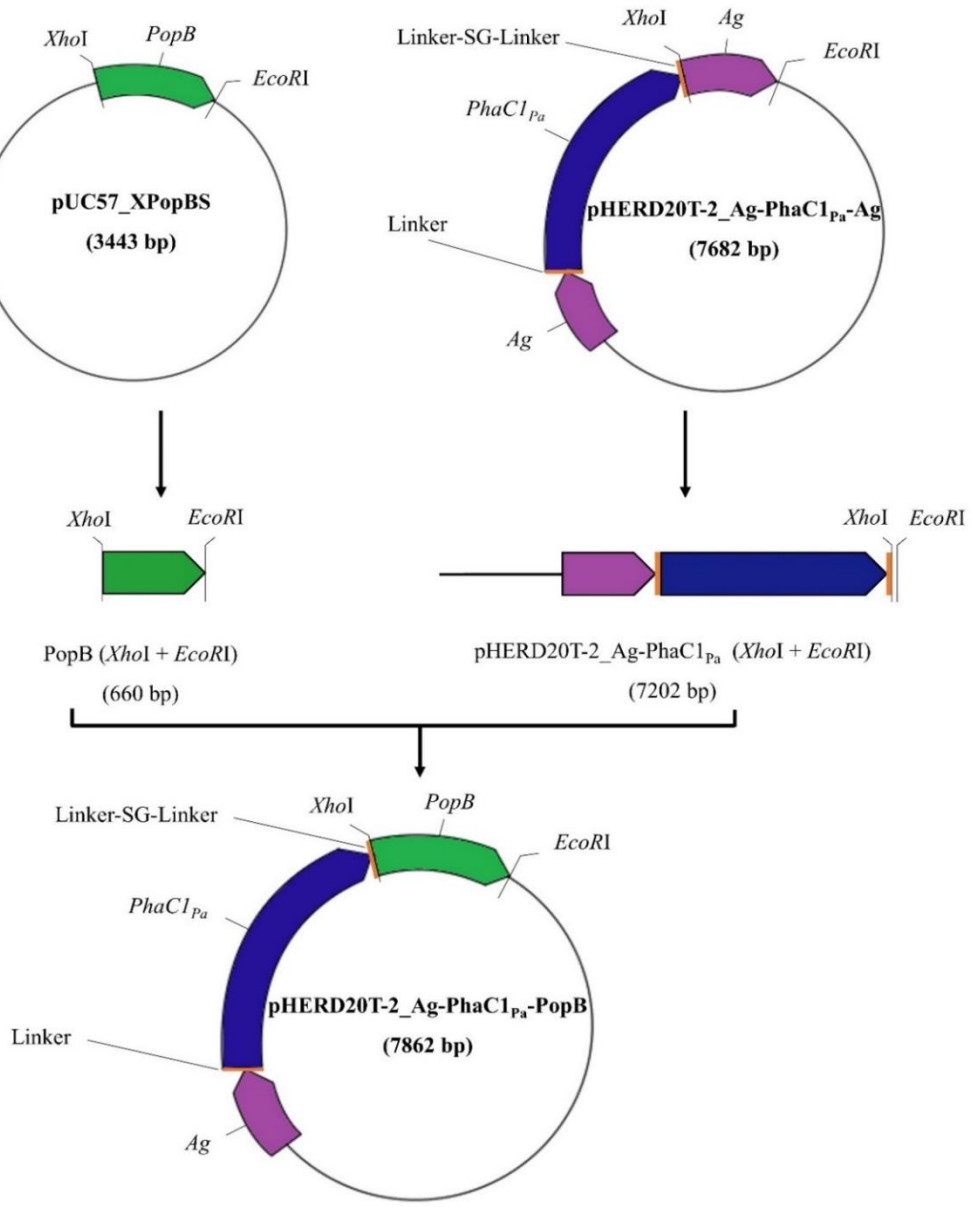

Figure 12. Strategy for the construction of pHERD20T-2_Ag-PhaC1Pa-PopB. The *Pseudomonas* codon optimized *PopB* gene was isolated from pUC57_XPopBS by PCR amplification using primers Primer 5' (XhoI) and Primer 3' (EcoRI) (Section 2.7.3), followed by the recovery of DNA fragments using agarose gel electrophoresis (Section 2.7.4) and gel purification (Section 2.7.5). The recovered PopB fragment was digested using restriction enzymes *Xho*I and *EcoR*I (Section 2.7.2), and purified (Section 2.7.1.2). The PopB fragment was ligated using T4 DNA ligase (Section 2.7.6) into the linearized vector pHERD20T-2_Ag-PhaC1Pa which was generated by restriction enzyme digest with *Xho*I and *EcoR*I, generating the final plasmid pHERD20T-2_Ag-PhaC1Pa-PopB.

Construction of pHERD20T-2_PhaC1$_{Pa}$-PopBAg was performed due to the inability of pHERD20T-2_Ag-PhaC1$_{Pa}$-PopB to produce PHA$_{MCL}$ beads (Section 2.4.1.1) with the objective of displaying the single fusion of Ag and PopB on the PHA$_{MCL}$ beads, giving a total of four antigens. The strategy was similar to the approach above and is presented in Figure 13, the PopBAg from pHERD20T-2_PopBAg-PhaC1$_{Pa}$ was amplified by PCR (Section 2.7.3) using XhoI-2 and EcoRI-2 primers, isolated via AGE (Section 2.7.4) followed by gel purification (Section 2.7.5). The PopBAg fragment and vector pHERD20T-2_PhaC1$_{Pa}$-Ag were hydrolysed using *Xho*I and *EcoR*I REs (Section 2.7.2), and subsequently separated from the digestion mixture (Section 2.7.1.2). The PopBAg fragment was ligated to the linearized vector, generating the final plasmid, pHERD20T-2_PhaC1$_{Pa}$-PopBAg. The plasmid was used to transform (Section 2.6.1.2) *E. coli* XL1-Blue (Table 3) and spread plated onto LB-agar media containing carbenicillin (Section 2.3). Single colonies were selected and the successful transformants were verified using *Xho*I and *EcoR*I restriction enzyme digestion (Section 2.7.2), and DNA sequencing (Section 2.7.7) using the same primers above, pHERD20T_fwd and 5' phaC1_rev primers.

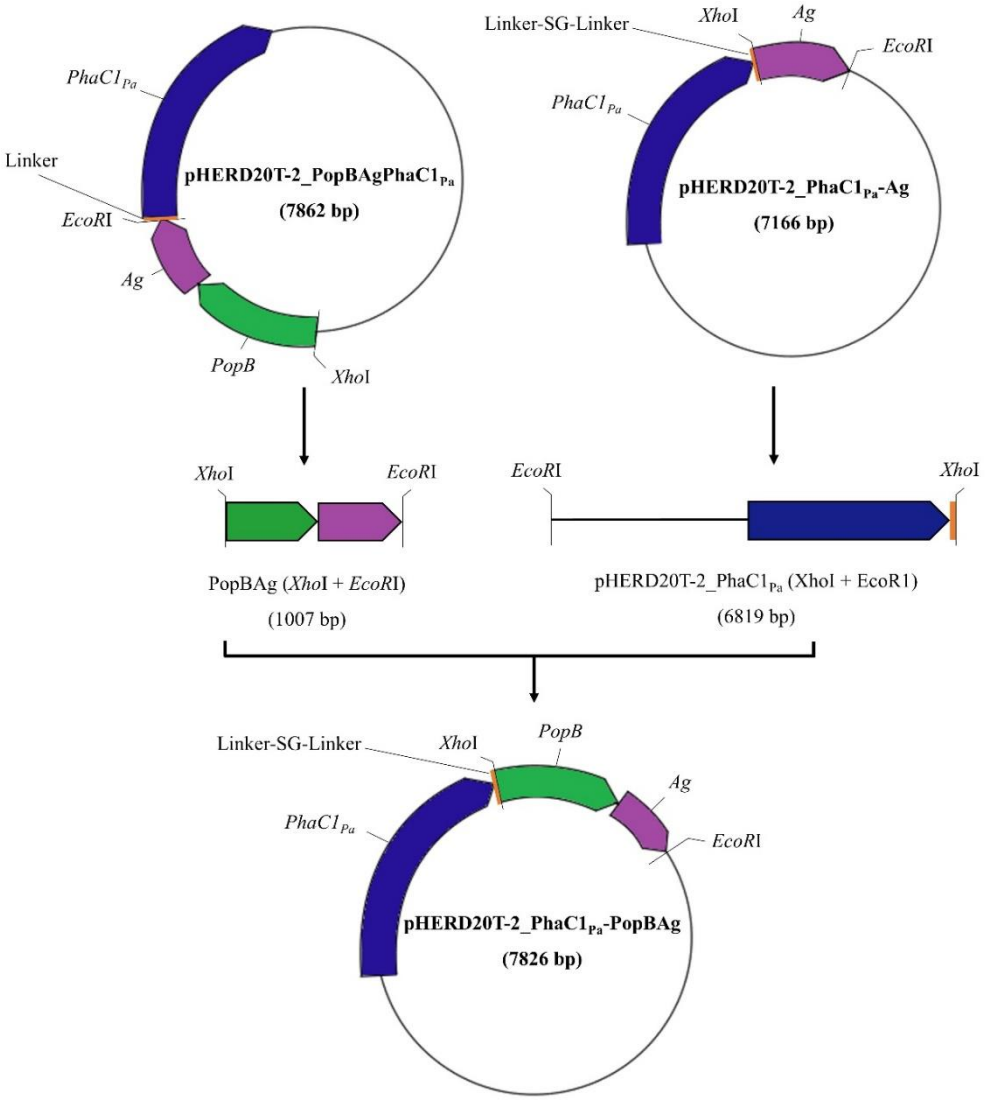

Figure 13. Strategy for the construction of pHERD20T-2_PhaC1$_{Pa}$-PopBAg. The PopBAg fragment was isolated from pHERD20T-2_ PopBAg-PhaC1$_{Pa}$ by PCR amplification (Section 2.7.3) using primers XhoI-2 and EcoRI-2, followed by separation of DNA fragments using agarose gel electrophoresis (Section 2.7.4) and gel purification (Section 2.7.5). Subsequently, the recovered PopBAg fragment was digested by *Xho*I and *EcoR*I restriction enzymes (Section 2.7.2) and purified from the digestion mixture (Section 2.7.1.2). The PopBAg fragment was ligated using T4 DNA ligase (Section 2.7.6) into the linearized vector pHERD20T-2_PhaC1$_{Pa}$ which was generated by restriction enzyme digest with *Xho*I and *EcoR*I, generating the final plasmid pHERD20T-2_PhaC1$_{Pa}$-PopBAg.

3.1.3 Gene expression and PHA_{MCL} bead production

The pHERD20T (Qiu et al., 2008), an arabinose inducible system was chosen as an *Escherichia-Pseudomonas* shuttle vector for the expression of genes required for the production of PHA_{MCL} beads displaying antigens in *P. aeruginosa*. It has the advantage of readily transferring from *E. coli* into *Pseudomonas* species by electroporation. Alteration of the pHERD20T was essential for the removal of an alternative start site encoded by *LacZ*. The vector was linearized by restriction enzyme digestion using *Nco*I and *Eco*RI. T4 DNA polymerase blunted the cohesive ends of the resulting linear vector fragment, permitting re-ligation of the vector, resulting in the final pHERD20T-2 vector (Lee et al., 2017). The pHERD20T-2 expression vector contains a multiple cloning site within *Lac*Z α, origin of replication, araC regulator, P_{BAD} promoter, and a carbenicillin resistance gene. The araC regulator and the P_{BAD} promoter cassette controls gene expression, allowing the induction of the cloned gene in the presence of L-arabinose.

P. aeruginosa naturally forms PHA inclusions composing of medium chain length 3-hydroxy fatty acids (MCL) of which polymerization is catalysed by the class II MCL-PHA synthase ($PhaC1_{Pa}$) (Draper et al., 2013; Rehm, 2003). The gene encoding $PhaC1_{Pa}$ and the *Pseudomonas* antigens (PopB and Ag) were incorporated into the pHERD20T-2 expression vector. These recombinant expression vectors were used to transform *P. aeruginosa* PAO1 ΔCΔ8ΔF or PAO1 ΔCΔ8ΔFΔP production strains via electroporation (Section 2.6.2) for *in vivo* PHA_{MCL} bead production. *Pseudomonas* cells harbouring the various plasmids were cultivated under nitrogen limiting conditions to promote PHA bead inclusion formation (Section 2.4.1.1) and produce PHA_{MCL} beads displaying *Pseudomonas* antigens. Subsequently, the beads were isolated (Section 2.8).

Cultures (400 mL) of *P. aeruginosa* strain PAO1 ΔCΔ8ΔF containing pHERD20T-2_PopB-$PhaC1_{Pa}$, pHERD20T-2_PopBAg-$PhaC1_{Pa}$, pBBR1JO-5_$PhaC1_{Pa}$ (control) and pHERD20T-2_Ag-$PhaC1_{Pa}$ (control) were used to test the PHA_{MCL} bead production of the production strains containing the *PopB* gene. The controls were used to assess the reproducibility of PHA_{MCL} bead isolation from the previous study (Lee et al., 2017) that used a different cell disruption method of a French press aided by the addition of lysozyme. As expected, PHA_{MCL} beads were isolated from the controls as

indicated by the brownish white pellet. However, no beads were isolated and only cell debris manifested by the brown colour was produced from the production strains containing pHERD20T-2_PopB-PhaC1$_{Pa}$ and pHERD20T-2_PopBAg-PhaC1$_{Pa}$. Furthermore, protein profiles were assessed and confirmed the display of PhaC1$_{Pa}$ and Ag-PhaC1$_{Pa}$ on the surface of the PHA$_{MCL}$ beads at 62.5 kDa and 77.75 kDa, respectively, as previously shown (Lee et al., 2017). Hence, this showed the reproducibility of the PHA$_{MCL}$ bead isolation from different disruption methods. The current isolation method of omitting lysozyme and using the Microfluidizer (Section 2.8.2.2) for cell disruption is faster and more efficient than using the French press. In the final PHA$_{MCL}$ bead isolation and characterisation, the positive control PAO1 ΔCΔ8ΔF pBBR1JO-5_PhaC1$_{Pa}$ was replaced with PAO1 ΔCΔ8ΔFΔP pHERD20T-2_PhaC1$_{Pa}$ to have a uniform expression vector system and as the production of PhaC1$_{Pa}$ protein from the latter was significantly higher.

PopB may have a negative impact on the amount of beads produced. Therefore, a larger culture of 2 L was used to try and overcome such effects, but still no beads were isolated. The results suggest that PopB fused to the N-terminus of PhaC1$_{Pa}$ may deactivate PHA synthase activity, abrogating PHA$_{MCL}$ bead production. Hence, PopB was fused to the C-terminal of PhaC1$_{Pa}$ resulting in the isolation of PhaC1$_{Pa}$-PopB beads indicated by the brownish white pellet upon harvesting, but still only cell debris was harvested from constructs encoding Ag-PhaC1$_{Pa}$-PopB. Another attempt to combine PopB and Ag for display on the PHA$_{MCL}$ beads was made by constructing pHERD20T-2_PhaC1$_{Pa}$-PopBAg; this resulted in the successful isolation of PhaC1$_{Pa}$-PopBAg beads.

3.1.4 Characterisation of PHA$_{MCL}$ beads displaying *P. aeruginosa* antigens

PHA-accumulating *P. aeruginosa* cells and the isolated PHA beads were stained with Nile-red and visualised by fluorescence microscopy (Section 2.9.1). Fluorescence indicated the presence of intracellular PHA$_{MCL}$ beads in *P. aeruginosa* cells and activity of PHA synthase (Figure 14). As expected, no fluorescence was observed in negative controls PAO1 ΔCΔ8ΔF and PAO1 ΔCΔ8ΔF + pHERD20T-2 because PhaC1$_{Pa}$ was deleted in the production strain; hence the production of PHA$_{MCL}$ beads was disabled. Fluorescence was detected for the rest of the *P. aeruginosa* cells containing the respective plasmids and all of the isolated beads, indicating the action

of PHA synthase to catalyse PHA_{MCL} bead production. Moreover, further verification was done through TEM analysis of the recombinant *P. aeruginosa* cells and the isolated PHA_{MCL} beads (Figure 15). The TEM images showed the formation of PHA_{MCL} beads mediated by the respective fusion proteins inside recombinant *P. aeruginosa* cells. Confirming the fluorescence microscopy data, the negative controls did not produce PHA_{MCL} beads. Accumulation of the intracellular PHA beads was further confirmed and quantified by GC-MS (Section 2.9.2). GC-MS analysis showed the quantification and composition of intracellular PHA_{MCL} and the purity of the bead material (Figure 16). There were low levels of 3-hydroxyalkanoic acids in the negative control PAO1 ΔCΔ8ΔF + pHERD20T-2 contributing to 2.21% (w/w) of cellular dry weight (CDW) and mainly composed of 3-hydroxydecanoate (C10) and 3-hydroxydodecanoate (C12) which may be derived from rhamolipid synthesis. PAO1 ΔCΔ8ΔF cells harbouring the plasmid encoding $PhaC1_{Pa}$ accumulated PHA_{MCL} contributing to 17.88% of CDW while the strain PAO1 ΔCΔ8ΔF containing plasmid encoding Ag-$PhaC1_{Pa}$ and $PhaC1_{Pa}$ –PopB accumulated PHA_{MCL} contributing to 21.39% and 15.24% of CDW, respectively. The $PhaC1_{Pa}$, Ag-$PhaC1_{Pa}$ and $PhaC1_{Pa}$-PopB beads were purified to approximately 46%, 69% and 52%, respectively. The isolated PHA_{MCL} beads were mainly composed of 3-hydroxyoctanoate (C8), 3-hydroxydecanoate (C10) and 3-hydroxydodecanoate (C12) and reflected the PHA_{MCL} composition in whole cells.

The whole-cells of pHERD20T-2_$PhaC1_{Pa}$-PopBAg and $PhaC1_{Pa}$-PopBAg beads were not further characterised due to the very small amounts of PHA_{MCL} beads isolated of approximately 0.2 grams in 15 L of culture. Furthermore, there was very low production of fusion protein that was only detected in immunoblot analysis and not in SDS-PAGE (Appendix I).

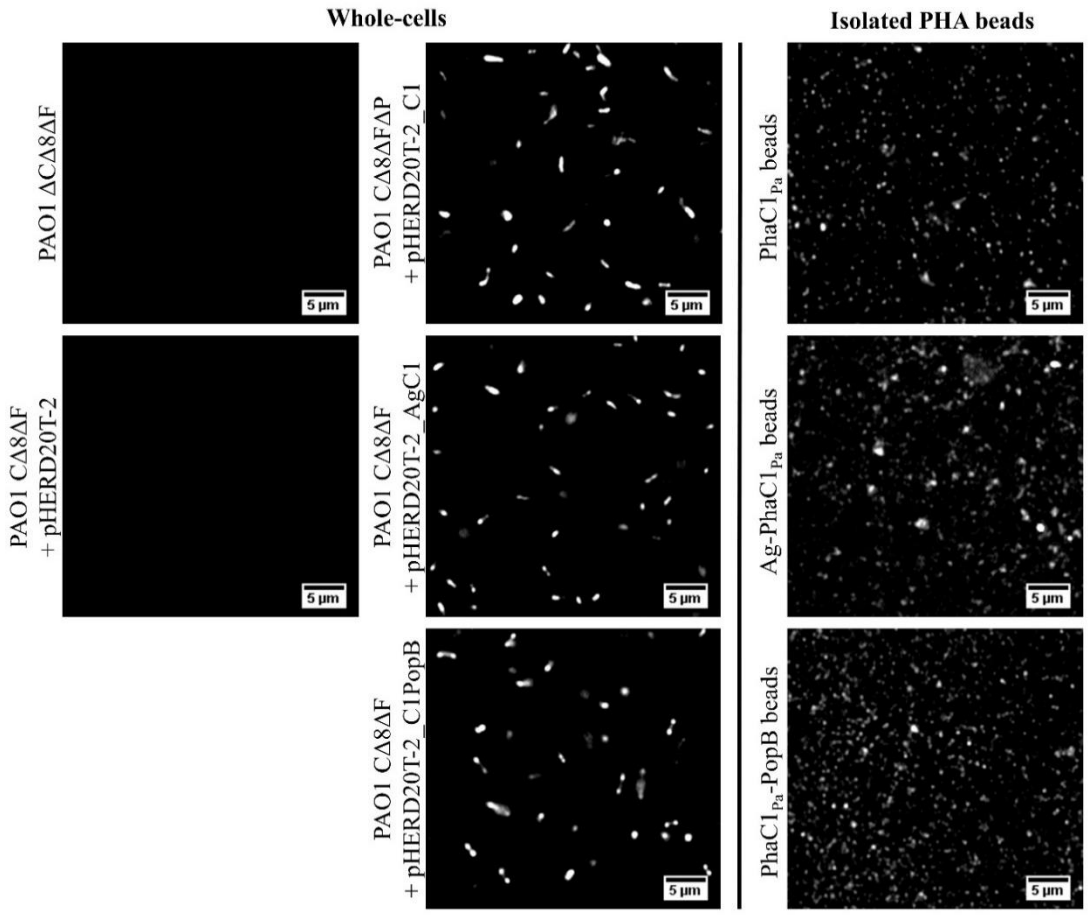

Figure 14. Fluorescence microscopy images of whole-cells and PHA$_{MCL}$ beads produced in recombinant *P. aeruginosa* PAO1 ΔCΔ8ΔF or PAO1 ΔCΔ8ΔFΔP harbouring various fusion protein-encoding pHERD20T-2 expression vectors stained with Nile-red. Fluorescence was detected in whole cells with pHERD20T-2_C1, pHERD20T-2_AgC1 and pHERD20T-2_C1PopB encoding PhaC1$_{Pa}$, and fusion proteins Ag-PhaC1$_{Pa}$ and PhaC1$_{Pa}$-PopB, respectively. Also, fluorescence was detected in all corresponding PHA$_{MCL}$ bead samples. No fluorescence was detected in the negative controls PAO1 ΔCΔ8ΔF and PAO1 ΔCΔ8ΔF pHERD20T-2. PhaC1$_{Pa}$ is designated as C1.

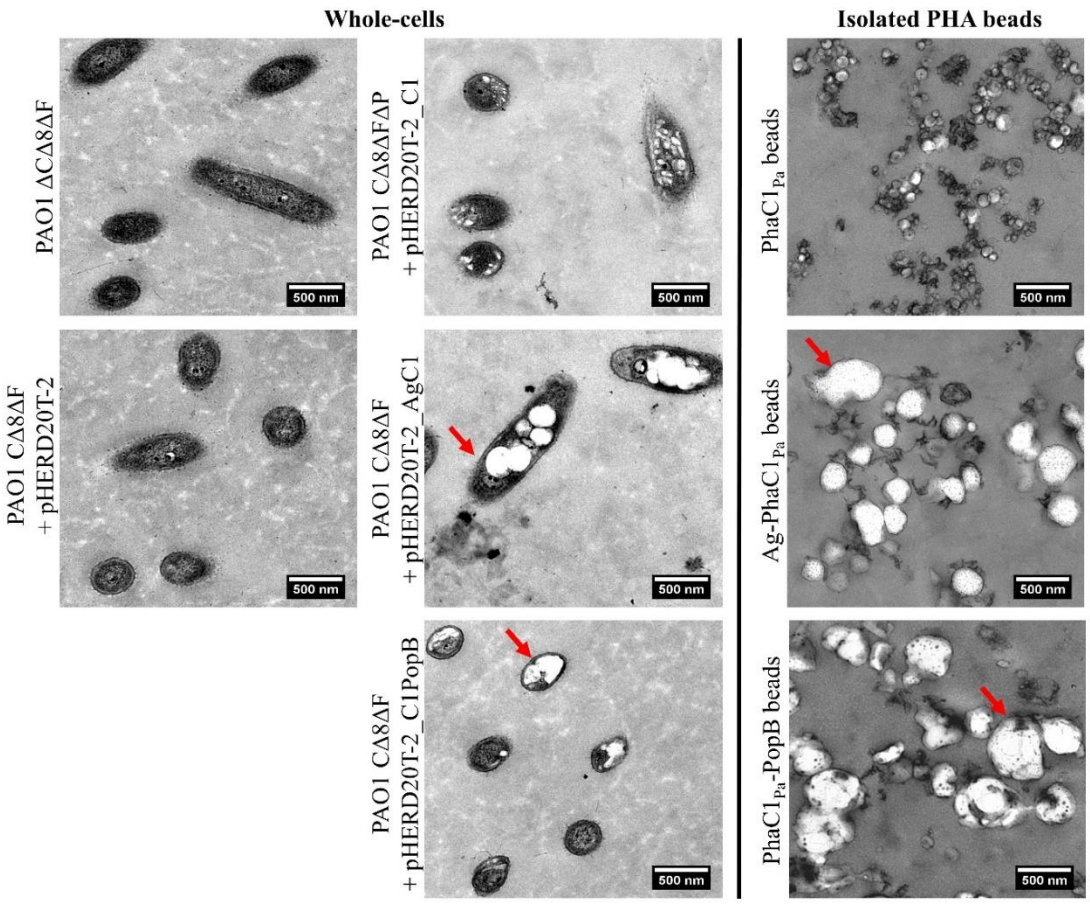

Figure 15. TEM analysis of recombinant *P. aeruginosa* harbouring various plasmids and the isolated PHA_{MCL} beads displaying *P. aeruginosa* antigens. Absence of PHA_{MCL} accumulation in the negative controls PAO1 ΔCΔ8ΔF and PAO1 ΔCΔ8ΔF + pHERD20T-2 confirmed the fluorescence microscopy data. Larger beads were observed in cells with plasmids pHERD20T-2_AgC1 and pHERD20T-2_C1PopB encoding fusion proteins Ag-$PhaC1_{Pa}$ and $PhaC1_{Pa}$-PopB, respectively, as well as their corresponding isolated PHA_{MCL} beads (indicated by red arrows) compared to pHERD20T-2_C1 and $PhaC1_{Pa}$ beads. $PhaC1_{Pa}$ is designated as C1.

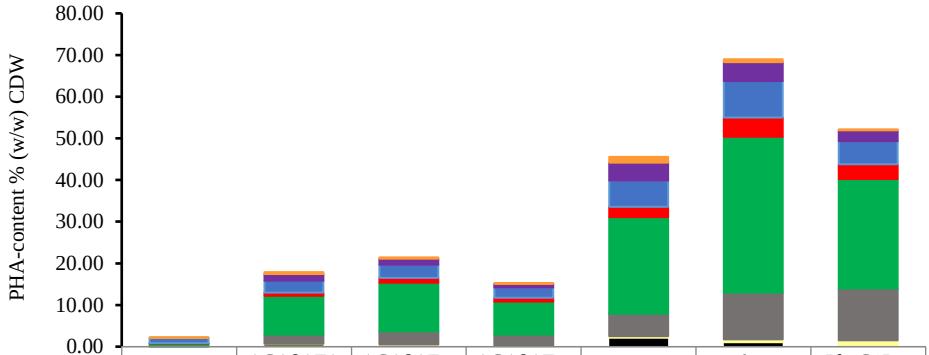

	ΔCΔ8ΔF + 20T-2	ΔCΔ8ΔFΔP + 20T-2_C1	ΔCΔ8ΔF + 20T-2_Ag-C1	ΔCΔ8ΔF + 20T-2_C1-PopB	PhaC1Pa beads	Ag-PhaC1Pa beads	PhaC1Pa-PopB beads
3-HHD (C16)	0.07	0.48	0.26	0.12	1.39	0.69	0.28
3-HTD (C14)	0.00	1.57	1.44	0.89	4.29	4.51	2.61
3-HDD (C12)	1.28	2.86	3.15	2.51	6.32	8.75	5.55
3-HDD isomer (C12)	0.08	0.75	1.22	0.87	2.42	4.63	3.47
3-HD (C10)	0.79	9.33	11.63	7.96	23.21	37.41	26.29
3-HO (C8)	0.00	2.21	3.20	2.61	5.41	11.21	12.45
3-HH (C6)	0.00	0.13	0.18	0.18	0.32	0.68	1.17
3-HB (C4)	0.00	0.56	0.31	0.10	2.17	1.08	0.36

Figure 16. GC-MS analysis of recombinant *P. aeruginosa* harbouring various plasmids and the isolated PHA_{MCL} beads displaying *P. aeruginosa* antigens. In negative control PAO1 ΔCΔ8ΔF + 20T-2, low levels of 3-hydroxyalkanoic acids were detected, mainly composed of 3-HD (C10) and 3-HDD (C12), contributing to about 2.21% (w/w) of cellular dry weight (CDW). PAO1 ΔCΔ8ΔF harboring the plasmid encoding $PhaC1_{Pa}$ accumulated PHA_{MCL}, contributing to 17.88% (w/w) of CDW, while strain PAO1 ΔCΔ8ΔF harboring the plasmid encoding Ag-$PhaC1_{Pa}$ or $PhaC1_{Pa}$-PopB accumulated PHA_{MCL}, contributing to 21.39% and 15.24% (w/w) of CDW, respectively. The composition of the PHA_{MCL} between the different beads showed only slight variation. The beads were composed mainly of 3-HO (C8), 3-HD (C10), 3-HDD (C12) and 3-HTD (C14) and the composition of PHA_{MCL} is reflected in the whole cells. The PHA_{MCL} purity of the isolated $PhaC1_{Pa}$, Ag-$PhaC1_{Pa}$, $PhaC1_{Pa}$-PopB beads are 46%, 69% and 52%, respectively. $PhaC1_{Pa}$ and pHERD20T-2 are designated as C1 and 20T-2, respectively. The 3-hydroxybutanoate is designated as 3-HB (C4); 3-hydroxyhexanoate as 3-HH (C6); 3-hydroxyoctanoate as 3-HO (C8); 3-hydroxynonanoate as 3-HN (C9); 3-hydroxydecanoate as 3-HD (C10); 3-hydroxydodecanoate isomer as 3-HDD isomer (C12); 3-hydroxydodecanoate as 3-HDD (C12); 3-hydroxytetradecanoate as 3-HTD (C14); and 3-hydroxyhexadecanote as 3-HHD (C16).

3.1.5 Display of recombinant PhaC1$_{Pa}$-antigen fusion protein on the surface of PHA$_{MCL}$ beads

The presence of the recombinant fusion proteins on the surface of the PHA$_{MCL}$ beads was confirmed using SDS-PAGE (Section 2.10.1). In addition, protein profiles of the recombinant fusion proteins were analysed using SDS-PAGE (Figure 17). The theoretical molecular weight of recombinant proteins in this study were calculated utilizing the ProtParam tool from the ExPASy Proteomics Server (http://www.expasy.org/). Dominant protein bands were observed corresponding to proteins with theoretical molecular weights of 62.5 kDa for PhaC1$_{Pa}$; 75.8 kDa for Ag-PhaC1$_{Pa}$; and 84.7 kDa for PhaC1$_{Pa}$-PopB. These were identified and confirmed by mass spectrometry (Section 2.10.4; Appendix II). Moreover, densitometry analysis (Section 2.10.2) of the SDS-PAGE showed that PhaC1$_{Pa}$ accounted for 68.1% of the total protein in the PhaC1$_{Pa}$ bead fraction; and Ag-PhaC1$_{Pa}$ and PhaC1$_{Pa}$-PopB accounted for 40.6% and 9.1% of the total protein in their corresponding bead fractions.

Several additional co-purifying host cell proteins (HCPs) were identified within the PHA$_{MCL}$ beads, and the major distinct bands were labelled I-XII (Figure 17) and selected for identification using mass spectrometry (MS). The MS data was filtered according to peptide (PeptideProphet ≥ 0.995) and protein (UniquePeptide ≥ 6) to help reveal the identity of the HCPs. Subsequently, the data was filtered based on the approximate molecular weight of the selected bands. In general, the potential identities of protein(s) represented by each band were ranked according to the number of unique hits revealed during MS and shown in Table 18 in descending order (the highest number of matching peptide hits has the highest rank). The findings show that PHA synthase, OMPs (OprF), ribosomal proteins, and heat-shock proteins are likely to be common contaminating HCPs.

The protein profile of the PhaC1$_{Pa}$-PopBAg beads was analysed using SDS-PAGE and there was no dominant band at the theoretical weight 100 kDa (Appendix I). Hence, immunoblot analysis using PhaC1_529 antibody (Section 2.10.3) was carried out and there was detection of the band at 100 kDa. The presence of the band only in immunoblot analysis indicates a very low production of the PhaC1$_{Pa}$-PopBAg fusion protein. Hence, the low production of PhaC1$_{Pa}$-PopBAg beads (Section 3.1.4) and the

low levels of fusion protein suggest that PhaC1$_{Pa}$-PopBAg bead is unsuitable for mass production preparation for animal testing. Therefore, an alternative strategy of using a different production strain was explored in order to achieve the combination of PopB and Ag. Furthermore, the PAO1 ΔCΔ8ΔF pBBR1JO-5_PhaC1$_{Pa}$ was replaced with PAO1 ΔCΔ8ΔFΔ*Psl* pHERD20T-2_PhaC1$_{Pa}$ as positive control to have a uniform expression vector system and the production of PhaC1$_{Pa}$ protein from the latter was significantly higher. Mass production of the PHA$_{MCL}$ beads for isolation used 4-8 L of cultures.

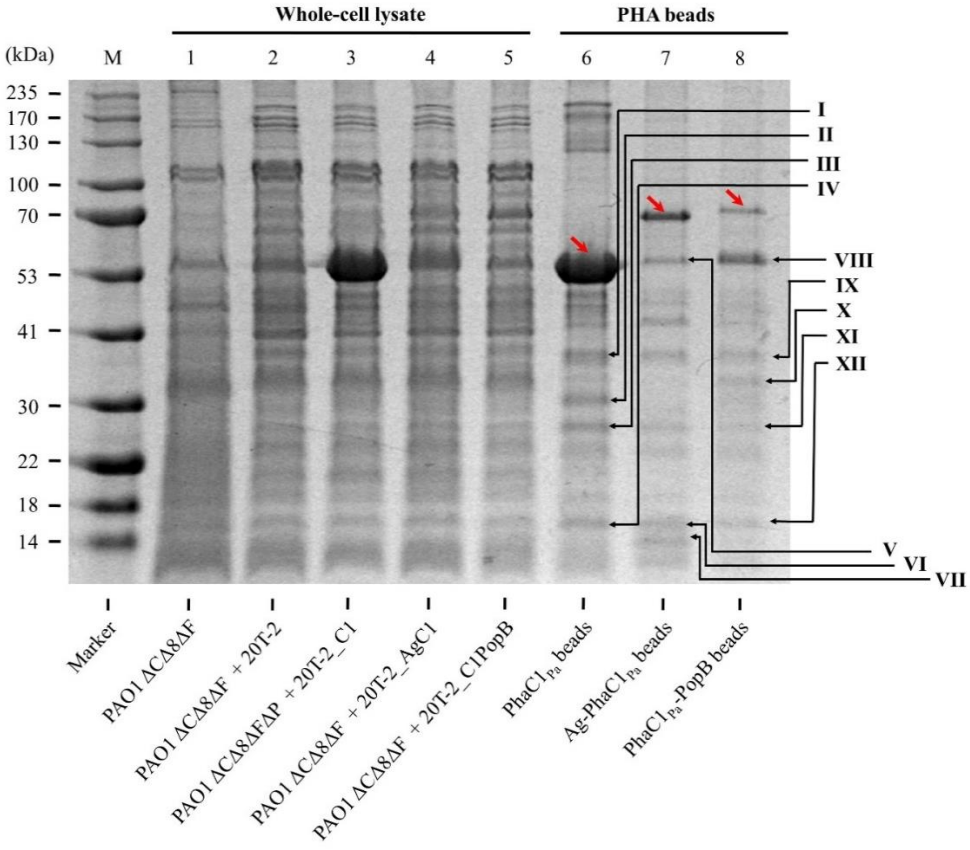

Figure 17. Protein profile analysis of whole-cell lysate and the PHA$_{MCL}$ beads separated by SDS-PAGE and gel stained with Coomassie Blue. PhaC1$_{Pa}$ (62.5 kDa), Ag-PhaC1$_{Pa}$ (75.8 kDa), and PhaC1$_{Pa}$-PopB (84.7 kDa) fusion proteins (indicated by red arrows) and co-purifying proteins (black arrows) were isolated from *P. aeruginosa* PAO1 ΔCΔ8ΔF strain (PAO1 ΔCΔ8ΔFΔP for the PhaC1$_{Pa}$ beads) containing the respective plasmids. The twelve HCP bands of interest, indicated in roman numerals (I-XII) were selected if they were distinct and dominant. These HCPs were isolated for protein identification by MS (Table 18). The presence of PhaC1$_{Pa}$ and PhaC1$_{Pa}$-antigen fusion proteins were confirmed by mass spectrometry (Appendix II). PhaC1$_{Pa}$ is designated as C1.

Table 18. Identification of the PHA$_{MCL}$ bead associated host cell proteins (HCPs) by MS.

Band[a]	Rank[b]	Database hits
I	1	RecName: Full=Outer membrane porin F; Flags: Precursor
	2	RecName: Full=Outer membrane protein assembly factor BamD; Flags: Precursor
	3	2-alkenal reductase [*Pseudomonas aeruginosa*]
	4	hypothetical protein [*Pseudomonas aeruginosa*]
	5	efflux RND transporter periplasmic adaptor subunit [*Pseudomonas aeruginosa*]
	6	RecName: Full=UDP-N-acetylglucosamine--N-acetylmuramyl-(pentapeptide) pyrophosphoryl-undecaprenol N-acetylglucosamine transferase; AltName: Full=Undecaprenyl-PP-MurNAc-pentapeptide-UDPGlcNAc GlcN...
II	1	alpha/beta hydrolase *[Pseudomonas aeruginosa*]
	2	MULTISPECIES: type VI secretion-associated lipoprotein TagQ [*Pseudomonas*]
	3	RecName: Full=ATP synthase gamma chain; AltName: Full=ATP synthase F1 sector gamma subunit; AltName: Full=F-ATPase gamma subunit
	4	ABC transporter permease, partial [*Pseudomonas aeruginosa*]
	5	universal stress protein, partial [*Pseudomonas aeruginosa*]
	6	acyl dehydratase [*Pseudomonas aeruginosa*]
	7	hypothetical protein [*Pseudomonas aeruginosa*]
III	1	peptidylprolyl isomerase [*Pseudomonas aeruginosa*]
	2	RecName: Full=30S ribosomal protein S2
	3	ParA family protein [*Pseudomonas aeruginosa*]
	5	RecName: Full=50S ribosomal protein L1
IV	1	RecName: Full=Peptidoglycan-associated lipoprotein; Flags: Precursor
	2	nuclear transport factor 2 family protein [*Pseudomonas aeruginosa*]
	3	RecName: Full=Phosphopantetheine adenylyltransferase; AltName: Full=Dephospho-CoA pyrophosphorylase; AltName: Full=Pantetheine-phosphate adenylyltransferase; Short=PPAT
	4	3-hydroxyacyl-[acyl-carrier-protein] dehydratase FabZ [*Pseudomonas aeruginosa*]
V	1	class II poly(R)-hydroxyalkanoic acid synthase [*Pseudomonas aeruginosa*]
	2	molecular chaperone GroEL [*Pseudomonas aeruginosa*]
	3	MULTISPECIES: ShlB/FhaC/HecB family hemolysin secretion/activation protein [*Pseudomonas*]
	4	MULTISPECIES: hypothetical protein [*Pseudomonas*]
	5	methyl-accepting chemotaxis protein [*Pseudomonas aeruginosa*]
	6	methyl-accepting chemotaxis protein [*Pseudomonas aeruginosa*]

	7	RecName: Full=Glutamine synthetase; Short=GS; AltName: Full=Glutamate--ammonia ligase; AltName: Full=Glutamine synthetase I beta; Short=GSI beta
	8	MULTISPECIES: ATP-dependent RNA helicase RhlB [*Pseudomonas*]
VI	1	RecName: Full=Peptidoglycan-associated lipoprotein; Flags: Precursor
	2	RecName: Full=30S ribosomal protein S7
	3	3-hydroxyacyl-[acyl-carrier-protein] dehydratase FabZ [*Pseudomonas aeruginosa*]
VII	1	heat-shock protein IbpA [*Pseudomonas aeruginosa* PAO1]
	2	hypothetical protein PA5178 [*Pseudomonas aeruginosa* PAO1]
VIII	1	class II poly(R)-hydroxyalkanoic acid synthase [*Pseudomonas aeruginosa*]
	2	hypothetical protein PA2540 [*Pseudomonas aeruginosa* PAO1]
	3	hypothetical protein [*Pseudomonas aeruginosa*]
	4	ShlB/FhaC/HecB family hemolysin secretion/activation protein [*Pseudomonas aeruginosa*]
IX	1	RecName: Full=Outer membrane porin F; Flags: Precursor
	2	RecName: Full=Outer membrane protein assembly factor BamD; Flags: Precursor
	3	MULTISPECIES: glycoside hydrolase family 43 [*Pseudomonas*]
	4	AraC family transcriptional regulator [*Pseudomonas aeruginosa*]
	5	serine/threonine protein kinase [*Pseudomonas aeruginosa*]
	6	alpha/beta hydrolase [*Pseudomonas aeruginosa*]
	7	RecName: Full=Dihydroorotate dehydrogenase (quinone); AltName: Full=DHOdehase; Short=DHOD; Short=DHODase; AltName: Full=Dihydroorotate oxidase
	8	RecName: Full=UDP-N-acetylglucosamine--N-acetylmuramyl-(pentapeptide) pyrophosphoryl-undecaprenol N-acetylglucosamine transferase; AltName: Full=Undecaprenyl-PP-MurNAc-pentapeptide-UDPGlcNAc GlcN...
X	1	rhamnosyltransferase [*Pseudomonas aeruginosa* PAO1]
	2	cell division protein ZipA [*Pseudomonas aeruginosa*]
	3	imelysin [*Pseudomonas aeruginosa*]
	4	RNA-directed DNA polymerase [*Pseudomonas aeruginosa*]
	5	alpha/beta hydrolase [*Pseudomonas aeruginosa*]
	6	AraC family transcriptional regulator [*Pseudomonas aeruginosa*]
	7	biofilm formation protein PslC [*Pseudomonas aeruginosa* PAO1]
XI	1	RecName: Full=30S ribosomal protein S2
	2	MULTISPECIES: serine acetyltransferase [*Pseudomonas*]
	3	RecName: Full=50S ribosomal protein L1
XII	1	RecName: Full=Peptidoglycan-associated lipoprotein; Flags: Precursor

2	RecName: Full=Phosphopantetheine adenylyltransferase; AltName: Full=Dephospho-CoA pyrophosphorylase; AltName: Full=Pantetheine-phosphate adenylyltransferase; Short=PPAT
3	RecName: Full=30S ribosomal protein S7

[a] Protein bands identified on SDS-PAGE.

[b] Peptide filter (PeptideProphet ≥ 0.995), protein filter (UniquePepties ≥ 6) and filtered by approximate molecular weight. The rank is based on the number of 'unique peptides'; the higher the number of 'unique peptides', the higher is the ranking.

3.2 Development of antigen-displaying PHA_{SCL} beads produced in *E. coli* strain ClearColi™

The advantage of producing PHA beads in *E. coli* compared with *P. aeruginosa* is the faster and more efficient process. Most importantly, the fusion protein is dominant and the impurities are removed making it easier to assess the protein of interest. Moreover, production of PHA beads in *E. coli* strain ClearColi™ has an advantage of the absence of LPS production, thereby producing endotoxin-free PHA beads. The *E. coli* ClearColi™ production strain was used due to the lack of successful production of PHA_{MCL} beads displaying sufficient amount of PopBAg in *P. aeruginosa* production strain (Section 3.1).

It was necessary to develop corresponding plasmids to those used for the *P. aeruginosa* production strain, to compare the protein production levels in *E. coli* strain ClearColi™, and to create the PopB and Ag single fusion. To do this, genes optimized for codon usage to *E. coli* were used to generate four plasmids: (1) pET-14b_PhaC; (2) pET-14b_Ag-PhaC; (3) pET-14b_PhaC-PopB; and (4) pET-14b_PhaC-PopBAg (Table 5). The first plasmid which is the wild-type PhaC was constructed previously (Peters & Rehm, 2005) while the author constructed the remaining 3 plasmids described in Section 3.2.1.

The hypotheses for this part of the study were: (1) the *E. coli* ClearColi™ production strain containing the respective plasmids produce PHA_{SCL} beads displaying Ag, PopB, and fusion of PopB and Ag on the surface of the PHA_{SCL} beads, and (2) the PHA_{SCL} beads produced in (1) have less impurities (without the HCPs) compared to the PHA_{MCL} beads from *P. aeruginosa* production strain. To test the hypotheses, plasmids were constructed and used to transform XL1-Blue *E. coli* and for bead production

plasmids were used to transform *E. coli* strain ClearColi^{TM}. The production of PHA_{SCL} beads were assessed and characterized via Nile-red staining and fluorescence microscopy (Section 2.9.1), TEM (Section 2.9.3), and GC-MS (Section 2.9.2). The fusion proteins were analysed and confirmed using SDS-PAGE (Section 2.10.1) and MS (Section 2.10.4).

3.2.1 Construction of pET-14b_Ag-PhaC, pET-14b_PhaC-PopB and pET-14b_PhaC-PopBAg

Construction of the corresponding plasmids to the *P. aeruginosa* PHA_{MCL} bead study (Section 3.1) used a pET-14b expression vector. For the N-terminal fusion of Ag to PhaC, a plasmid construct corresponding to pHERD20T-2_Ag-$PhaC1_{Pa}$ was made. The strategy of the construction of pET-14b_Ag-PhaC is presented in Figure 18. The *Ag* gene codon optimised for *E. coli* was amplified by PCR (Section 2.7.3) from pET-16b_His_{10}-Ag (Table 6) using primers NdeI_fwdAg and SpeI_revAg. The Ag fragment was recovered by AGE (Section 2.7.4) and gel purified (Section 2.7.5). Subsequently, Ag fragment was hydrolysed using *Nde*I and *Spe*I REs (Section 2.7.2), and separated from the digestion mixture (Section 2.7.1.2). In parallel, the plasmid pET-14b_ObodyB7-PhaC was digested (Section 2.7.2) with *Nde*I and *Spe*I REs, resulting in linearized vector pET-14b_PhaC which was isolated by AGE (Section 2.7.4) and subjected to gel purification (Section 2.7.5). Subsequently, the Ag fragment was ligated (Section 2.7.6) to the linearized vector fragment, generating the final plasmid, pET-14b_Ag-PhaC. The plasmid was used to transform (Section 2.6.1.2) *E. coli* XL1-Blue (Table 3) and spread-plated onto LB-agar media containing ampicillin (Section 2.3). Single colonies were selected and the successful transformants were verified via plasmid DNA hydrolysis (Section 2.7.2) using *Nde*I and *Spe*I REs. Final confirmation of the plasmid was done by DNA sequencing (Section 2.7.7) using primers 5' pET-14b and N-PhaC_rev.

The strategy for the construction of pET-14b_PhaC-PopB, the plasmid corresponding to pHERD20T-2_$PhaC1_{Pa}$-PopB, is presented in Figure 19. The *PopB* gene from pET-16b_His_{10}-PopBAg was amplified by PCR (Section 2.7.3) using Xho1_fwdPopBAg and BamHI_revPopB primers, followed by isolation by AGE (Section 2.7.4), and gel purification (Section 2.7.5). The PopB fragment was hydrolysed using *Xho*I and *BamH*I REs (Section 2.7.2), and separated from the digestion mixture (Section

2.7.1.2). In parallel, pET-14b_PhaC-RV1626 vector was hydrolysed using *Xho*I and *BamH*I REs (Section 2.7.2), separated from the digestion mixture using AGE with SYBR safe stain (Section 2.7.4), recovered and purified by gel purification (Section 2.7.5). The PopB fragment was ligated to the linearized vector, generating the final plasmid, pET-14b_PhaC-PopB. The plasmid was used to transform (Section 2.6.1.2) *E. coli* XL1-Blue (Table 3) and spread-plated onto LB-agar media containing ampicillin (Section 2.3). Single colonies were selected and the successful transformants were verified using plasmid DNA hydrolysis *Xho*I and *BamH*I REs (Section 2.7.2), and DNA sequencing (Section 2.7.7) using C-PhaC_fwd and T7_terminator primers.

The strategy of the construction of pET-14b_PhaC-PopBAg is presented in Figure 20. The *PopBAg* gene was amplified by PCR (Section 2.7.3) from pET-16b_His_{10}-PopBAg (Table 6) using primers Xho1_fwdPopBAg and BamHI_revPopBAg. The PopBAg fragment was recovered by AGE (Section 2.7.4) and gel purified (Section 2.7.5). Subsequently, PopBAg fragment was hydrolysed using *Xho*I and *BamH*I REs (Section 2.7.2), and separated from the digestion mixture (Section 2.7.1.2). In parallel, the vector pET-14b_PhaC-RV1626 was digested (Section 2.7.2) with *Xho*I and *BamH*I REs, resulting in a linearized vector pET-14b_PhaC which was isolated via AGE (Section 2.7.4) and gel purified (Section 2.7.5). Subsequently, the PopBAg fragment was ligated (Section 2.7.6) to linearized vector fragment, generating the final plasmid, pET-14b_PhaC-PopBAg. The plasmid was used to transform (Section 2.6.1.2) *E. coli* XL1-Blue (Table 3) and spread-plated onto LB-agar media containing ampicillin (Section 2.3). Single colonies were selected and the successful transformants were verified via plasmid DNA hydrolysis (Section 2.7.2) using *Xho*I and *BamH*I, and DNA sequencing (Section 2.7.7) using primers T7_terminator and T7_terminator.

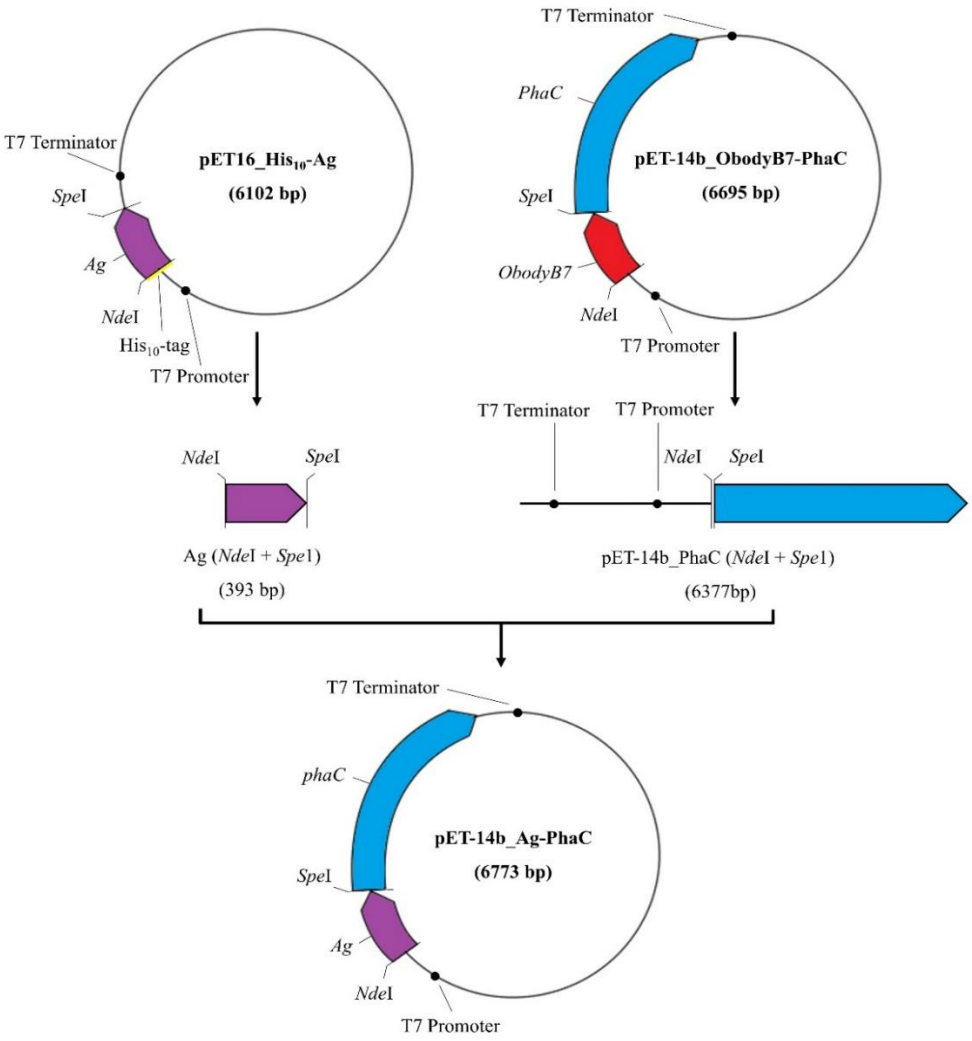

Figure 18. Strategy for the construction of pET-14b_Ag-PhaC for PHA$_{SCL}$ bead production in *E. coli* strain ClearColi^{TM}. The DNA fragment encoding *Ag* genes was isolated from pET-16b_His$_{10}$-Ag by PCR amplification using primers NdeI_fwdAg and SpeI_revAg (Section 2.7.3), followed by separation of DNA fragments using agarose gel electrophoresis (Section 2.7.4) and gel purification (Section 2.7.5). Subsequently, the recovered Ag fragment was digested by *Nde*I and *Spe*I restriction enzymes (Section 2.7.2) and purified from the digestion mixture (Section 2.7.1.2). The Ag fragment was ligated using T4 DNA ligase (Section 2.7.6) into the linearized vector pET-14b_PhaC which was generated by restriction enzyme digest with *Nde*I and *Spe*I, generating the final plasmid pET-14b_Ag-PhaC.

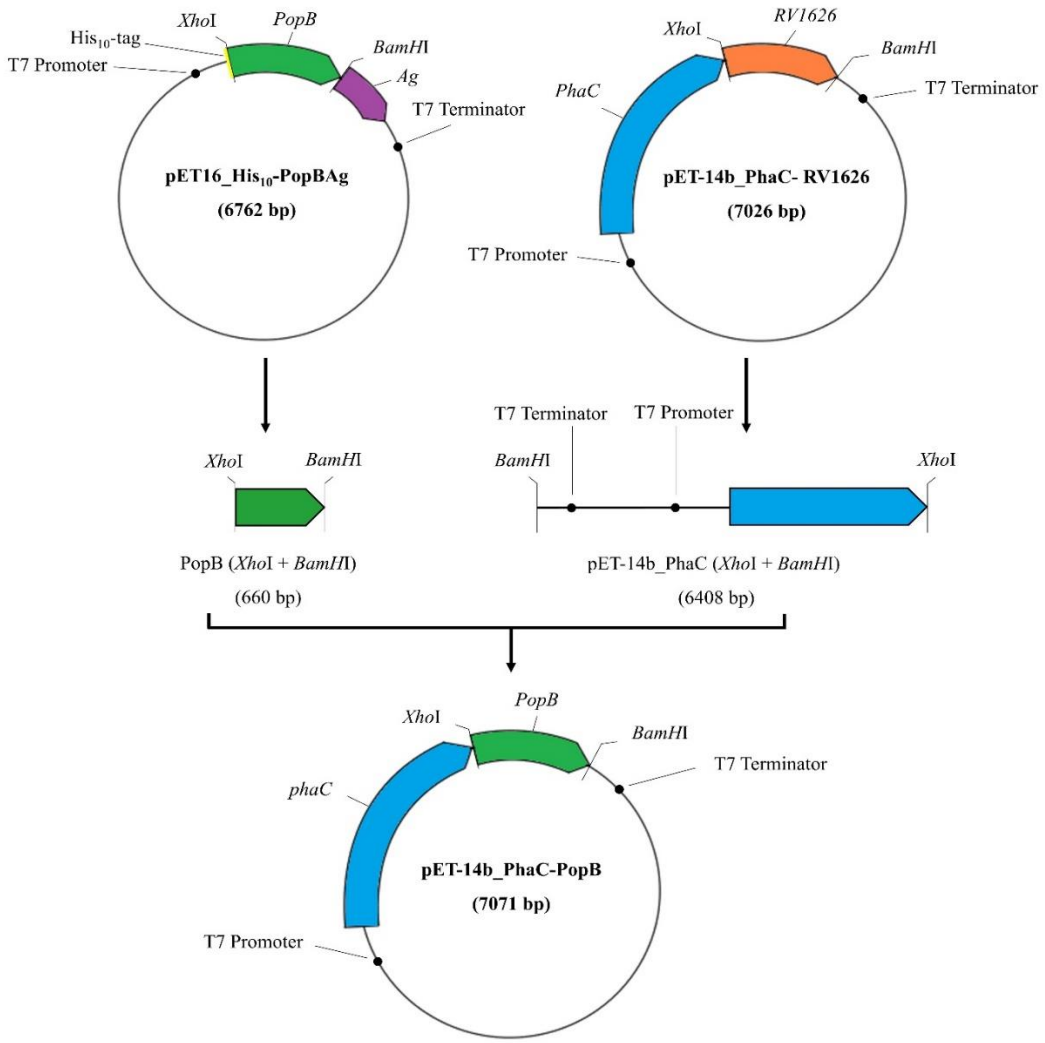

Figure 19. Strategy for the construction of pET-14b_PhaC-PopB for PHA$_{SCL}$ bead production in *E. coli* strain ClearColi^{TM}. The DNA fragment encoding *PopB* gene was isolated from pET-16b_His$_{10}$-PopBAg by PCR amplification using primers Xho1_fwdPopBAg and BamHI_revPopB (Section 2.7.3), followed by separation of DNA fragments using agarose gel electrophoresis (Section 2.7.4) and gel purification (Section 2.7.5). Subsequently, the recovered PopB fragment was digested by *Xho*I and *BamH*I restriction enzymes (Section 2.7.2) and purified from the digestion mixture (Section 2.7.1.2). The PopB fragment was ligated using T4 DNA ligase (Section 2.7.6) into the linearized vector pET-14b_PhaC which was generated by restriction enzyme digest with *Xho*I and *BamH*I, generating the final plasmid pET-14b_PhaC-PopB.

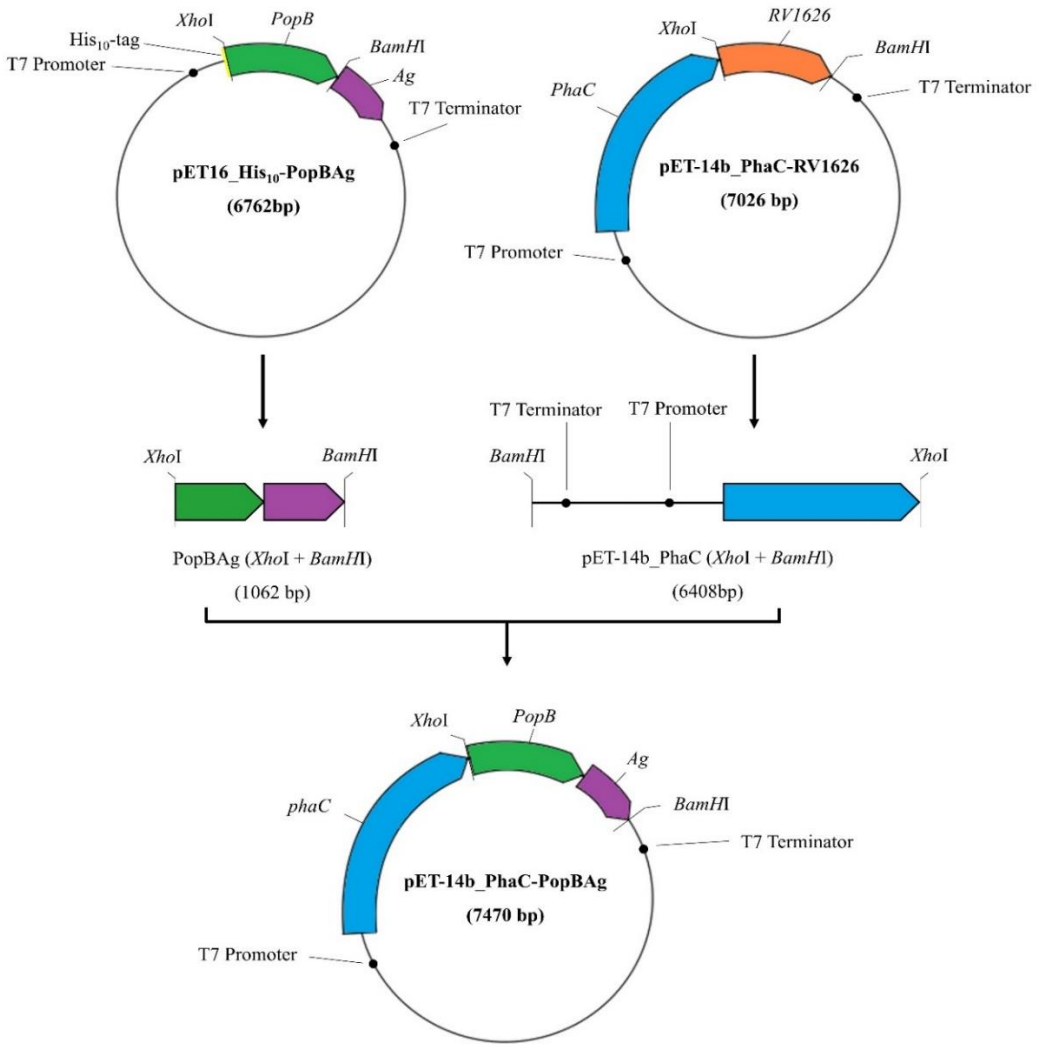

Figure 20. Strategy for the construction of pET-14b_PhaC-PopBAg for PHA$_{SCL}$ bead production in *E. coli* strain ClearColi^{TM}. The DNA fragment encoding *PopBAg* genes was isolated from pET-16b_His$_{10}$-PopBAg by PCR amplification using primers Xho1_fwdPopBAg and BamHI_revPopBAg (Section 2.7.3), followed by separation of DNA fragments using agarose gel electrophoresis (Section 2.7.4) and gel purification (Section 2.7.5). Subsequently, the recovered PopBAg fragment was digested by *Xho*I and *BamH*I restriction enzymes (Section 2.7.2) and purified from the digestion mixture (Section 2.7.1.2). The PopBAg fragment was ligated using T4 DNA ligase (Section 2.7.6) into the linearized vector pET-14b_PhaC which was generated by restriction enzyme digest with *Xho*I and *BamH*I, generating the final plasmid pET-14b_PhaC-PopBAg.

3.2.2 Construction pET-16b_His$_{10}$-PopBAg for the production of soluble protein

The pET-16b_His$_{10}$-PopBAg was needed for the isolation of the soluble PopBAg and would serve as a positive control in animal testing (Section 3.3). The pUC57 plasmid containing NPopBN antigen fragment which was codon optimised for *E. coli* was obtained from Genescript Corporation (USA). The plasmid was hydrolysed (Section 2.7.2) with *Nco*I and *Nde*I REs (Figure 21). Separately, pET-16b_His$_{10}$-Ag (Table 6) was hydrolysed with the same REs, *Nco*I and *Nde*I resulting in linearized vector backbone fragment. The DNA fragments (PopB and linearized vector pET-16b_His$_{10}$-Ag) were separated from the digestion mixture using AGE with SYBR safe stain (Section 2.7.4) and recovered and purified by gel purification (Section 2.7.5). Subsequently, the PopB fragment and the vector fragment were ligated (Section 2.7.6), generating the final plasmid pET-16b_His$_{10}$-PopBAg. The plasmid was used to transform (Section 2.6.1.2) *E. coli* XL1-Blue (Table 3) and spread-plated onto LB agar medium containing ampicillin (Section 2.3). Single colonies were selected and confirmed for the presence of the insert using plasmid isolation (Section 2.7.1) and, *Nco*I and *Nde*I RE digest (Section 2.7.2). Lastly, final confirmation by DNA sequencing (Section 2.7.7) using primers HisAg_fwd and HisAg_rev was performed.

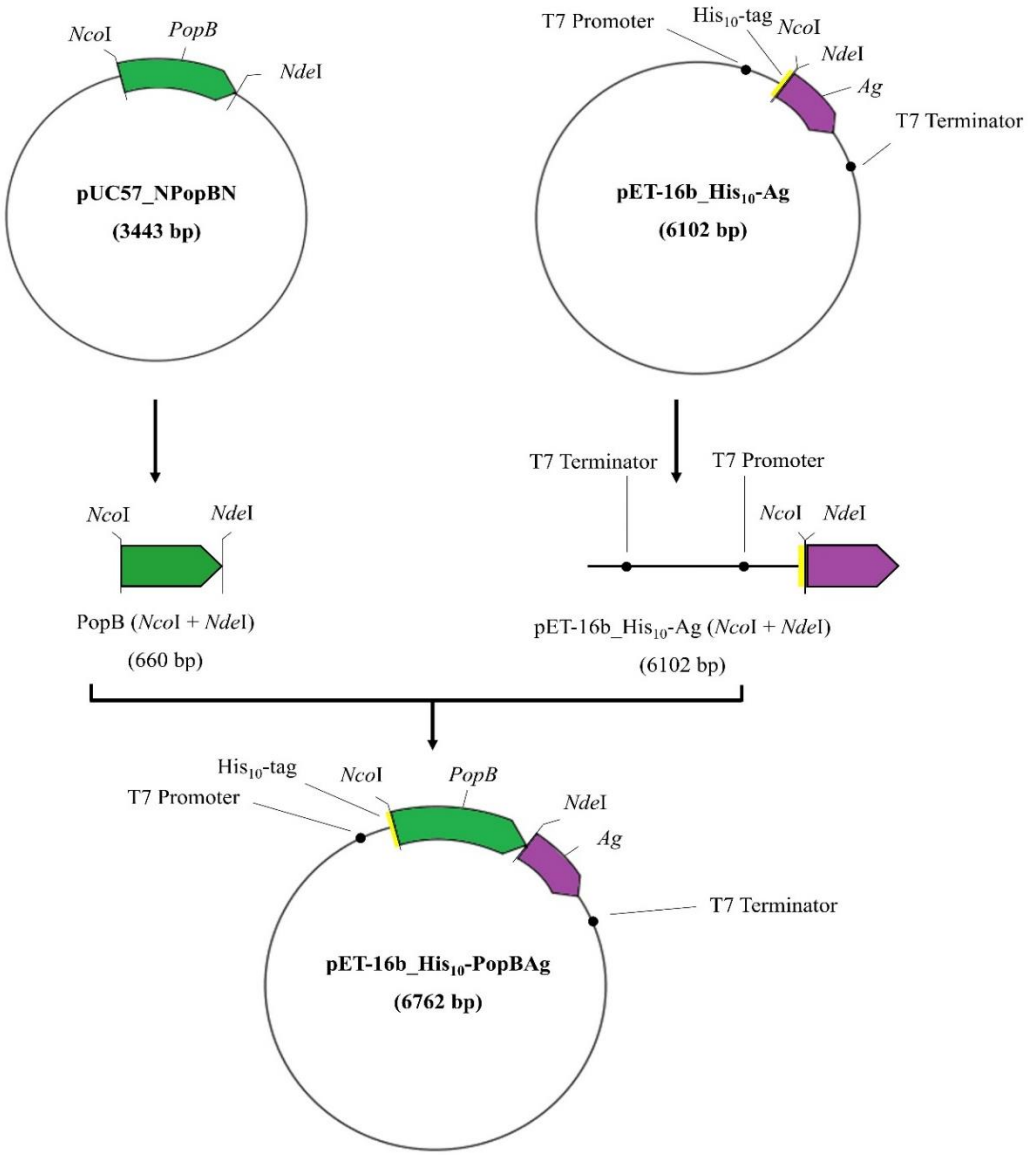

Figure 21. Strategy for the construction of pET-16b_His$_{10}$-PopBAg. The DNA fragment encoding *PopB* gene, codon optimised for *E. coli* was isolated from pUC57_NPopBN, followed by restriction enzyme digestion using *Nco*I and *Nde*I (Section 2.7.2). The DNA fragment was recovered using AGE (Section 2.7.4) and gel purification (Section 2.7.5). The PopB fragment was ligated using T4 DNA ligase (Section 2.7.6) into the linearized vector pET-16b_His$_{10}$-Ag which was generated by restriction enzyme digest with *Nco*I and *Nde*I, generating the final plasmid pET-16b_His$_{10}$-PopBAg.

3.2.3 Gene expression and PHA_{SCL} bead production

The pET expression vector has several features including a lacI gene encoding a *lac* repressor, a *lac* operator, a fl origin of replication, a strong T7 promoter which is specific for T7 RNA polymerase, an ampicillin resistance gene, and ColE1 origin of replication. The main advantage of the pET expression system is allowing the overproduction of fusion proteins through over-expression of recombinant genes placed under the control of the T7 promoter.

The gene encoding the Class I PHA synthase PhaC of *C. necator* and the *Pseudomonas* antigens (Ag and PopB) were integrated into the pET-14b expression vector. For *in vivo* PHA bead production, the recombinant expression vectors were used to transform *E. coli* ClearColi^{TM} production strain (Table 3; Section 2.6.1.2), harbouring pMCS69. Plasmid pMCS69 comprises the genes encoding PhaA and PhaB enzymes of *C. necator* (Table 5) that produce the precursors for PHA_{SCL} synthesis. The *E. coli* cells harbouring various plasmids were cultivated under PHA_{SCL} accumulating conditions (Section 2.4.1.2) to produce PHA_{SCL} beads displaying the *Pseudomonas* antigens. Subsequently, the beads were isolated (Section 2.8).

The pET-16b expression vector was used for production of the soluble proteins, Ag and PopBAg. These plasmids were designed to produce fusion proteins which have an N-terminal polyhistidine-tag fused to the N-terminus of Ag and PopBAg. The recombinant expression vectors were used to transform *E. coli* ClearColi^{TM} production strain (Table 3; Section 2.6.1.2). Furthermore, to confirm the production of PopBAg, the recombinant vector was used to transform (Section 2.6.1.2) *E. coli* production strains BL21 (DE3), BL21 Star^{TM} (DE3), pLysS, Star^{TM} (DE3) pLysS and Shuffle (Table 3). The *E. coli* cells harbouring various plasmids were cultivated under optimum protein isolating conditions (Section 2.4.2) to produce soluble proteins His_{10}-Ag and His_{10}-PopBAg. Subsequently, the soluble proteins were isolated and purified (Section 2.8).

3.2.4 Characterisation of PHA_{SCL} beads displaying *P. aeruginosa* antigens

PHA-accumulating *E. coli* and the isolated PHA_{SCL} beads displaying *Pseudomonas* antigens were stained with Nile-red and visualised by fluorescence microscopy (Section 2.9.1). Fluorescence indicated the presence of intracellular PHA_{SCL} beads in *E. coli* cells and activity of PHA synthase. No fluorescence was observed in negative controls ClearColi^{TM} and ClearColi^{TM} + pET-14b (Figure 22). Fluorescence was detected in the rest of the whole-cells containing plasmid constructs encoding PhaC and the fusion proteins: Ag-PhaC, PhaC-PopB and PhaC-PopBAg. Furthermore, fluorescence was noted in all the isolated PHA_{SCL} beads. The results were confirmed by TEM analysis of the recombinant *E. coli* cells harbouring various plasmids and the PHA_{SCL} beads isolated from the production strain (Figure 23). The TEM images showed the formation of PHA_{SCL} beads facilitated by the respective fusion protein inside recombinant *E. coli* cells. Confirming the fluorescence microscopy data, there was absence of the PHA_{SCL} bead formation in the negative controls. Accumulation and purity of the intracellular PHA_{SCL} beads was further confirmed and quantified by GC-MS (Section 2.9.2). GC-MS analysis showed that cells were accumulating the polyester polyhydroxybutyrate (PHB), which contributes to approximately 60%, 52%, 51% and 31% of CDW when genes encoding PhaC, Ag-PhaC, PhaC-PopB and PhaC-PopBAg, respectively, were present (Figure 24). In addition, the PhaC, Ag-PhaC, PhaC-PopB and PhaC-PopBAg beads were purified to approximately 100%, 92%, 94% and 94% PHB of CDW, respectively.

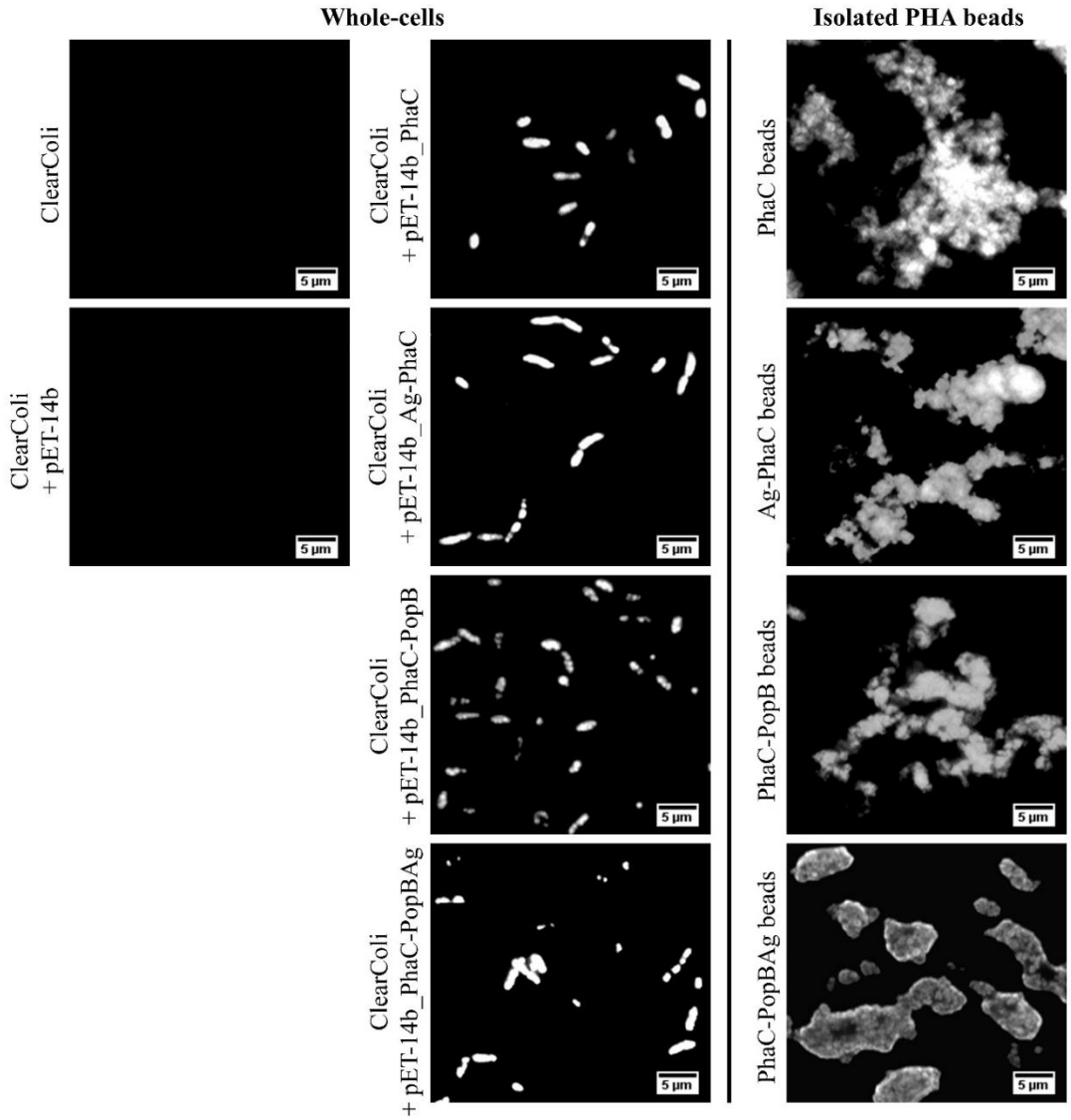

Figure 22. Fluorescence microscopy images of whole-cells and the isolated PHA_{SCL} beads produced in recombinant *E. coli* ClearColi™ strain, harbouring pMCS69 and various fusion protein encoding pET expression vectors stained with Nile red. Fluorescence was detected in all the samples except the negative controls ClearColi™ and ClearColi™ + pET-14b.

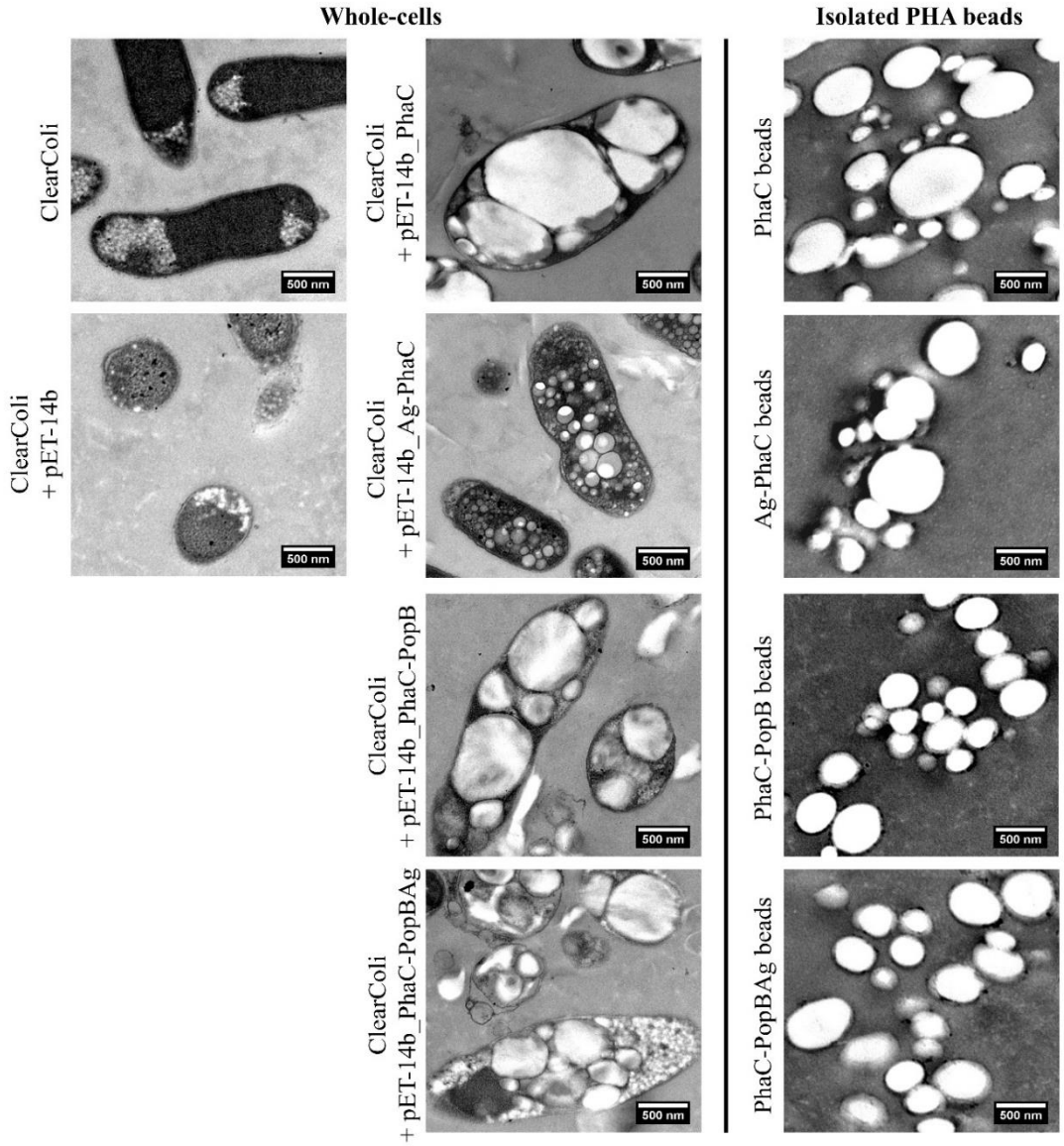

Figure 23. TEM analysis of recombinant *E. coli* harbouring pMCS69 and various fusion protein encoding pET expression vectors, and the isolated PHA$_{SCL}$ beads displaying *P. aeruginosa* antigens. The absence of PHA accumulation in the negative controls ClearColi^{TM} and ClearColi^{TM} + pET-14b and the presence of PHA accumulation in the rest of the whole-cell samples and PHA$_{SCL}$ beads confirmed the fluorescence microscopy data.

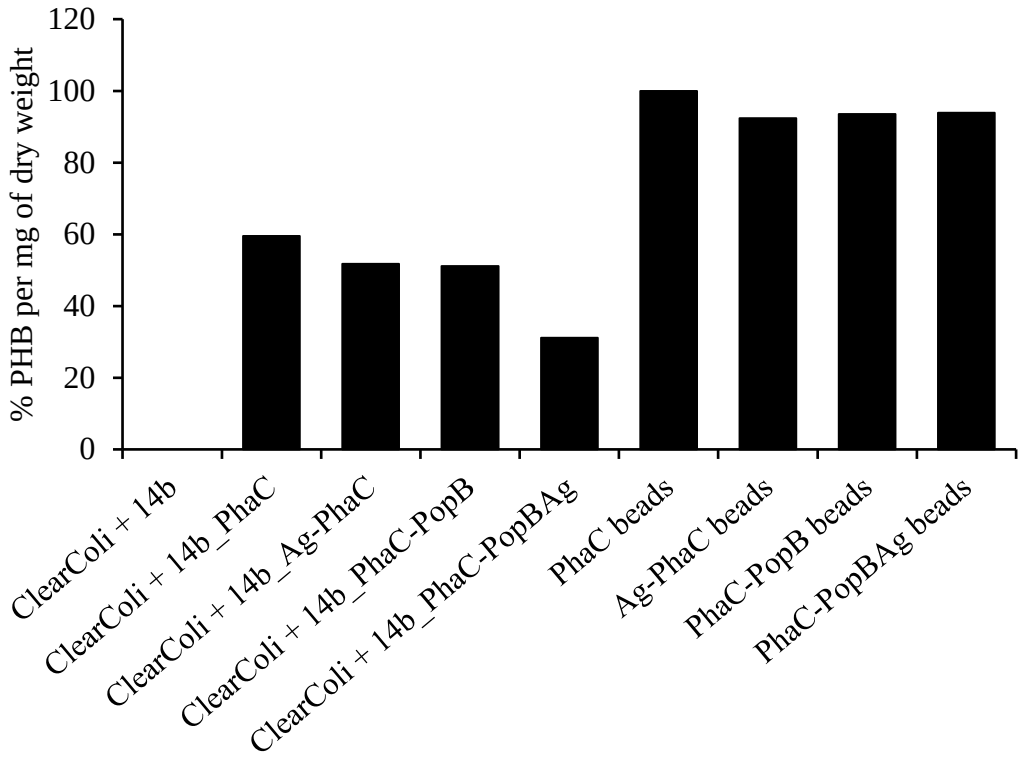

Figure 24. GC-MS analysis of recombinant *E. coli* strain ClearColi^{TM} harbouring various plasmids and of the isolated PHA$_{SCL}$ beads displaying antigens. There was no PHB detected in the negative control ClearColi^{TM} + 14b. Accumulation of PHB was observed in PhaC, Ag-PhaC, PhaC-PopB and PhaC-PopBAg beads with 100%, 92%, 94% and 94% PHB of CDW, respectively. The pET-14b is designated as 14b.

3.2.5 Display of recombinant PhaC-antigen fusion protein on the surface of PHA_{SCL} beads

The presence of the recombinant fusion proteins on the surface of the PHA_{SCL} beads was confirmed using SDS-PAGE (Section 2.10.1). Furthermore, protein profiles of the recombinant fusion proteins were analysed using SDS-PAGE (Figure 25). The theoretical molecular weight of recombinant proteins in this study were calculated utilizing the ProtParam tool from the ExPASy Proteomics Server (http://www.expasy.org/). Dominant protein bands were observed corresponding to proteins with theoretical molecular weights of 64.2 kDa for PhaC; 78.6 kDa for Ag-PhaC; 86.5 kDa for PhaC-PopB and 101.2 kDa for PhaC-PopBAg. These were identified and confirmed by mass spectrometry (Section 2.10.4; Appendix II). Moreover, densitometry analysis (Section 2.10.2) of the SDS-PAGE showed that PhaC accounted for 82.9% of the total protein in the PhaC bead fraction; Ag-PhaC, PhaC-PopB and PhaC-PopBAg accounted for 90.4%, 60.1% and 71.3% of the total protein in their corresponding bead fractions, resectively.

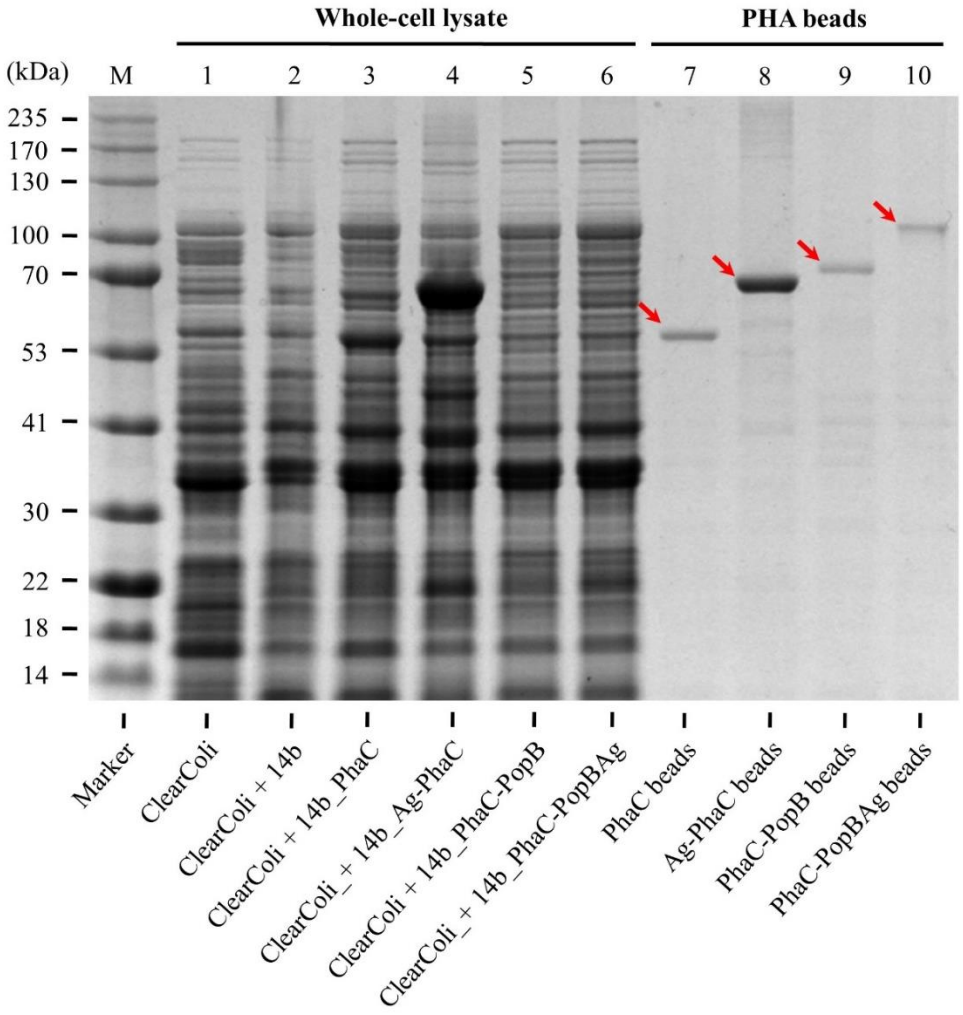

Figure 25. Protein profile analysis of the whole-cell lysate and the isolated PHA$_{SCL}$ beads separated by SDS-PAGE and gel stained with Coomassie Blue. PhaC (64.2 kDa), Ag-PhaC (78.6 kDa), PhaC1-PopB (86.5 kDa) and PhaC1-PopB (101.2 kDa) fusion proteins (marked with red arrows) were isolated from *E. coli* strain ClearColi^{TM} containing the respective plasmids. The presence of the PhaC-antigen fusion proteins was confirmed by mass spectrometry (Appendix II).

3.2.6 The protein profiles of soluble proteins His_{10}-Ag and His_{10}-PopBAg

Evaluation of the successful isolation (Section 2.8) and purification (Section 2.8.4) of the soluble proteins, His_{10}-Ag and His_{10}-PopBAg was confirmed using SDS-PAGE (Section 2.10.1). Furthermore, protein profiles of the whole-cell lysate and soluble proteins were analysed using SDS-PAGE (Figure 26). The theoretical molecular weight of recombinant proteins in this study were calculated utilizing the ProtParam tool from the ExPASy Proteomics Server (http://www.expasy.org/). Dominant protein bands were observed corresponding to proteins with theoretical molecular weights of 15.8 kDa for His_{10}-Ag and 37.3 kDa for His_{10}-PopBAg. These were identified and confirmed by mass spectrometry (Section 2.10.4; Appendix II). Moreover, band percentage analysis of the SDS-PAGE showed 100% for both His_{10}-Ag and His_{10}-PopBAg.

For soluble protein analysis, Ag had a high level of production when isolated from the *E. coli* ClearColi™ production strain (Figure 26; Appendix III). However, the addition of PopB to Ag (PopBAg) resulted in a very low level of production compared to Ag in the ClearColi™ production strain. Hence, several *E. coli* strains were tested for the confirmation of the isolation of the fusion protein His_{10}-PopBAg, and overexpression was observed in *E. coli* pLysS, *E. coli* Star™ (DE3) pLysS and *E. coli* Shuffle but not in ClearColi™ BL21 (DE3), BL21 (DE3) or BL21 Star™ (DE3) (Appendix III). The results indicate that PopB reduced the expression of the fusion protein in ClearColi™ but can be overexpressed using other *E. coli* strains. To be consistent with the PHA_{SCL} bead production in ClearColi™ and the advantage of the absence of endotoxin, ClearColi™ strain was used to produce the final soluble proteins for mice vaccination study (Section 3.3).

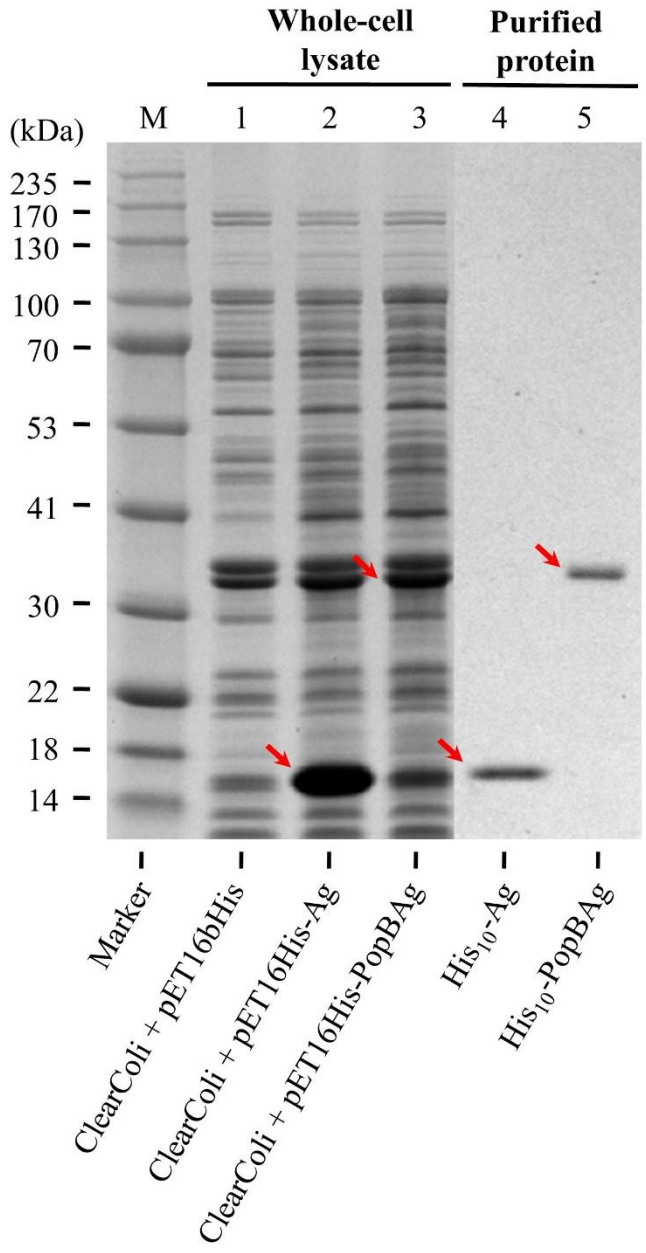

Figure 26. Protein profile analysis of the whole-cell lysate and the isolated soluble proteins separated by SDS-PAGE and gel stained with Coomassie Blue. His_{10}-Ag (15.8 kDA) and His_{10}-PopBAg (37.3 kDa) soluble proteins (marked with red arrows) were isolated from *E. coli* strain ClearColi^{TM} BL21 (DE3) containing the respective plasmids. The soluble proteins were purified using the Zymo (Irvine, CA), His-Spin Protein Miniprep affinity purification (Section 2.8.4). Mass spectrometry (Section 2.10.4) confirmed the isolation of the soluble proteins (Appendix II).

3.3 Immunological analysis of the PHA_{SCL} beads and soluble proteins

The custom-made PHA beads obtained from *P. aeruginosa* and *E. coli*, and the soluble proteins from *E. coli* were prepared by the author to act as particulate vaccines to prevent *P. aeruginosa* infections. The plasmids ultimately used for the production of the PHA beads and soluble proteins are outlined in Figure 27.

The hypotheses of this animal testing study were: (1) the PopB displayed on the surface of PHA beads would stimulate IL-17 suggesting Th17 immune response in immunised mice, (2) the immunised mice would be protected and survive the challenge with *P. aeruginosa*. To assess the candidate vaccines and identify the vaccine with the highest immune response, two sets of experiments were carried out: (1) mice vaccination using the PHA_{MCL} beads from *P. aeruginosa*, and (2) mice vaccination using the PHA_{SCL} beads and soluble proteins from *E. coli* strain ClearColi^{TM}. Female FVN/NJ mice aged 6-7 weeks were immunised once every two weeks for 6 weeks, for a total of 3 immunisations (Section 2.11.1). Blood was collected via retro-orbital technique for the analysis of IgG responses (Section 2.11.2). Immunised mice were challenged with *P. aeruginosa* N13 strain and survival percentage was measured (Section 2.11.3).

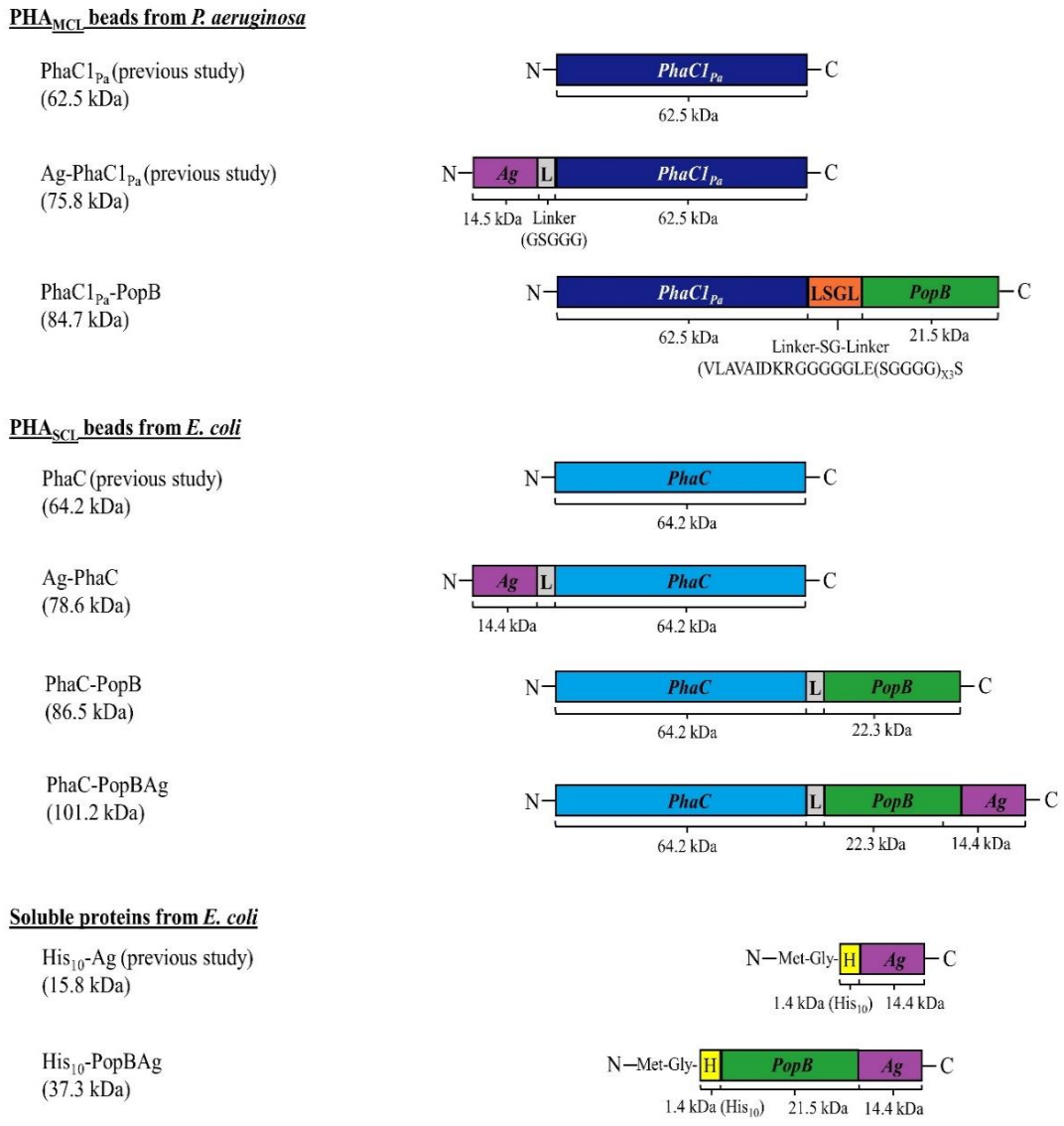

Figure 27. A schematic representation of the plasmid constructs for the production of PHA$_{MCL}$ beads from *P. aeruginosa*, and PHA$_{SCL}$ beads and soluble proteins from *E. coli* strain ClearColi^{TM} for animal testing.

3.3.1 Vaccine formulations and mice vaccination

The isolated PHA beads and soluble proteins were quantified by densitometry (Section 2.10.2). Furthermore, the antigen versus the recombinant protein ratios were calculated based on the densitometry results and are presented in Tables 19, 20 and 21 for PHA_{MCL} beads from *P. aeruginosa*, PHA_{SCL} beads from *E. coli* strain ClearColi^{TM} and soluble proteins from *E. coli* strain ClearColi^{TM}, respectively. The PHA beads and soluble proteins were shipped to the Harvard Medical School, Boston's Children Hospital, USA for animal testing. The dosage of the PHA beads and soluble proteins were based on the maximum amount that can be injected into mice.

Animal testing was set up as two major experiments: (1) mice immunization with PHA_{MCL} beads from *P. aeruginosa*, and (2) mice immunization with PHA_{SCL} beads from *E. coli*. A schematic overview of the production and immunological evaluation of custom-made PHA beads along with the negative and positive controls is presented in Figure 28. For the first experiment using the PHA_{MCL} beads from *P. aeruginosa*, 7 immunization groups were used: (1) Alum (negative control), (2) $PhaC1_{Pa}$, beads, (3) Ag-$PhaC1_{Pa}$ beads, (4) $PhaC1_{Pa}$-PopB beads, (5) PopB/PcrH (PopB with the chaperon PcrH as positive control), (6) OprF/I fusion protein (positive control), and (7) PopB/PcrH + OprF/I (positive control). All the 7 groups were prepared with alum as adjuvant with a final concentration of 1.25 mg/ml in 10 mM Tris saline. The negative and positive controls were provided by the Harvard Medical School. The second experiment using the PHA_{SCL} beads from *E. coli* had 8 immunization groups: (1) Alum (negative control), (2) PhaC beads, (3) Ag-PhaC beads, (4) PhaC-PopB beads, (5) PhaC-PopBAg beads, (6) His_{10}-Ag (positive control), (7) His_{10}-PopBAg (positive control), and (8) PopB/PcrH (positive control). Similar to the first experiment, all the 8 groups were prepared in Tris saline plus alum. Alum and PopB/PcrH were provided by the Harvard Medical School.

Table 19. Formulation of the PHA_{MCL} beads from *P. aeruginosa* (PA).

Vaccine samples	**Polymer beads (WT)_$PhaC1_{Pa}$**	**Polyester beads_Ag-$PhaC1_{Pa}$**	**Polyester beads_$PhaC1_{Pa}$-PopB**
Protein in 10% beads slurry (μg/μl)	3.5535	0.21585	0.1059
MW ratio: PA antigen VS Recombinant (Rec) protein	N/A	Ag:Rec protein =14.5:62.5 =1:4.31034	PopB:Rec protein =22.2:62.5 =1:2.8153
Antigen in 10% beads slurry (μg/μl)	N/A	0.05008	0.03762
Amount of PA antigen for injection	7 μg/dose	7 μg/dose	7 μg/dose
Final concentration of the adjuvant	1.25mg/ml	1.25mg/ml	1.25mg/ml
Injection volume of formulated vaccines	200 μL	200 μL	200 μL
Formulation (8 doses)	PHA beads: 15.76 μL	PHA beads: 1118.21 μL	PHA beads: 1488.57 μL

Table 20. Formulation of the PHA_{SCL} beads from *E. coli*.

Vaccine samples	Polymer beads (WT)_PhaC	Polyester beads_Ag-PhaC	Polyester beads_PhaC-PopB	Polyester beads_PhaC-PopBAg
Protein in 10% beads slurry (μg/μl)	0.08205	0.287	0.06249	0.03369
MW ratio: PA antigen VS Recombinant (Rec) protein	N/A	Ag:Rec protein =14.4:64.2 =1:4.458	PopB:Rec protein =22.2:64.3 =1:2.896	PopBAg:Rec protein =36.9:64.3 =1:1.74
Antigen in 10% beads slurry (μg/μl)	N/A	0.06438	0.02158	0.01936
Amount of PA antigen for injection	3 μg/dose	3 μg/dose	5 μg/dose	5 μg/dose
Amount of adjuvant for injection	1.25mg/ml	1.25mg/ml	1.25mg/ml	1.25mg/ml
Injection volume of formulated vaccines	200 μL	200 μL	200 μL	200 μL
Formulation (8 doses)	PHA beads: 292.50 μL	PHA beads: 372.79 μL	PHA beads: 1853.59 μL	PHA beads: 2066.12 μL

Table 21. Formulation of the soluble proteins from *E. coli*.

Vaccine samples	His_{10}_Ag	His_{10}_PopBAg
Protein (μg/μl)	0.05889	0.0738
MW ratio: PA antigen VS rec protein	Ag: HisAg 14.4:17.1(His10 Ag) 1:1.1875	36.6 (PopBAg):39.3(His10 PopBAg) =1:1.0738
Antigen (μg/μl)	0.04959	0.0687
Amount of PA antigen for injection	7 μg/dose	7 μg/dose
Amount of adjuvant for injection	1.25mg/ml	1.25mg/ml
Injection volume of formulated vaccines (8 doses)	1129.26 μL	815.14 μL

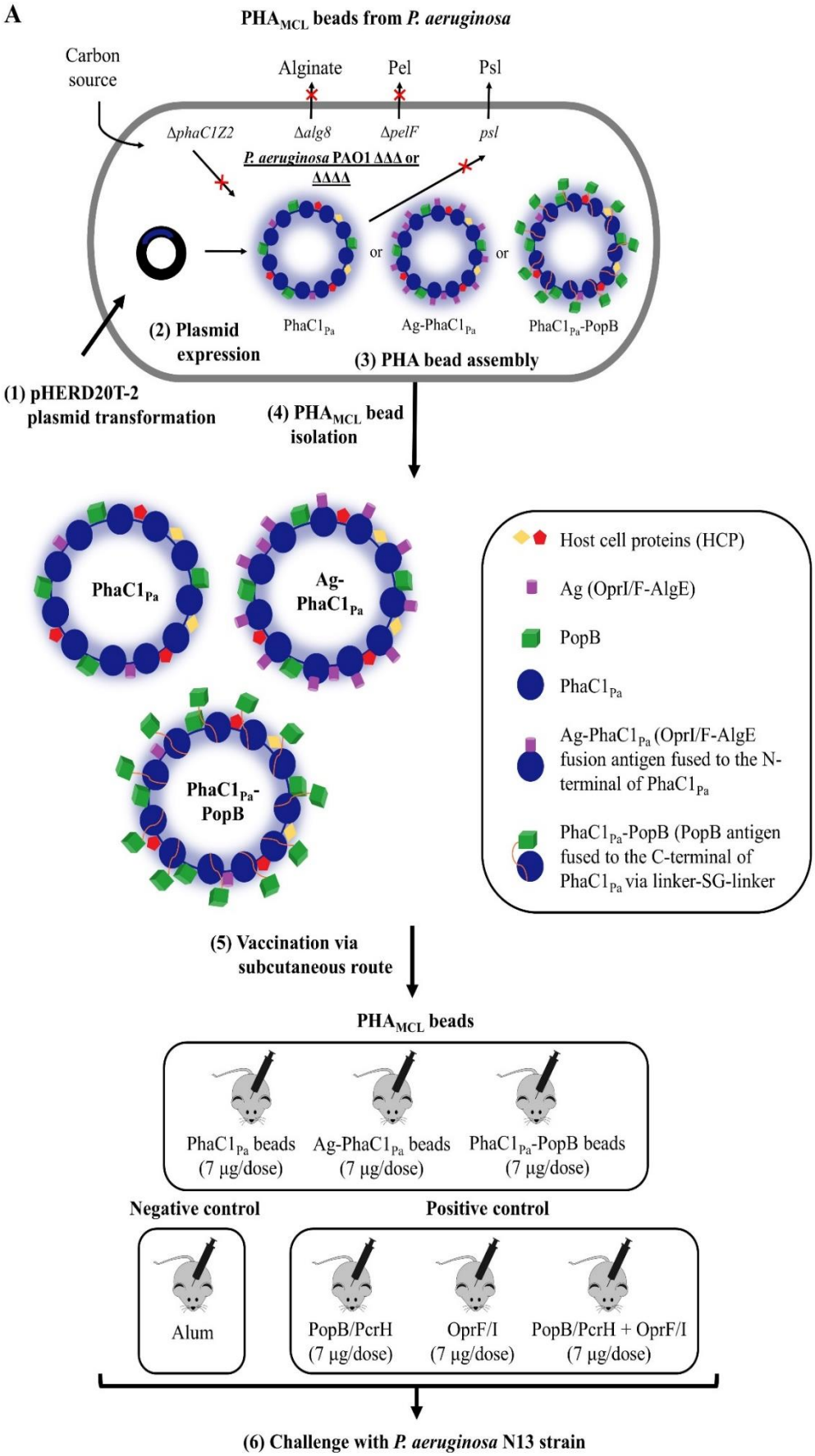
A
PHA$_{MCL}$ beads from *P. aeruginosa*
Carbon source
Alginate
Pel
Psl
ΔphaC1Z2
Δalg8
ΔpelF
psl
P. aeruginosa PAO1 ΔΔΔ or ΔΔΔΔ
or
or
PhaC1$_{Pa}$
Ag-PhaC1$_{Pa}$
PhaC1$_{Pa}$-PopB
(2) Plasmid expression
(3) PHA bead assembly
(1) pHERD20T-2 plasmid transformation
(4) PHA$_{MCL}$ bead isolation
PhaC1$_{Pa}$
Ag-PhaC1$_{Pa}$
PhaC1$_{Pa}$-PopB
Host cell proteins (HCP)
Ag (OprI/F-AlgE)
PopB
PhaC1$_{Pa}$
Ag-PhaC1$_{Pa}$ (OprI/F-AlgE fusion antigen fused to the N-terminal of PhaC1$_{Pa}$
PhaC1$_{Pa}$-PopB (PopB antigen fused to the C-terminal of PhaC1$_{Pa}$ via linker-SG-linker
(5) Vaccination via subcutaneous route
PHA$_{MCL}$ beads
PhaC1$_{Pa}$ beads (7 µg/dose)
Ag-PhaC1$_{Pa}$ beads (7 µg/dose)
PhaC1$_{Pa}$-PopB beads (7 µg/dose)
Negative control
Positive control
Alum
PopB/PcrH (7 µg/dose)
OprF/I (7 µg/dose)
PopB/PcrH + OprF/I (7 µg/dose)
(6) Challenge with *P. aeruginosa* N13 strain

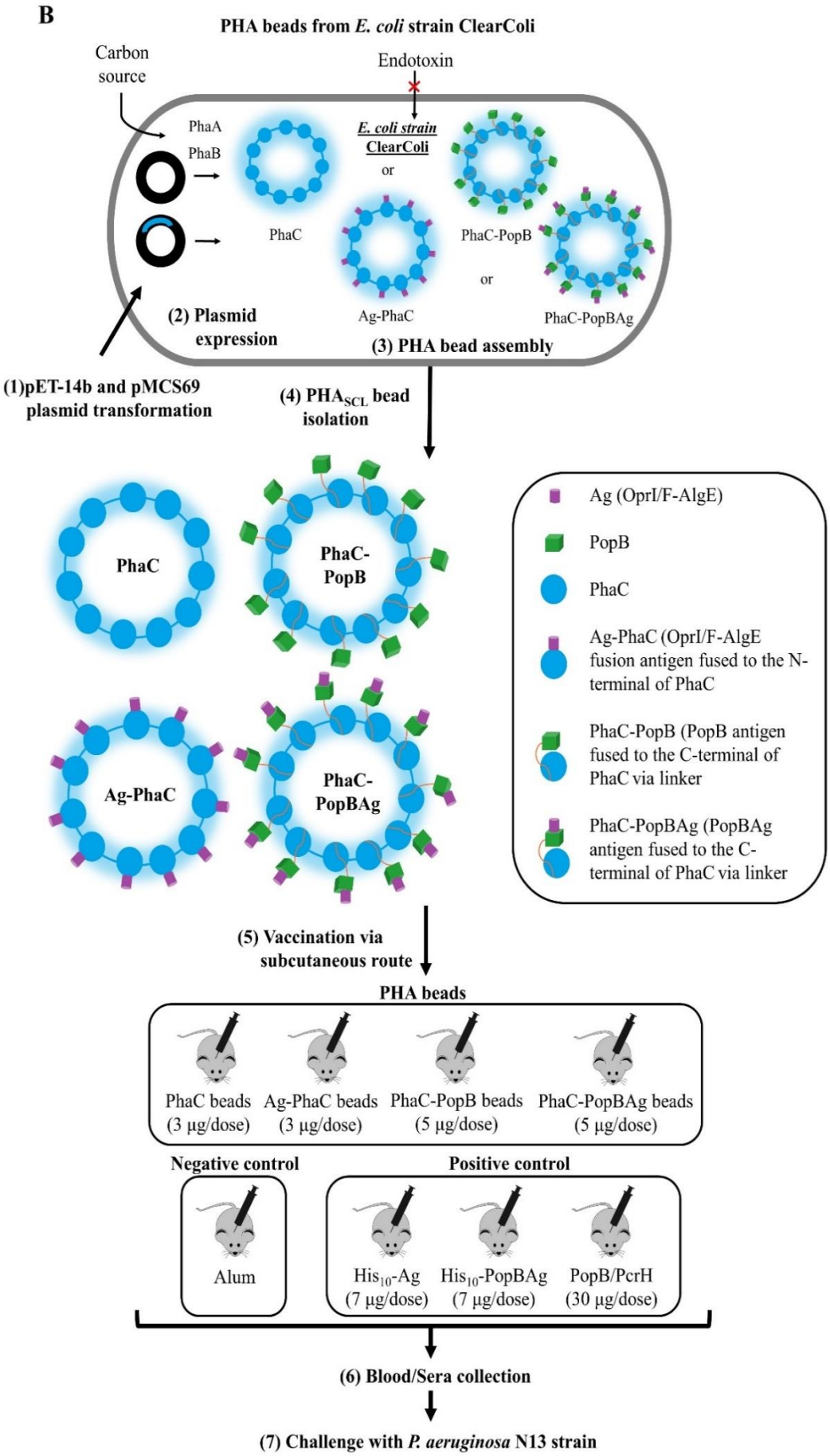
B
PHA beads from E. coli strain ClearColi
Carbon source
Endotoxin
PhaA
PhaB
E. coli strain ClearColi
or
PhaC
PhaC-PopB
or
Ag-PhaC
PhaC-PopBAg
(2) Plasmid expression
(3) PHA bead assembly
(1)pET-14b and pMCS69 plasmid transformation
(4) PHASCL bead isolation
PhaC
PhaC-PopB
Ag-PhaC
PhaC-PopBAg
Ag (OprI/F-AlgE)
PopB
PhaC
Ag-PhaC (OprI/F-AlgE fusion antigen fused to the N-terminal of PhaC
PhaC-PopB (PopB antigen fused to the C-terminal of PhaC via linker
PhaC-PopBAg (PopBAg antigen fused to the C-terminal of PhaC via linker
(5) Vaccination via subcutaneous route
PHA beads
PhaC beads (3 µg/dose)
Ag-PhaC beads (3 µg/dose)
PhaC-PopB beads (5 µg/dose)
PhaC-PopBAg beads (5 µg/dose)
Negative control
Positive control
Alum
His10-Ag (7 µg/dose)
His10-PopBAg (7 µg/dose)
PopB/PcrH (30 µg/dose)
(6) Blood/Sera collection
(7) Challenge with P. aeruginosa N13 strain

Figure 28. A schematic overview of the production and immunological evaluation of custom-made PHA beads displaying *P. aeruginosa* candidate antigens derived from *P. aeruginosa* and *E. coli*. (A) For PHA_{MCL} beads from *P. aeruginosa*: (1) plasmid encoding $PhaC1_{Pa}$ or Ag antigen fused to the N-terminal of $PhaC1_{Pa}$ or PopB fused to the C-terminal of $PhaC1_{Pa}$ via linker-SG-linker were used to transform *P. aeruginosa* PAO1 ΔCΔ8ΔF mutant strain (ΔCΔ8ΔFΔP for $PhaC1_{Pa}$). This strain is defective in production of native PHA_{MCL} and of EPS alginate and Pel (additional Psl knockout for $PhaC1_{Pa}$). (2) Plasmid harbouring strains are then grown under PHA_{MCL} accumulating conditions to mediate overproduction of the fusion protein and subsequent PHA_{MCL} bead assembly. (3) Formation of PHA_{MCL} beads results in the display of fusion antigens covalently linked to the PHA synthase along with the HCPs. (4) PHA_{MCL} beads were isolated from the host by mechanical disruption and subsequently purified. (5) FVB/NJ mice were vaccinated with sterilized PHA_{MCL} beads, negative control alum, and positive controls PopB/PcrH, OprI/F and PopB/PcrH + OprI/F via subcutaneous route three times at biweekly intervals. (6) Mice were challenged with *P. aeruginosa* N13 strain and survival percentage was measured. (B) For PHA_{SCL} beads from *E. coli*: (1) plasmid encoding wild-type PhaC or Ag antigen fused to the N-terminal of PhaC or PopB fused to the C-terminal of PhaC via linker or PopBAg fused to the C-terminal of PhaC via linker were used to transform *E. coli* ClearColi^{TM} production strain. (2) Strains harbouring various plasmids plus pMCS69 were grown under PHA_{SCL} accumulating conditions to mediate overproduction of the fusion protein and subsequent PHA_{SCL} bead assembly. (3) Formation of PHA_{SCL} beads results in the display of fusion antigens covalently linked to the PhaC. (4) PHA_{SCL} beads were isolated from the host by mechanical disruption and subsequently purified. (5) FVB/NJ mice were vaccinated with sterilized PHA_{SCL} beads, negative control alum, and positive controls His_{10}-Ag, His_{10}-PopBAg and PopB/PcrH via subcutaneous route three times at biweekly intervals. 6) Blood was collected from mice three-weeks after the last vaccination for IgG responses via retro-orbital bleeding. (7) Mice were challenged with *P. aeruginosa* N13 strain and survival percentage was measured.

3.3.2 Immunological response to the antigen-displaying PHA beads

Only the mice vaccinated with the PHA_{SCL} beads from *E. coli* had blood available for testing as this was collected by retro-orbital bleeding technique. The tail bleeding did not work in the first experiment with mice vaccinated with beads from *P. aeruginosa*. IL-17 cytokine analysis was done using the solid phase sandwich ELISA (Figure 29). All splenocytes were stimulated with PopB/PcrH, His_{10}-Ag, His_{10}-PopBAg or PhaC beads. Vaccination with PhaC and PhaC-PopBAg beads induced significantly more ($p < 0.05$) IL-17 in PopB/PcrH stimulation than the alum (negative control), PopB/PcrH and Ag-PhaC beads (Figure 29A). On the other hand, PhaC-PopBAg beads produced significantly more IL-17 in His_{10}-Ag stimulation compared to alum (negative control), PopB/PcrH, His_{10}-Ag and Ag-PhaC beads (Figure 29B). In the His_{10}-PopBAg (Figure 29C) and PhaC beads (Figure 29D) stimulations, there was significant induction of IL-17 in both PhaC-PopB and PhaC-PopBAg beads compared to the other treatments. Highest production of IL-17 was observed in PhaC beads stimulation of 368 pg/ml and 341 pg/ml for PhaC-PopB and PhaC-PopBAg beads, respectively.

IgG1 and IgG2c responses were evaluated by ELISA (Figure 30) using microtiter plates coated with PopB/PcrH, His_{10}-Ag, or PhaC beads. The results showed strong IgG1 and IgG2 responses in mice vaccinated with the PhaC and PhaC-antigen fusion beads (Figure 30C). The IgG1 responses of the beads were significantly higher ($p < 0.05$) than IgG1 responses produced by mice vaccinated with alum (negative control) or soluble proteins. Although not statistically significant, there was a positive trend of higher IgG2c responses elicited by mice vaccinated with the PhaC and PhaC-antigen fusion beads compared to the other treatments. Taken together, these findings suggest that bead preparations containing PhaC or PhaC-fused-antigens elicited greater immunogenic response than the negative control (Alum) or soluble proteins.

In the PopB/PcrH induced condition (Figure 30A), there was a significant IgG1 response in mice vaccinated with PopB/PcrH compared to the rest of the vaccine groups, indicating specificity in the host immune response. PhaC and PhaC-antigen fusion beads as well as the soluble protein His_{10}-PopBAg elicited significantly higher IgG1 response than alum (negative control) and PopB/PcrH induced by His_{10}-Ag (Figure 30B). Furthermore, a similar positive trend was observed in the IgG2c

responses to PhaC, PhaC-antigen fusion beads, and soluble proteins His_{10}-Ag and His_{10}-PopBAg compared to Alum (negative control) and PopB/PcrH, although this is not statistically significant.

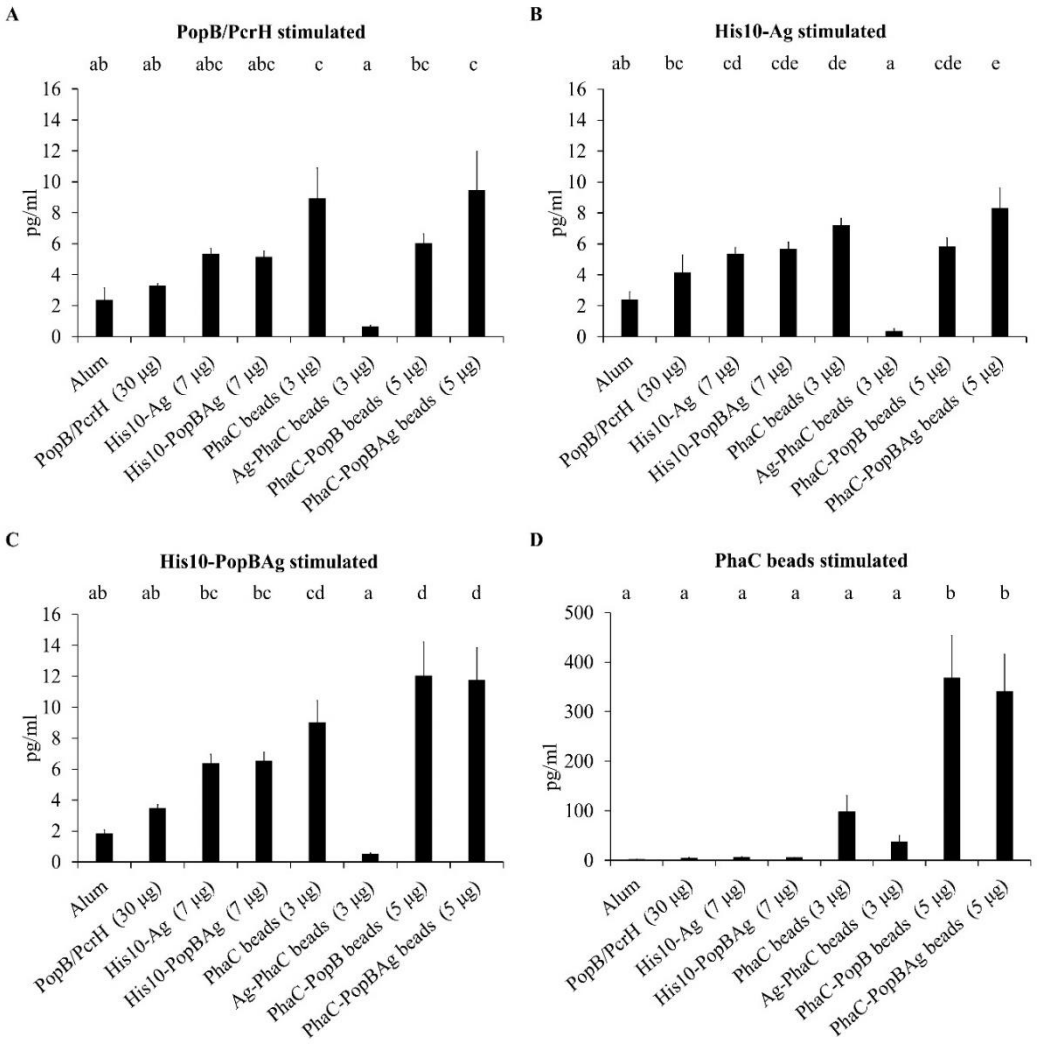

Figure 29. IL-17 cytokine analysis from mice splenocytes stimulated with PopB/PcrH, His_{10}-Ag, His_{10}-PopBAg or PhaC beads and analysed by solid-phase sandwich ELISA. Each data point represents the mean ± the standard error of the mean. PhaC beads and PhaC-antigen fusion beads; soluble PopB/PcrH, His_{10}-Ag and His_{10}-PopBAg were used as a positive control; and Alum adjuvant used for vaccine formulation and as a negative control. Statistical significance ($p < 0.05$) is indicated by letter-based representation of pairwise comparison between groups. The experiments were replicated twice.

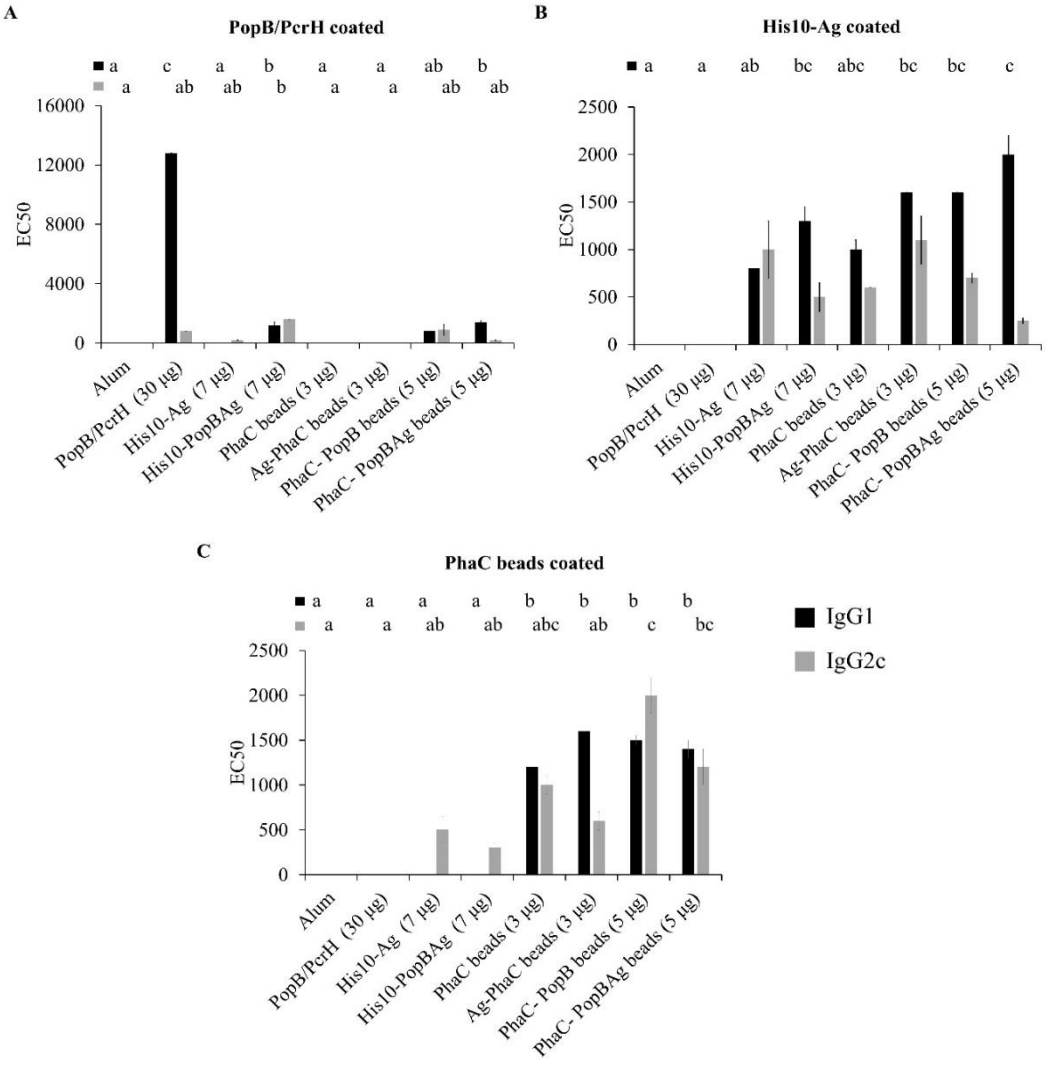

Figure 30. IgG1 and IgG2c titers expressed in EC50 values in response to PopB/PcrH, His_{10}-Ag and PhaC beads analysed by ELISA for each immunized group. Each data point represents the mean ± the standard error of the mean. PhaC beads and PhaC-antigen fusion beads; PopB/PcrH, His_{10}-Ag and His_{10}-PopBAg used as positive control; and Alum adjuvant used for vaccine formulation and as a negative control. Statistical significance ($p < 0.05$) is indicated by letter-based representation of pairwise comparison between groups. The experiments were replicated twice.

3.3.3 Challenge with *P. aeruginosa* N13 strain

To assess the efficacy of the PHA beads as particulate vaccines, mice were challenged with the *P. aeruginosa* N13 strain. Challenge was administered through the nostril. All immunization groups started with 8 mice per group. However, in the experiment with PHA_{MCL} beads from *P. aeruginosa*, 5 mice immunized with Alum got sick for an unexplained reason, and as a result only 3 mice were used for the challenge. Similarly, in the experiment with PHA_{SCL} beads from *E. coli*, one mouse immunized with PopB/PcrH became sick for an unexplained reason, leaving 7 mice in this group available for the challenge experiment. Figure 31 shows the survival percentage analysis of the vaccinated mice challenged with *P. aeruginosa* N13 strain. Mice vaccinated with $PhaC1_{Pa}$-PopB beads from *P. aeruginosa* were the most promising with the highest survival rate of 40% at 40 hours after the challenge (Figure 31A). On the other hand, among the PHA beads from *E. coli*, Ag-PhaC had the highest survival rate of 25% at 40 hours after the challenge despite the lower dosage of 3 μg/dose (Figure 31B). The dosage of PopB/PcrH was increased to 30 μg/dose because in the first experiment with PHA_{MCL} beads from *P. aeruginosa*, there was almost no protection detected in the group of the mice immunised with PopB/PcrH (positive control) compared to $PhaC1_{Pa}$-PopB using the same quantity. However, comparing the level of protection from beads obtained from *P. aeruginosa* and *E. coli*, $PhaC1_{Pa}$-PopB (from *P. aeruginosa*) had better protection, indicated by higher survival rate compared to the best *E. coli* beads, Ag-PhaC. The soluble version of the antigens had no protection except the PopB/PcrH with 30 μg dosage but not in the lower dose of 7 μg (positive control).

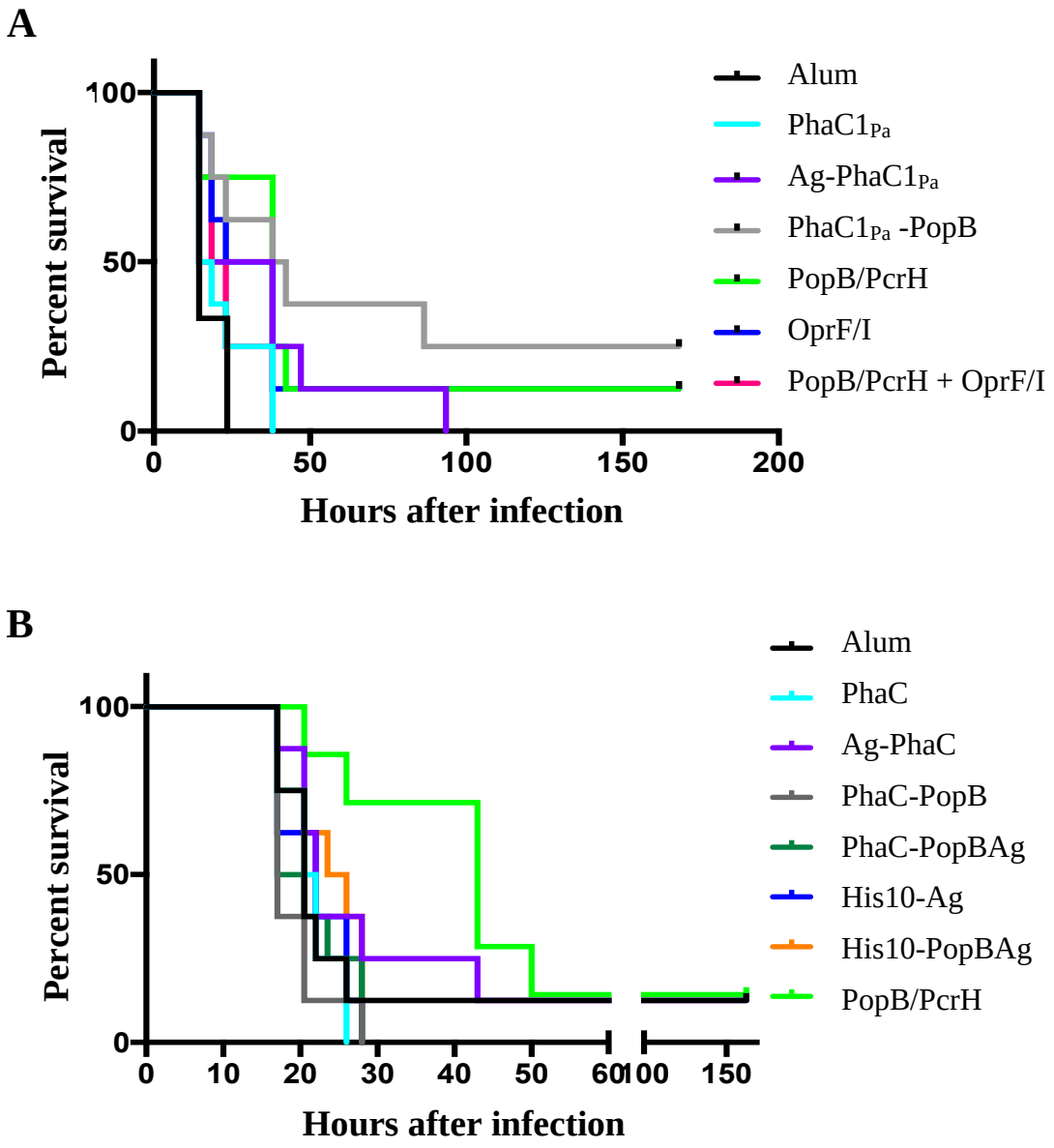

Figure 31. Survival percentage analysis of the vaccinated mice challenged with *P. aeruginosa* N13 strain. The challenge was administered via the nostril. (A) Mice vaccinated with PHA_{MCL} beads from *P. aeruginosa*, $PhaC1_{Pa}$, Ag- $PhaC1_{Pa}$ and $PhaC1_{Pa}$-PopB along with the negative control Alum and positive controls PopB/PcrH, OprF/I and PopB/PcrH + OprF/I. Eight mice per vaccine group were used, except for the Alum which used only 3 mice. $PhaC1_{Pa}$-PopB showed potential protection. (B) Mice vaccinated with PHA_{SCL} beads from *E. coli*, PhaC, Ag-PhaC, PhaC-PopB and PhaC-PopBAg along with the negative control Alum and positive controls His_{10}-Ag, His_{10}-PopBAg and PopB/PcrH. Eight mice per vaccine group were used, except for the PopB/PcrH which used only 7 mice. Ag-PhaC showed potential protection.

3.4 Generation of the *cdrA* knockout mutant strain and characterisation

To generate a *cdrA* knockout mutant for the production of Psl as a potential vaccine target and which can be used for future studies (Section 1.7), an isogenic *cdrA* deletion mutant was generated from the *P. aeruginosa* PAO1 Δ*phaC1ZC2* Δ*alg8* Δ*pelF* (PAO1 ΔCΔ8ΔF or ΔΔΔ) (Table 3). This mutant was assessed for Psl production (Section 2.12). The pEX4625 (Table 7) used to create the mutant was previously generated by Borlee et al. (2010). Previous studies have shown that CdrA directly binds to Psl polysaccharide promoting biofilm formation (Borlee et al., 2010). The hypothesis of this study is that the *cdrA* knockout mutant overproduces free Psl. In order to test the hypothesis, *P. aeruginosa* PAO1 ΔΔΔΔ*cdrA* (Section 3.4.1) was generated by transconjugation (Section 2.6.3) and Psl production of the mutant (Section 3.4.2) was analysed by solid surface attachment (SSA) assay (Section 2.12.1) and ELISA (Section 2.12.2). The strategy of producing the *P. aeruginosa* PAO1 ΔΔΔΔ*cdrA* and analysis is presented in Figure 32.

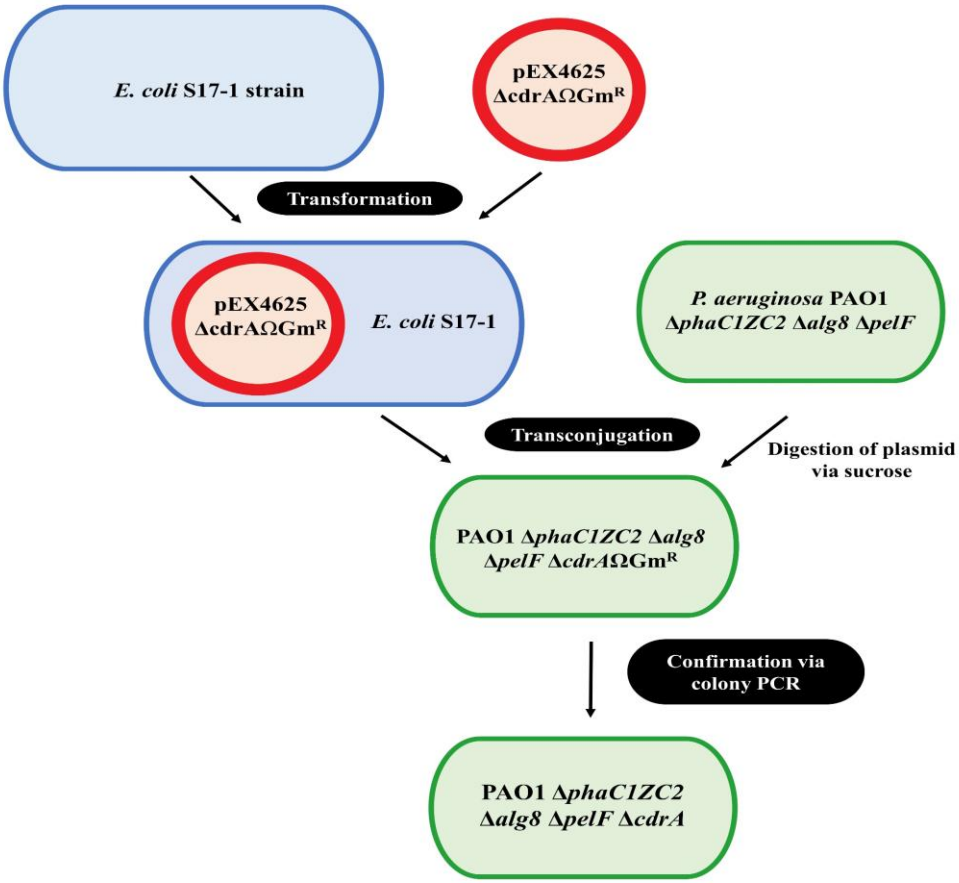

Figure 32. Strategy for the generation of *cdrA* knockout mutant. Plasmid pEX4625Δ*cdrA*ΩGm^R, a *cdrA* deletion construct carrying gentamicin resistant cassette was used to transform (Section 2.6.1.2) *E. coli* S17-1 strain. The *E. coli* S17-1 containing the plasmid acts as a donor and *P. aeruginosa* PAO1 Δ*phaC1ZC2* Δ*alg8* Δ*pelF* was the recipient in the transconjugation (Section 2.6.3), generating PAO1 Δ*phaC1ZC2* Δ*alg8* Δ*pelF* Δ*cdrA*ΩGm^R. The mutant was grown in PIA agar plates containing 100 µg/ml gentamicin and subsequently on PIA containing 5% sucrose (w/v) to isolate double recombinants. Confirmation of the generated *cdrA* knockout mutant was done via colony PCR (Section 2.7.3) using cdrAout40_fwd and cdrAoutout32_rev primers (Table 10), generating the final PAO1 Δ*phaC1ZC2* Δ*alg8* Δ*pelF* Δ*cdrA.*

3.4.1 Generation of *P. aeruginosa* PAO1 ΔΔΔΔ*cdrA*

The pEX4625Δ*cdrA*ΩGm^R containing the *cdrA* deletion construct with gentamicin resistance cassette was transformed (Section 2.6.1.2) into *E. coli* S17-1 (ATCC47055), the basic conjugative donor strain containing the tra gene on the chromosome (Phornphisutthimas et al., 2007). Subsequently, transconjugation (Section 2.6.3) with the transformed *E. coli* serving as the donor strain and the recipient strain *P. aeruginosa* PAO1 ΔCΔ8ΔF resulted in PAO1 ΔCΔ8ΔFΔ*cdrA*ΩGm^R. Transconjugants were selected on PIA (Section 2.2.2.1) containing 100 μg/ml gentamicin (Section 2.3) and subsequently on 5% (w/v) sucrose. Under these conditions, a double cross over event was selected, creating the strain PAO1 ΔCΔ8ΔFΔ*cdrA* which was verified by PCR (Section 2.7.3) using cdrAout40_fwd and cdrAoutout32_rev primers (Table 11), yielding approximately 231 bp PCR product (Figure 33). Gentamicin sensitivity was tested, however despite several attempts to remove the resistance marker, the mutant strain was still resistant to gentamicin. The plasmid was designed with the gentamicin cassette outside of the gene; hence this may not impact the Psl overproduction which is the main aim of this study. The mutant was analysed for Psl production (Section 3.4.2).

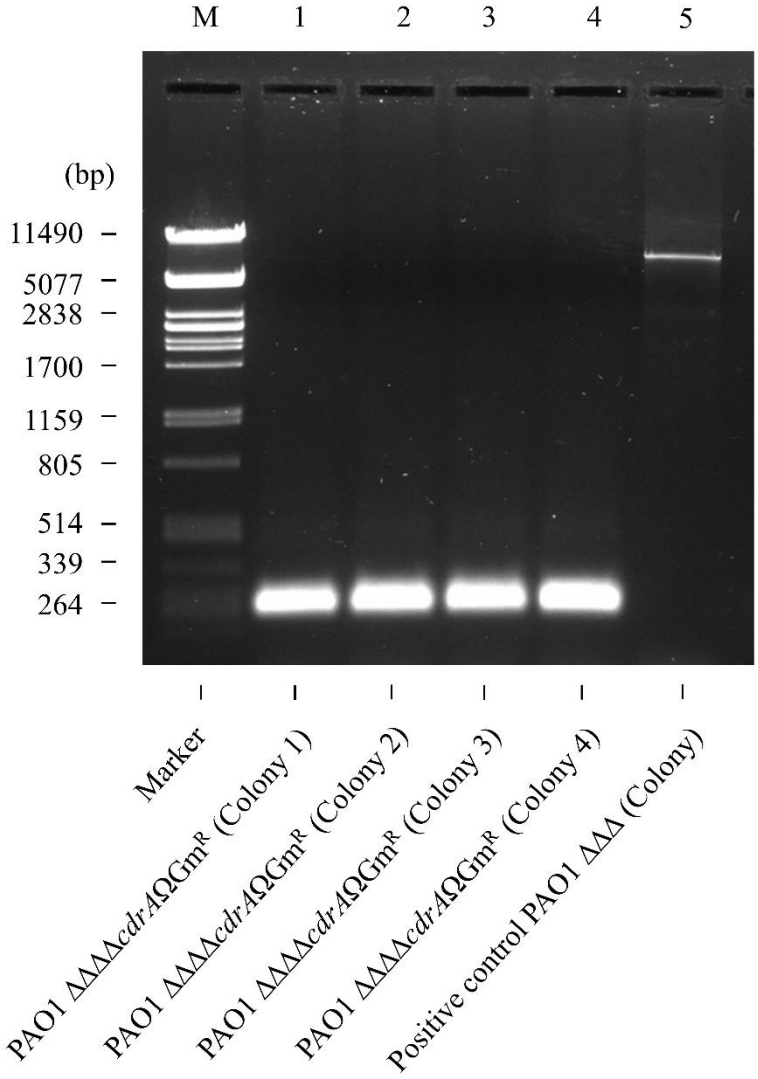

Figure 33. Confirmation of *cdrA* deletion mutant. Colony PCR (Section 2.7.3) using cdrAout40_fwd and cdrAoutout32_rev primers (Table 11) was used to confirm deletion of *cdrA* in *P. aeruginosa* PAO1 Δ*phaC1ZC2* Δ*alg8* Δ*pelF* strain. *P. aeruginosa* PAO1 Δ*phaC1ZC2* Δ*alg8* Δ*pelF* was also used as a positive control in the confirmation test.

3.4.2 Psl production of the *P. aeruginosa* PAO1 ΔCΔ8ΔFΔ*cdrA* mutant

To test whether the PAO1 ΔCΔ8ΔFΔ*cdrA* mutant can overproduce Psl, solid surface attachment (SSA) assay (Section 2.12.1) and ELISA (Section 2.12.2) using the *Hippeastrum hybrid* lectin (HHA)-HRP which directly binds to Psl, were used to measure the absorbance correlating to the production of Psl. Psl acts as an anchor or crosslinking protein to CdrA. Hence, deletion of *cdrA* gene would generate a mutant which sheds Psl into the medium, thereby allowing the recovery of Psl and its purification for potential vaccine use.

Three time points were tested for the SSA assay: 12, 20 and 96 hours. Figure 34 shows the best time point was the lowest incubation period of 12 hours, indicated by positive absorbance values, while the 20 and 96 hour incubation periods resulted in negative absorbance values. All three incubation periods had similar results in which the negative control with Psl knockout phenotype, PAO1 ΔCΔ8ΔFΔ*pslA* had negative values in all the time points. Furthermore, the positive control producing Psl, PAO1 ΔCΔ8ΔF, had higher absorbance than the negative control. Interestingly, the *cdrA* knockout mutant grown in the presence and absence of gentamicin had significantly higher absorbance ($p < 0.05$) than the positive control (Figure 34A), suggesting higher production of Psl than the positive control. This confirmed that the *cdrA* knockout mutant is a strain that can over produce Psl and potentially can be used for purification processes and other applications.

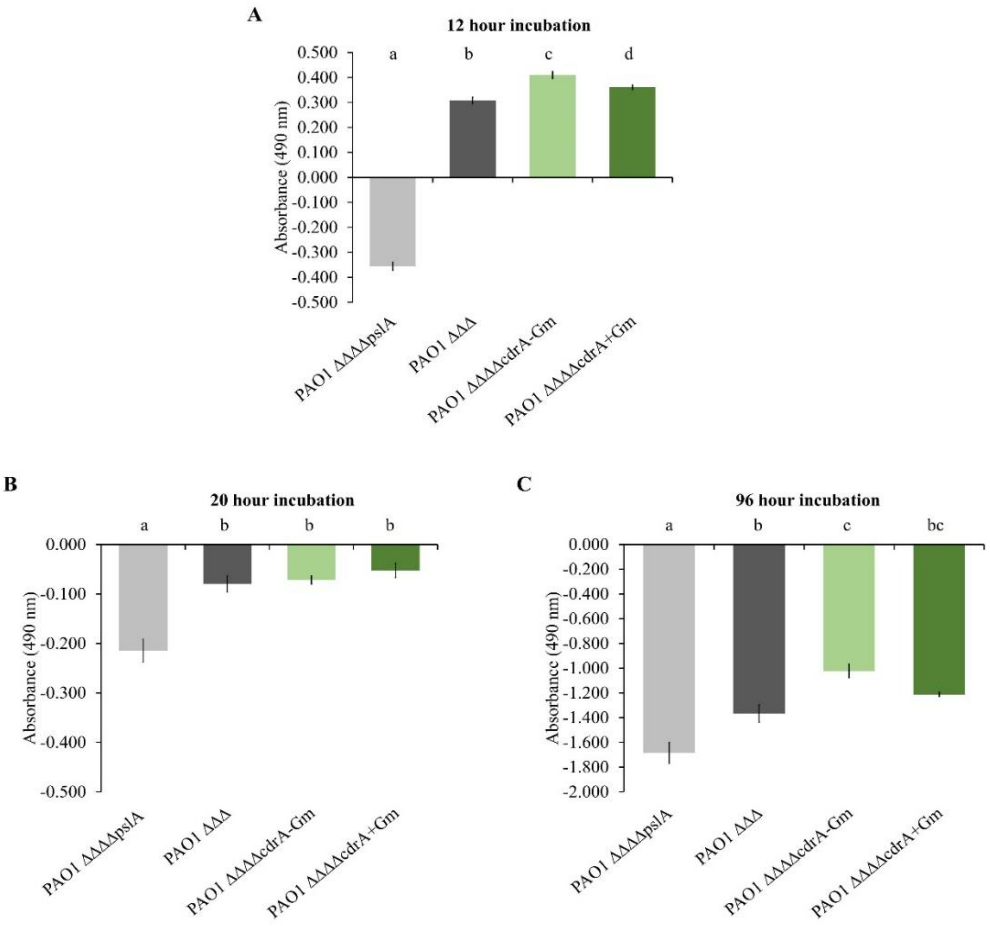

Figure 34. Psl production analysis of the *cdrA* knockout mutant using solid surface attachment (SSA) assay and ELISA. Three incubation periods, (A) 12, (B) 20 and (C) 96 hours were tested for the Psl production phenotype of the PAO1 ΔCΔ8ΔFΔ*cdrA* along with the negative control PAO1 ΔCΔ8ΔFΔ*pslA* and positive control PAO1 ΔCΔ8ΔF. The *cdrA* knockout mutant was grown both in the presence and absence of gentamicin. The data represents the mean of three experiments. Statistical significance ($p < 0.05$) is indicated by letter-based representation of pairwise comparison between groups. –Gm was the strain grown in the absence of gentamicin while +Gm was the strain grown in the presence of gentamicin.

Chapter 4: Discussion

4.1 Successful PhaC1$_{Pa}$-PopB bead production but unacceptable yields of PhaC1$_{Pa}$-PopBAg beads produced in *P. aeruginosa*

This part of the study aimed to produce functionalized PHA$_{MCL}$ beads displaying PopB alone, and the combination of PopB and Ag, at high copy number in *P. aeruginosa* suitable as candidate bead vaccines for animal testing. Vaccine development against *P. aeruginosa* using the traditional approaches have been unsuccessful (Priebe & Goldberg, 2014) and, to date, there is still no commercially available vaccine against *P. aeruginosa*. *P. aeruginosa* naturally produces PHA composed of medium chain length 3-hydroxy fatty acids (MCL) for which polymerization is catalyzed by the PHA$_{MCL}$ synthase (PhaC1$_{Pa}$) (Draper et al., 2013; Rehm, 2003). Hence, this study utilised PHA$_{MCL}$ beads, produced by their native host as a delivery system and as a novel approach to vaccine development, potentially providing improved immune responses over traditional means. Previous studies had shown that PhaC1$_{Pa}$ of *P. aeruginosa* can be bioengineered to produce custom made PHA$_{MCL}$ beads displaying antigen fusions that can serve as a particulate vaccine (Lee et al., 2017). Promising antigens against *P. aeruginosa* include OprI, OprF, and AlgE, and combinations of these (designated as Ag), were previously displayed on PHA$_{MCL}$ beads, and Ag-PhaC1$_{Pa}$ beads showed dominant Th1 immune response in mice vaccination (Lee et al., 2017). PopB is of particular interest as it is believed to provide a novel mechanism of immune response through inducing Th17 immunity (Wu et al., 2012). PopB was identified as a potential antigen using combined reverse vaccinology and screening of antigens stimulating Th-17 using the splenocytes of the mice vaccinated with live-attenuated *P. aeruginosa* vaccine (Montor et al., 2009; Wu et al., 2012). Stimulation of IL-17 production from the mice immunised with PopB was observed, inducing Th17 immune response leading to lung and spleen clearance from the *P. aeruginosa* challenge experiment. Moreover, IL-17 was shown to be essential in LPS serotype-independent protection against *P. aeruginosa* and allied to rapid recruitment of neutrophils (Priebe et al., 2008).

P. aeruginosa strain PAO1 ΔCΔ8ΔF was used as the production strain and was derived from PAO1 that was genetically engineered by deleting key genes required for synthesis of PHA, alginate, and pel polysaccharide (Figure 6) to permit improved recombinant production of PHA$_{MCL}$ beads displaying the vaccine candidates PopB

and combination of PopB and Ag on the surface of the beads. This process was accomplished via genetic engineering of the gene encoding $PhaC1_{Pa}$, the enzyme that catalyzes PHA_{MCL} synthesis facilitating PHA_{MCL} bead assembly, while remaining covalently fused to the surface of PHA_{MCL} beads (Amara & Bernd, 2003). The approach of producing the PHA beads using the target microorganism causing the disease has the potential advantage of avoiding extensive downstream processing because it is not necessary to remove host cell derived impurities (such as host cell proteins, HCPs). Also, the host cell impurities originating from *P. aeruginosa* could be valuable in providing additional antigens, thereby resulting in a larger antigen repertoire that may act as adjuvants to improve the protective immunity to diseases caused by this organism (Lee et al., 2017).

To determine the best orientation for the production of the fusion protein, gene constructs were made to produce both N-terminal and C-terminal fusions of PopB to $PhaC1_{Pa}$. PHA_{MCL} beads were not produced when PopB was fused to the N-terminal of $PhaC1_{Pa}$ and Ag-$PhaC1_{Pa}$ (Figure 10 and 9, respectively). PopB may negatively impact the production of PHA_{MCL} bead; however there are no reports stating the effect of N-terminal fusions inactivating PHA synthase. In fact, the N-terminus has been shown not to be important for PHA synthase activity (Rehm, 2003, 2007). Hence, a different orientation strategy was necessary to produce PHA_{MCL} beads. For these initial investigations, it was determined that the most efficient design of PopB was a C-terminal fusion with $PhaC1_{Pa}$ (Figure 11). A C-terminal fusion of PopB to $PhaC1_{Pa}$ enabled PHA_{MCL} bead formation. Furthermore, the isolated beads showed the $PhaC1_{Pa}$-PopB fusion protein stably and abundantly produced at the bead surface (Figure 17). However, interestingly, the C-terminal fusion of PopB to Ag-$PhaC1_{Pa}$ (Figure 12) abolished PHA_{MCL} bead production. This may be due to PopB inactivating $PhaC1_{Pa}$ when fused to the C-terminus of the enzyme, as the C-terminus of $PhaC1_{Pa}$ was reported to be essential for enzyme activity (Rehm et al., 2002). Furthermore, the C-terminus of PHA synthases was reported to be hydrophobic suggesting its interaction with the hydrophobic core of PHA inclusions (Rehm, 2003). Maintaining the hydrophobic environment of the C-terminus of PHA synthase was shown to be crucial in retaining enzyme activity (Rehm, 2003; Rehm et al., 2002). Hence, the addition of PopB probably disrupted the hydrophobic environment of the C-terminus of $PhaC1_{Pa}$, inactivating the enzyme and preventing PHA_{MCL} bead production.

However, this might not be the only explanation since a C-terminal fusion of only PopB to PhaC1$_{Pa}$ did not disrupt PHA biosynthesis. In some cases like the PhaC1$_{Pa}$-PopBAg combination (Figure 13), PHA$_{MCL}$ beads were produced but the fusion protein was not detectable by SDS-PAGE analysis (Appendix I). The hydrophobic C-terminus of PhaC1$_{Pa}$ predicted to be attached to the hydrophobic PHA core may require a specially designed linker to permit surface exposure of the fusion partner (Jahns & Rehm, 2009). Thus, the very low production of the PhaC1$_{Pa}$-PopBAg fusion protein, only detected in immunoblot (Appendix I) but not on SDS-PAGE, may be due to the insufficient length of the linker used that was not enough to fully display the fusion protein. In future work, the addition of such an optimised linker placed between PhaC and its C-terminal fusion partners may increase its enzymatic activity, potential improving the PHA bead yield and display of desired proteins on bead surfaces.

The composition of PHA$_{MCL}$ beads (3-hydroxybutanoate, 3-hydroxyhexanoate, 3-hydroxyoctanoate, 3-hydroxynonanoate, 3-hydroxydecanoate, 3-hydroxydodecanoate isomer, 3-hydroxydodecanoate, 3-hydroxytetradecanoate, and 3-hydroxyhexadecanote) remained the same regardless of whether there was fusion of PopB or Ag with the wild-type PhaC1$_{Pa}$. However, there was an increase in PHA$_{MCL}$ accumulation in Ag-PhaC1$_{Pa}$ (69% w/w CDW) and PhaC1$_{Pa}$-PopB (52% w/w CDW) beads in comparison to the wild-type PhaC1$_{Pa}$ (46% w/w CDW) suggesting the effect of the fusion on *in vivo* bead accumulation (Figure 16). In addition, an increase in PHA$_{MCL}$ formation was observed in the N-terminal fusion of Ag to PhaC1$_{Pa}$ compared to the C-terminal fusion of PopB to PhaC1$_{Pa}$.

The plasmid encoding PhaC1$_{Pa}$-PopB mediated PHA$_{MCL}$ bead production in *P. aeruginosa* as assessed by FM (Figure 14), TEM (Figure 15) and GC-MS (Figure 16), indicating that the PHA synthase PhaC1$_{Pa}$ remained active catalysing the synthesis of PHA$_{MCL}$ (Rehm, 2006, 2007). Furthermore, SDS-PAGE analysis of the PhaC1$_{Pa}$-PopB fusion protein displayed on the surface of PHA$_{MCL}$ beads showed the production of the full length of fusion protein as indicated by the detection of a dominant protein with the expected molecular weight at 84.7 kDa along with the co-purifying HCPs (Figure 17). The identification of the fusion proteins PhaC1$_{Pa}$, Ag-PhaC1$_{Pa}$ and PhaC1$_{Pa}$-PopB, and the selected HCPs were confirmed by mass spectrometry (Table

18; Appendix II) (Jahns & Rehm, 2009). The results suggest that production of PHA_{MCL} beads in *P. aeruginosa* is challenging as only $PhaC1_{Pa}$-PopB beads were successfully produced at an acceptable yield displaying $PhaC1_{Pa}$-PopB fusion proteins at high copy number. The C-terminal fusion of PopB to $PhaC1_{Pa}$ was successful in bead production but not the N-terminal fusion counterpart. The PopBAg beads were produced in *P. aeruginosa* but the yield of the beads as well as the PopBAg fusion protein displayed on the beads were very low.

4.2 Successful display of PopBAg on the PHA_{SCL} bead surface at high copy number produced in *E.coli* strain ClearColi™

There were several problems producing the PHA_{MCL} beads displaying PopB and the combination of PopB and Ag in *P. aeruginosa*. The inability of *P. aeruginosa* production strain to produce acceptable PHA_{MCL} bead yields and inadequate $PhaC1_{Pa}$-PopBAg fusion protein production on the bead surface opened the way to explore another production strain. Non-PHA producing bacteria such as *E. coli* can manufacture PHA beads via recombinant DNA technology. Several studies have shown genetic engineering of bead-associated proteins such as PHA synthase to display target proteins on the surface of the PHA beads (Blatchford et al., 2012; Grage et al., 2009). Furthermore, foreign proteins displayed on PHA beads were successfully synthesized by the recombinant *E. coli* (Blatchford et al., 2012; Peternel & Komel, 2011). There are several advantages of producing PHA_{SCL} beads in *E. coli* strains including ease of production due to faster growth of *E. coli*, high PHA_{SCL} bead yield, overexpression of proteins attached on the bead surface, and obtaining a high level of purity of the proteins on the beads, making them more reproducible. Previous studies have demonstrated PHA beads displaying the antigens of interest produced in *E. coli* and attaining overexpression of proteins on the bead surface (Parlane et al., 2011; Parlane et al., 2012; Parlane et al., 2009). However, the Gram negative *E. coli* strains used contained LPS endotoxins which may contaminate the beads (Cotten et al., 1994; Parlane et al., 2012). The presence of endotoxins limits the application of PHA beads produced from *E. coli* or requiring extensive downstream processing for human use. Hence, this study utilized the breakthrough development of *E. coli* strain ClearColi™, a novel strain derived from the commonly used BL21 (DE3) strain. The ClearColi™ expression system has the advantage of the production of endotoxin free products (Mamat et al., 2013; Woodard et al., 2007). Recent studies successfully used the *E.*

coli strain ClearColi™ to produce PHA beads displaying antigens (González-Miro et al., 2017; Reyes et al., 2016).

This part of the study aimed to produce functionalized PHA_{SCL} beads-displaying Ag alone, PopB alone, and combination of PopB and Ag from *E. coli* ClearColi™ production strain. Furthermore, it aimed to produce adequate amounts of PHA_{SCL} beads displaying fusion proteins at high copy number. In contrast to the PHA_{MCL} beads produced from *P. aeruginosa*, PHA_{SCL} beads produced from *E. coli* strain ClearColi™ had no host cell proteins (HCPs), which may be a limitation of the *E. coli* production strain as there will be no additional antigens that can act as adjuvants to enhance the immune response. On the other hand, the absence of HCPs and having purer PHA beads produced from *E. coli* can be beneficial for reproducibility purposes (Figure 25). In contrast to the PHA_{MCL} beads from *P. aeruginosa*, PHA_{SCL} beads from *E. coli* were composed only of PHB and demonstrated higher PHA purity at more than 80% of the cellular dry weight, similar to that previously reported (Madison & Huisman, 1999). The N-terminal fusion of Ag and C-terminal fusion of PopB and PopBAg to wild-type PhaC did not impact PHA composition (all showed the presence of PHB), but reduced PHA accumulation of Ag (92% of CDW), PopB (94% of CDW) and PopBAg (94% of CDW) beads compared to the wild-type PhaC (100% of CDW) implying the effect of the fusion on *in vivo* activity (Figure 24). The hybrid genes mediated PHA_{SCL} bead production in *E. coli* strain ClearColi™ as assessed by FM (Figure 22), TEM (Figure 23) and GC-MS (Figure 24), suggesting that the PHA synthase PhaC remained active catalysing the synthesis of PHA_{SCL} (Rehm, 2006, 2007). Moreover, SDS-PAGE analysis of the fusion proteins displayed on the respective PHA beads surface showed the production of the full length of fusion proteins as indicated by the detection of dominant protein with the expected molecular weight (Figure 25). The identification of the fusion proteins were further assessed by mass spectrometry (Appendix II) (Jahns & Rehm, 2009). The results highlighted the simpler and successful approach of using *E. coli* strain ClearColi™ in producing the PHA_{SCL} beads displaying Ag, PopB and combination of PopB and Ag at high copy number. The production of PopBAg beads that was not accomplished in the *P. aeruginosa* production strain was achieved easily using the *E. coli* strain ClearColi™. Although there are no HCPs that can expand the antigenic repertoire like the PHA_{MCL} beads from *P. aeruginosa*, PHA_{SCL} beads from *E. coli* strain ClearColi™ has

advantages of being an endotoxin free product suitable for human use and an easier approach in designing and production of the beads.

4.3 Mice vaccinated with PhaC-PopB and PhaC-PopBAg beads produced from *E. coli* strain ClearColi^{TM} induced high levels of IL-17 cytokine

Immune response was only measured from mice vaccinated with *E. coli* derived PHA_{SCL} beads because obtaining blood from mice vaccinated with *P. aeruginosa* derived PHA_{MCL} beads was unsuccessful. Blood collection in the first experiment with PHA_{MCL} beads from *P. aeruginosa* was performed via tail bleeding and was unsuccessful as insufficient volumes were obtained for the assays. Hence, a different technique of retro-orbital whole blood collection was used for the mice vaccinated with *E. coli* derived PHA_{SCL} beads; this resulted in adequate amounts. This part of the study aimed to determine the effect of the addition of PopB to the surface of the PHA beads on IL-17 cytokine production inducing Th17 immune response. Furthermore, the Th1 and Th2 immune responses of the mice vaccinated with bead samples were assessed.

There are several considerations in developing PHA bead based vaccines. One is the orientation of the fusion proteins. The recognition and uptake of the PHA bead vaccines as antigens by antigen presenting cells (APCs) may differ between the N-terminal fusion of Ag and C-terminal fusion of PopB to PhaC due to their mode of display when presented to immune cells. As discussed in Sections 4.1 and 4.2, both the N-terminal fusion of Ag and C-terminal fusion of PopB did not impact PHA composition produced by *P. aeruginosa* (Figure 16) and *E. coli* (Figure 24). However, PHA accumulation in *E. coli*-derived PHA_{SCL} beads decreased in Ag-PhaC, PhaC-PopB and PhaC-PopBAg beads compared to the wild-type (PhaC), implying an effect of the fusion on *in vivo* activity (Figure 24). In contrast, PHA accumulation was increased in *P. aeruginosa*-derived PHA_{MCL} beads displaying Ag-$PhaC1_{Pa}$ and $PhaC1_{Pa}$-PopB compared to the wild-type ($PhaC1_{Pa}$) (Figure 16). This result is opposite to the findings of Lee et al. (2017) which is possibly due to the different production hosts used for the wild-type $PhaC1_{Pa}$ (PAO1 ΔCΔ8ΔF for both Ag-$PhaC1_{Pa}$ and $PhaC1_{Pa}$-PopB while PAO1 ΔCΔ8ΔFΔP for $PhaC1_{Pa}$). An effect of the fusion on *in vivo* PHA synthase activity of bead formation has been reported for PHA

synthase of *R. eutropha* and was reliant on the PHA synthase fusion partner (Chen et al., 2014; Hooks et al., 2013; Jahns & Rehm, 2009).

Aside from the orientation of the fusion proteins, the amount of the antigen protein that can be administered to animals needs to be taken into account due to the viscosity of the bead suspensions. Lee et al. (2017) were able to use 20 μg of the antigen displayed on *P. aeruginosa* beads in their mice vaccination studies while this study used a lower dosage ranging from 3 to 7 μg. This is one of the limitations of this study. Bead size is another important factor that may influence the immune response. This may have an impact as the PhaC1$_{Pa}$ beads were smaller than the Ag-PhaC1$_{Pa}$ and PhaC1$_{Pa}$-PopB beads, but the cytokine profiles of these beads were not analysed in this study, as mentioned above. Bead size is a main contributing factor inducing particulate antigen uptake by APCs (Bachmann & Jennings, 2010). The antigen uptake mechanism can influence the type of immune response, inducing cell-mediated and/or humoral mediated immunity. However, the optimum size for the most efficient uptake of particulates by APCs is still unknown as effectiveness can be influenced by several factors including surface charge, shape, hydrophobicity/hydrophilicity and mode of administration (Bachmann & Jennings, 2010). The PHA beads produced from *P. aeruginosa* and *E. coli* in this study were all within the range of the accepted effective size (<0.5 μm) for uptake by APCs to elicit an antigen-specific immune response (Xiang et al., 2006).

To assess the mode of immune response induced by the various *E. coli* derived PHA$_{SCL}$ beads, sera of vaccinated mice were stimulated with PopB/PcrH, His$_{10}$-Ag, His$_{10}$-PopBAg and PhaC beads, and IL-17 cytokine profiles were analysed (Figure 29). Mice vaccinated with PhaC-PopB and PhaC-PopBAg beads mediated Th17-type immune response as indicated by the higher production of IL-17 in all stimulations compared to the negative control (Alum). Furthermore, mice vaccinated with PhaC-PopB and PhaC-PopBAg beads had significantly higher IL-17 production than all the vaccination samples from the His$_{10}$-PopBAg and PhaC bead stimulations (Figure 29C and D). This confirms the previous finding of PopB as an effective stimulator of Th17 immune response through increased IL-17 production (Wu et al., 2012). IL-17 plays a key role in sustaining control of host defences against extracellular pathogens and induces a Th17 immune response (Wu et al., 2012). Hence, PhaC-PopB and PhaC-

PopBAg may provide a new mechanism and contribute to maintaining the regulation of host defences that can lead to clearance of infections caused by *P. aeruginosa*.

This part of the study showed that vaccination of mice with *E. coli* derived PHA_{SCL} beads with alum adjuvant induced a robust T cell immune response with both Th1 and Th2 patterns, characterized by enhanced production of IgG2c and IgG1 isotype titers, respectively (Figure 30C). Alum adjuvant was used in this experiment to be consistent with the literature, although PHA beads can act as adjuvant as well (O'Hagan et al., 1991; Singh et al., 2006). After immunization, the subclass of IgG or immunoglobulin induced is considered as an indirect measure of the influence of Th2-type cytokines versus Th1-type cytokines in the immune response (Finkelman et al., 1990). Specifically, IgG1 isotype is elevated in the Th2 type response while IgG2c is enhanced in the Th1 type response (Petrushina et al., 2003). Th1 type immune response is indicated by the production of interferon (IFN)-γ, interleukin (IL)-2 and tumor necrosis factor (TNF)-β, which induce cell-mediated immunity and phagocyte-dependent inflammation. On the other hand, Th2 type response is characterized by the production of IL-4, IL-5, IL-6, IL-9, IL-10, and IL-13, which induce strong antibody responses and accumulation of eosinophils (Romagnani, 2000). Hence, the PHA_{SCL} beads in this study inducing both Th1 and Th2 type immune responses are beneficial in fighting against *P. aeruginosa* by offering a broad immunological response that recruits both antibody and cell-mediated immunity. However, it is worth noting that Th2 immune response may potentially inhibit several functions of phagocytic cells.

To successfully control the diseases caused by many extracellular pathogens such as *P. aeruginosa*, a Th2 immune response, characterized by the production of IgG1 isotype is usually needed. However, in CF patients chronically infected with *P. aeruginosa*, this may not be the case as their response has been suggested to show bias towards a Th2 type immune response when compared to non-infected CF patients or healthy controls (Hartl et al., 2006; Moser et al., 2000). There is increasing evidence that a Th1 type immune response, characterized by increased IgG2c, may be favoured for the successful control of CF patients with acute and chronic infections (Hartl et al., 2006; Moser et al., 2002; Moser et al., 2000). The Th1 type response is also induced by enhanced $CD4^+$ type 1 (Parlane et al., 2014) T cell and activation of Toll-like receptors (TLR) (Van Duin et al., 2006). In this study, significant levels of

antigen-specific serum antibodies were induced with the mice vaccinated with the beads, in particular PhaC-PopB beads (Figure 30C). These antibodies may be due to the B cell class-switching to IgG2c isotype associated Th1 antigen-specific T cells activation (Braun et al., 2012), possibly playing the key role in the clearance of acute infection caused by *P. aeruginosa* (Brennan et al., 1999).

In comparison with the soluble antigens, PopB/PcrH, His_{10}-Ag and His_{10}-PopBAg, the PHA_{SCL} beads induced a significant immune response bias towards a Th2 pattern (Figure 30C). Furthermore, a dominant Th1 response was observed in PhaC-PopB and PhaC-PopBAg compared to the soluble proteins. The stronger immune response induced by PopB/PcrH compared to other vaccination groups may have been due to the higher dose used compared to other soluble proteins and PHA beads (Figure 30A). The His_{10}-Ag and His_{10}-PopBAg soluble proteins also induced a Th2 immune response but weaker than the PHA_{SCL} beads (Figure 30B). Soluble proteins need the addition of appropriate adjuvant and/or delivery system to generate an optimal immune response (Rosalia et al., 2013). Alum might not be the best adjuvant for these soluble proteins, hence the reason for their poor induction of immune response compared to PHA_{SCL} beads.

The results suggest that the addition of PopB to the surface of the PHA_{SCL} beads can increase the production of IL-17 cytokine inducing Th17 immunity. Furthermore, Th1 and Th2 immune responses were induced by all bead samples especially PhaC-PopB and PhaC-PopBAg. The higher immune response of the PHA_{SCL} beads displaying the antigens compared to the soluble counterparts indicates the effectiveness of PHA beads as delivery system of the antigens.

4.4 $PhaC1_{Pa}$-PopB and Ag-PhaC beads gave vaccinated mice some protection against *P. aeruginosa* infection

Mice vaccinated with *E. coli* or *P. aeruginosa* derived PHA beads were challenged with *P. aeruginosa* bacteria and showed the potential effectiveness of Ag-PhaC and $PhaC1_{Pa}$-PopB beads (Figure 31). However, $PhaC1_{Pa}$-PopB beads from *P. aeruginosa* performed better than the Ag-PhaC from *E. coli*, possibly due to the host derived proteins that act as additional antigens present on the beads from *P. aeruginosa* (Lee et al., 2017). Wu et al. (2012) vaccinated mice with PopB/PcrH and showed 62.5%

survival which is higher than the maximum survival observed in this study. This is probably due to the higher dosage used (35 μg vs 3-7 μg used in this study), or may be due to a difference in the adjuvant (curdlan vs alum in this study), mode of immunization (intranasal vs subcutaneous route in this study), strain (*P. aeruginosa* $ExoU^+$ PAO1 strain vs *P. aeruginosa* N13 strain used in this study), or inoculum size used in the bacterial challenge (1 $x10^6$ CFUs vs 2.6 $x10^6$ CFUs in this study). $PhaC1_{Pa}$-PopB beads induced Th1, Th2 and Th17 immune responses and gave some level of protection in mice challenged with *P. aeruginosa*. The dosage used for mice vaccination was 7 μg and increasing the dosage would potentially increase the level of protection. These findings add to the increasing number of reports on the importance of Th17 immune response against an expanding list of pathogens. In addition, PopB and Ag had no synergistic effects as there was no observed enhancement in Th1 and Th2 immune responses or improved survival of the mice vaccinated with PhaC-PopBAg beads compared to those vaccinated with Ag-PhaC. The different components may result in an antagonistic effect such as the delayed viral clearance reported from combinations of epitopes of influenza virus (Crowe et al., 2006).

A limitation of this study is the application of the acute *P. aeruginosa* mouse model to the chronic *P. aeruginosa* infection in humans, particularly CF patients. Individuals with CF have high septum and bronchoalveolar lavage levels of IL-17 (McAllister et al., 2005; Tan et al., 2011). In addition, infiltration of the airway submucosa with Th17 lymphocytes has been shown in humans with CF. However, these reports do not rule out the potential effectiveness of Th17 responses prior to the establishment of the infection. The results suggest the potential efficacy of Ag antigens consisting of OprI, OprF and AlgE as shown in the mice survival in the bacterial challenge. However, synergistic effects of PopB and Ag fusion was not observed in the challenge data but rather resulted to potential antagonistic effects. On the other hand, HCPs from *P. aeruginosa* beads revealed a great advantage and may have acted as additional antigens to boost immune response from mice vaccinated with $PhaC1_{Pa}$-PopB beads. The $PhaC1_{Pa}$-PopB beads can be conjugated with polysaccharides (such as Psl) that may be beneficial for CF patients - an option that can be explored in future works.

4.5 Creation of *cdrA* knockout mutant provides free Psl as potential novel vaccine target

Another antigen, Psl polysaccharide is especially important for CF patients as it is a component of the EPS matrix (Friedman & Kolter, 2004a, 2004b; Jackson et al., 2004). Psl can be found both in mucoid and non-mucoid phenotypes of *P. aeruginosa* (Byrd et al., 2009) and plays a key role in initial reversible surface attachment of the non-mucoid phenotypes of *P. aeruginosa* (Ma et al., 2009). Previous studies have revealed that CdrA directly binds to Psl promoting the formation of biofilm (Borlee et al., 2010). Furthermore, CdrA is essential for the structural integrity of the biofilm which is also dependent on the presence of Psl (Borlee et al., 2010). Protective activity of human monoclonal antibodies (mAbs) targeting Psl biofilm was demonstrated against planktonic bacteria in acute infection models (Ray et al., 2017). Hence, Psl is a potential vaccine target for *P. aeruginosa*. To date, there is still no commercially available Psl that can be used for applications such as conjugation with other proteins and PHA beads for vaccine development. Thus, this study aimed to produce free Psl by generating a *cdrA* knockout mutant.

This study showed the importance of incubation time for successful production of Psl (Figure 34). The production of Psl was significantly higher in the *cdrA* knockout mutant strain than the positive control PAO PAO1 ΔCΔ8ΔF at 12 hours of incubation (Figure 34A). In contrast, longer incubation times (20 and 96 hour periods) failed to detect the production of Psl. The detected Psl is assumed to be free and not bound to CdrA (Borlee et al., 2010). Hence, optimisation of the isolation conditions and exploring different protocols for its purification would lead directly to the production of a pure Psl suitable for several applications. Specifically, the pure Psl could be conjugated to PHA beads developed in this study, especially the promising Ag-PhaC beads produced from *E. coli* and $PhaC1_{Pa}$-PopB beads produced from *P. aeruginosa*. Furthermore, PHA beads displaying CdrA and conjugation with Psl would be a novel and promising target for vaccine development, beneficial especially to the CF patients as both CdrA and Psl are important for biofilm formation and integrity.

4.6 Future directions

P. aeruginosa is extremely problematic due to its multiple drug resistance with the current report of the World Health Organisation notifying it as a critical priority that poses a great threat to human health. The current lack of commercial vaccines aggravates this situation. The particulate vaccines developed in this study, especially the $PhaC1_{Pa}$-PopB beads from *P. aeruginosa* and the Ag-PhaC from *E. coli*, have the potential for further optimization and animal trials. This study provided preliminary results for the potential efficacy of the PHA beads isolated from *P. aeruginosa* and *E. coli*. Mice vaccinated with *P. aeruginosa* beads were not analysed for IgG responses due to the failure of tail bleeding technique to get blood sera. Splenocytes of the immunised mice should be further analysed for various cytokine profiles to determine and confirm the initial findings of induction of Th1, Th2 and Th17 immunity.

PHA beads isolated from both *P. aeruginosa* and *E. coli* requires optimization to improve PHA yield, uniformity, and removal of non-bead associated materials. Bead purification can be efficiently achieved in a scalable method using crossflow filtration (CFF). This purification technique was shown to be more efficient then gradient-based separation methods, leading to significantly cleaner PHA bead products. This study used caustic buffer wash to eliminate the unwanted contaminants but this method is harsh, and may reduce and remove the important antigens. Furthermore, the protein concentration used for mice vaccination in this study ranged from 3 to 7 μg and already showed Th1, Th2 and Th7 immune response. There is a need to increase the expression of the protein antigen on the surface of the PHA beads to obtain higher amounts of proteins and increasing the amount of protein antigens injectable for mice vaccination. This may potentially increase Th1, Th2 and Th17 immune responses critical for fighting against *P. aeruginosa* infections.

Addition of adjuvants have the potential to enhance protective immune response and induce long lasting immunity. Formulation of the PHA beads with the suitable adjuvants should be considered. In this study, alum adjuvant was used in the formulation of the PHA beads but lead to the bias of Th2 immune response especially with Ag-PhaC. Hence, exploring the use of different adjuvants could improve the immune response to PHA bead vaccines. However, there is a limitation of the selection of approved adjuvants for human use. Comparison of mice vaccination with

and without adjuvants is necessary to confirm the adjuvant property of PHA beads. This would also be advantageous in removing the necessity for the additional step of adjuvant formulation.

Optimization of the antigen display such as position of the antigens on the termini of PHA synthase, or rearrangement of the antigenic epitopes, may be necessary to fully display the antigens on the surface of PHA beads. As a result, this may allow better access and presentation of certain antigenic epitopes to APCs. For instance, N-terminal fusion of PopB and PopBAg to PhaC may produce an increased level of fusion proteins displayed on the surface of PHA beads produced from *E. coli*. This study has only shown the C-terminal fusion of PopB and PopBAg to PhaC. Alternatively, N-terminal fusions may lead to better immune responses and increased protective efficacy. In addition, optimisation of the linker may be necessary to enable the surface exposure of the fusion partner especially the PhaC1$_{Pa}$-PopBAg, allowing higher levels of fusion protein production.

This study successfully demonstrated the induction of Th1, Th2 and Th17 immune response in mice vaccinated with *E. coli*-derived PHA beads vaccines compared to the controls using mouse models. A relevant animal model needs to be identified for the assessment of PHA beads vaccine efficacy. Mouse models to study CF pathology are commonly used and are perceived as being cost effective, easily maintained, and are readily available. However, mouse models show limitations like other animal models due to physiological differences between mice and humans. Several factors such as the mouse strain, dose, and route of administration need to be considered for an appropriate mouse model to show vaccine efficacy of the PHA beads. In particular, for the application to CF disease, mucoid and non-mucoid phenotypes of *P. aeruginosa* need to be tested in vaccine efficacy studies.

Psl is a promising antigen that can potentially be conjugated to PHA beads and may be important in CF patients with chronic *P. aeruginosa* infections. There is evidence that CdrA binds directly to Psl, functioning as a Psl cross-linker and/or probably in tethering Psl to the cell surface (Borlee et al., 2010). Hence, the creation of the *cdrA* knockout mutant would enable the production of free Psl. A *cdrA* knockout mutant that produced Psl significantly more than a wild-type Psl producing strain was created.

From this strain, Psl can be isolated, purified and use for several applications such as vaccines, conjugating Psl with the most promising PHA beads developed in this study or perhaps novel PHA beads displaying CdrA. This approach may provide additional protection by inducing greater and wider immune responses earlier in infection.

4.7 Conclusions

This study focused on specific epitopes of antigens and PHA beads as an effective vaccine delivery system. PHA beads were utilised as a delivery system that facilitates the efficient display of vaccine candidate antigens relevant to *P. aeruginosa* infections. Genetic engineering of PHA synthase allowed the manipulation of the enzyme to produce the PHA beads displaying the antigens of interest. These antigen-displaying PHA bead vaccines were produced in engineered production hosts such as *P. aeruginosa* (the target organism) and *E. coli*. Each production strain has its advantages and disadvantages. *P. aeruginosa* production strain has the benefit of host derived proteins that may act as additional antigens, expanding the antigenic repertoire that may help boost the immune response as well as the potential benefit of the reduction for the need of extensive downstream processing to remove impurities. However, there was difficulty in gene construction and production of PHA beads from *P. aeruginosa*. On the other hand, the advantage of producing PHA beads in *E. coli* strain ClearColi^{TM} is an endotoxin-free bead vaccine product that has no limitation for human use. Having the *E. coli* production system could also lead to higher PHA yield, overexpression of the fusion proteins displayed on the surface of the beads and a simpler production process. However, like other subunit vaccines, the limitation of the PHA beads produced from *E. coli* is the limited repertoire of antigens for the disease-causing *P. aeruginosa*. The PHA bead delivery system demonstrated increased immunogenicity of the displayed vaccine candidate antigens over its soluble protein antigens counterpart.

PopB was the antigen of particular interest in this study. PopB was effectively displayed on the surface of PHA beads alone and combined with other antigens (Ag) using the expression systems pHERD20T-2 and pET-14b for *P. aeruginosa* and *E. coli* production strains, respectively. PopB induced Th17 immune response characterised by the increase in IL-17 production. Immunological analysis from the mice vaccinated with *E. coli* derived beads showed a significant increase in IL-17

production with both PhaC-PopB and PhaC-PopBAg beads. This confirmed that PopB can induce Th17 immune response that could help in the clearance of infections caused by extracellular pathogens such *P. aeruginosa*. Furthermore, the PHA bead vaccine especially induced Th1 and Th2 immune responses. PhaC-PopB induced a significantly dominant Th1 type immune response compared to other PHA bead vaccines. Challenge with *P. aeruginosa* showed promising results from the mice vaccinated with PhaC1$_{Pa}$-PopB (*P. aeruginosa* derived bead) and Ag-PhaC (*E. coli* derived bead). However, PhaC1$_{Pa}$-PopB bead vaccine performed better than Ag-PhaC probably because it had additional antigens derived from the pathogen in the form of HCPs, which were able to enhance the immune response. It is expected that further optimisation of the purification techniques and more subsequent animal testing may be done to verify these preliminary observations.

The interest in conjugating the developed PHA bead vaccines in this study with Psl polysaccharide led to the creation of a *cdrA* knockout mutant. Here, the *cdrA* knockout mutant successfully overproduced Psl which is anticipated to be free from the binding of CdrA. Hence, it should be relatively easy to isolate and purify the free Psl for applications such as conjugation with proteins and/or PHA beads for vaccine development.

APPENDIX I

SDS-PAGE and immunoblot analysis of the whole-cell lysate and the PHA$_{MCL}$ beads. PhaC1$_{Pa}$ (62.5 kDa), Ag-PhaC1$_{Pa}$ (75.8 kDa), PhaC1$_{Pa}$-PopB (84.7 kDa) and PhaC1$_{Pa}$-PopB (101.2 kDa) fusion proteins along, with the co-purifying proteins, were isolated from *P. aeruginosa* PAO1 ΔCΔ8ΔF strain containing the respective plasmids. PhaC1$_{Pa}$-PopBAg beads were only apparent in immunoblot analysis (indicated by the red arrows).

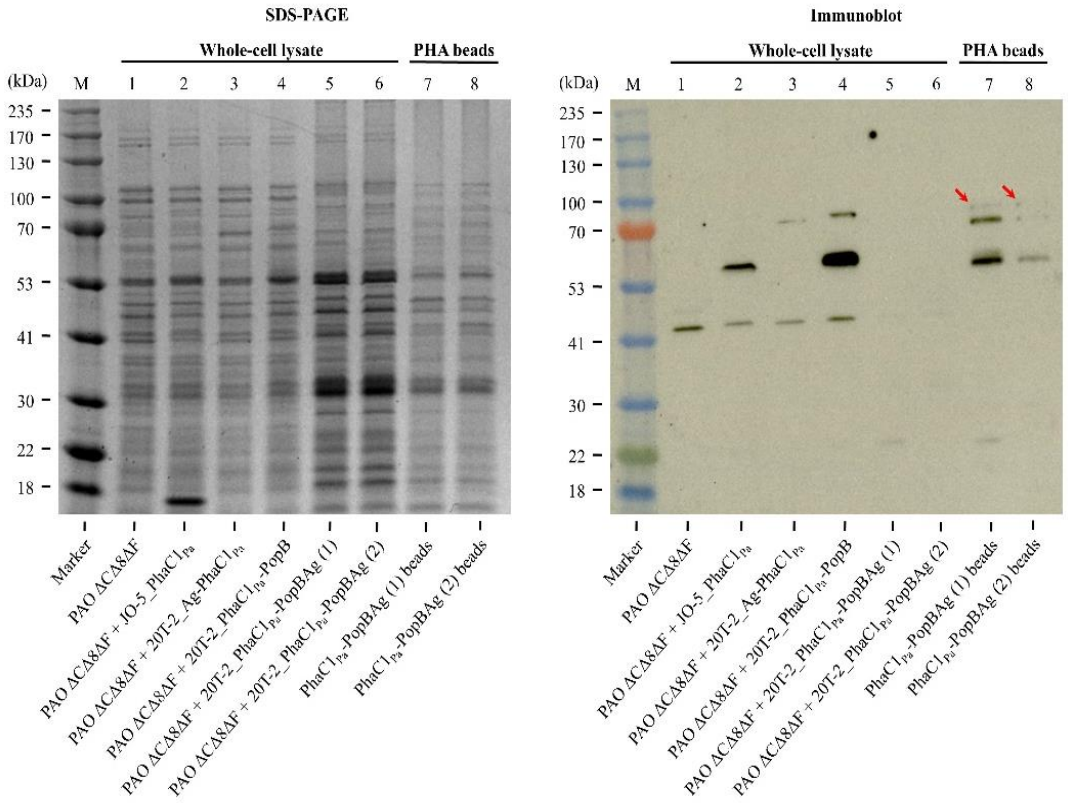

APPENDIX II

Mass Spectrometry (MS) analysis of PhaC1$_{Pa}$, PhaC1$_{Pa}$-fusion proteins, PhaC, PhaC-fusion proteins, and soluble proteins.

Protein/Protein Sequence	Percent fragments assigned to the various protein regions
PhaC1$_{Pa}$ and PhaC1$_{Pa}$-fusion proteins from *P. aeruginosa*	
PhaC1 (MW: 62.5 kDa) 1 MSQKNNNELP KQAAENTLNL NPVIGIRGKD LLTSARMVLL QAVRQPLHSA 51 RHVAHFSLEL KNVLLGQSEL RPGDDDRRFS DPAWSQNPLY KRYMQTYLAW 101 RKELHSWISH SDLSPQDISR GQFVINLLTE AMSPTNSLSN PAAVKRFFET 151 GGKSLLDGLG HLAKDLVNNG GMPSQVDMDA FEVGKNLATT EGAVVFRNDV 201 LELIQYRPIT ESVHERPLLV VPPQINKFYV FDLSPDKSLA RFCLRNGVQT 251 FIVSWRNPTK SQREWGLTTY IEALKEAIEV VLSITGSKDL NLLGACSGGI 301 TTATLVGHYV ASGEKKVNAF TQLVSVLDFE LNTQVALFAD EKTLEAAKRR 351 SYQSGVLEGK DMAKVFAWMR PNDLIWNYWV NNYLLGNQPP AFDILYWNND 401 TTRLPAALHG EFVELFKSNP LNRPGALEVS GTPIDLKQVT CDFYCVAGLN 451 DHITPWESCY KSARLLGGKC EFILSNSGHI QSILNPPGNP KARFMTNPEL 501 PAEPKAWLEQ AGKHADSWWL HWQQWLAERS GKTRKAPASL GNKTYPAGEA 551 APGTYVHER	PhaC1 (73%): N5- R27, F79-K91, Y93-R197, F228-R241, N246-R256, E264-K342, S351-K461, C470-K491,H514-R529, T544-R559
Ag-PhaC1 (MW: 75.8 kDa) Ag 1 MHLRRPGEEV NLTTTTVDDR RIATGKQNAT AEGRAINRRV ENATAEGRAI 51 NRRVENATAE GRAINRRVES SHSKETEARL TATEDAAARA QARADEAYRK 101 ADEALGAAQK AQQTADEANE RALRMLEKASRK PhaC1 1 MSQKNNNELP KQAAENTLNL NPVIGIRGKD LLTSARMVLL QAVRQPLHSA 51 RHVAHFSLEL KNVLLGQSEL RPGDDDRRFS DPAWSQNPLY KRYMQTYLAW 101 RKELHSWISH SDLSPQDISR GQFVINLLTE AMSPTNSLSN PAAVKRFFET 151 GGKSLLDGLG HLAKDLVNNG GMPSQVDMDA FEVGKNLATT EGAVVFRNDV 201 LELIQYRPIT ESVHERPLLV VPPQINKFYV FDLSPDKSLA RFCLRNGVQT 251 FIVSWRNPTK SQREWGLTTY IEALKEAIEV VLSITGSKDL NLLGACSGGI 301 TTATLVGHYV ASGEKKVNAF TQLVSVLDFE LNTQVALFAD EKTLEAAKRR 351 SYQSGVLEGK DMAKVFAWMR PNDLIWNYWV NNYLLGNQPP AFDILYWNND 401 TTRLPAALHG EFVELFKSNP LNRPGALEVS GTPIDLKQVT CDFYCVAGLN 451 DHITPWESCY KSARLLGGKC EFILSNSGHI QSILNPPGNP KARFMTNPEL 501 PAEPKAWLEQ AGKHADSWWL HWQQWLAERS GKTRKAPASL GNKTYPAGEA 551 APGTYVHER	Ag (13%): R4-R20 PhaC1 (73%): Q12-R27, F79-K91, Y93-R146, D165-R197, L201-K237, N246-R256, E264-K342, R350-K461, C470-K491, H514-R529, T544-R559
PhaC1-PopB (MW: 84.7 kDa) PhaC1 1 MSQKNNNELP KQAAENTLNL NPVIGIRGKD LLTSARMVLL QAVRQPLHSA 51 RHVAHFSLEL KNVLLGQSEL RPGDDDRRFS DPAWSQNPLY KRYMQTYLAW 101 RKELHSWISH SDLSPQDISR GQFVINLLTE AMSPTNSLSN PAAVKRFFET 151 GGKSLLDGLG HLAKDLVNNG GMPSQVDMDA FEVGKNLATT EGAVVFRNDV 201 LELIQYRPIT ESVHERPLLV VPPQINKFYV FDLSPDKSLA RFCLRNGVQT 251 FIVSWRNPTK SQREWGLTTY IEALKEAIEV VLSITGSKDL NLLGACSGGI	PhaC1 (71%): Q12-R27, F79-K91, Y93-R146, D165-K237, N246-R256, E264-K342, V365-K461, C470-K491, H514-R529, T544-R559

301 TTATLVGHYV ASGEKKVNAF TQLVSVLDFE LNTQVALFAD EKTLEAAKRR 351 SYQSGVLEGK DMAKVFAWMR PNDLIWNYWV NNYLLGNQPP AFDILYWNND 401 TTRLPAALHG EFVELFKSNP LNRPGALEVS GTPIDLKQVT CDFYCVAGLN 451 DHITPWESCY KSARLLGGKC EFILSNSGHI QSILNPPGNP KARFMTNPEL 501 PAEPKAWLEQ AGKHADSWWL HWQQWLAERS GKTRKAPASL GNKTYPAGEA 551 APGTYVHER PopB 1 FGWISAIASI IVGAIMVATG VGAAAGALMI AGGVMGVVSQ SVQQAAADGL 51 ISKEVMEKLG PALMGIEMAV ALLAAVVSFG GSAVGGLARL GAKIGGKAAE 101 MTASLASKVA DLGGKFGSLA GQSLSHSLKL GVQVSDLTLD VANGAAQATH 151 SGFQAKAANR QADVQESRAD LTTLQGVIER LKEELSRMLE AFQEIMERIF 201 AMLQAKGETL HNLSSRPAAI	PopB (34%): A98-K108, F114-K156, A169-R180, M188-R198
PhaC- and PhaC-fusion proteins from *E. coli*	
PhaC (MW: 64.2 kDa) 1 MATGKGAAAS TQEGKSQPFK VTPGPFDPAT WLEWSRQWQG TEGNGHAAAS 51 GIPGLDALAG VKIAPAQLGD IQQRYMKDFS ALWQAMAEGK AEATGPLHDR 101 RFAGDAWRTN LPYRFAAAFY LLNARALTEL ADAVEADAKT RQRIRFAISQ 151 WVDAMSPANF LATNPEAQRL LIESGGESLR AGVRNMMEDL TRGKISQTDE 201 SAFEVGRNVA VTEGAVVFEN EYFQLLQYKP LTDKVHARPL LMVPPCINKY 251 YILDLQPESS LVRHVVEQGH TVFLVSWRNP DASMAGSTWD DYIEHAAIRA 301 IEVARDISGQ DKINVLGFCV GGTIVSTALA VLAARGEHPA ASVTLLTTLL 351 DFADTGILDV FVDEGHVQLR EATLGGGAGA PCALLRGLEL ANTFSFLRPN 401 DLVWNYVVDN YLKGNTPVPF DLLFWNGDAT NLPGPWYCWY LRHTYLQNEL 451 KVPGKLTVCG VPVDLASIDV PTYIYGSRED HIVPWTAAYA STALLANKLR 501 FVLGASGHIA GVINPPAKNK RSHWTNDALP ESPQQWLAGA IEHHGSWWPD 551 WTAWLAGQAG AKRAAPANYG NARYRAIEPA PGRYVKAKA	PhaC (79%): V21-R74, D78-K90, F115-T140, F146-R180, N185-K234, Y250-R299, D306-R442, L456-K498, F501-K518, R521-562
Ag-PhaC (MW: 78.6 kDa) Ag 1 MSSHSKETEA RLTATEDAAA RAQARADEAY RKADEALGAA QKAQQTADEA 51 NERALRMLEK ASRKNATAEG RAINRRVENA TAEGRAINRR VENATAEGRA 101 INRRVENLTT TTVDDRRIAT GKQHLRRPGEEV PhaC 1 MATGKGAAAS TQEGKSQPFK VTPGPFDPAT WLEWSRQWQG TEGNGHAAAS 51 GIPGLDALAG VKIAPAQLGD IQQRYMKDFS ALWQAMAEGK AEATGPLHDR 101 RFAGDAWRTN LPYRFAAAFY LLNARALTEL ADAVEADAKT RQRIRFAISQ 151 WVDAMSPANF LATNPEAQRL LIESGGESLR AGVRNMMEDL TRGKISQTDE 201 SAFEVGRNVA VTEGAVVFEN EYFQLLQYKP LTDKVHARPL LMVPPCINKY 251 YILDLQPESS LVRHVVEQGH TVFLVSWRNP DASMAGSTWD DYIEHAAIRA 301 IEVARDISGQ DKINVLGFCV GGTIVSTALA VLAARGEHPA ASVTLLTTLL 351 DFADTGILDV FVDEGHVQLR EATLGGGAGA PCALLRGLEL ANTFSFLRPN 401 DLVWNYVVDN YLKGNTPVPF DLLFWNGDAT NLPGPWYCWY LRHTYLQNEL 451 KVPGKLTVCG VPVDLASIDV PTYIYGSRED HIVPWTAAYA STALLANKLR 501 FVLGASGHIA GVINPPAKNK RSHWTNDALP ESPQQWLAGA IEHHGSWWPD 551 WTAWLAGQAG AKRAAPANYG NARYRAIEPA PGRYVKAKA	Ag (11%): R101-I116 PhaC (79%): V21-R74, D78-K90, F115-T140, F146-R180, N185-K234, Y250-R299, D306-R442, L456-K498, F501-K518, S522-562
PhaC-PopB (MW: 86.5 kDa) PhaC 1 MATGKGAAAS TQEGKSQPFK VTPGPFDPAT WLEWSRQWQG TEGNGHAAAS 51 GIPGLDALAG VKIAPAQLGD IQQRYMKDFS ALWQAMAEGK AEATGPLHDR	PhaC (72%): V21-R74, D78-K90, F115-T140, F146-R180,

101 RFAGDAWRTN LPYRFAAAFY LLNARALTEL ADAVEADAKT RQRIRFAISQ 151 WVDAMSPANF LATNPEAQRL LIESGGESLR AGVRNMMEDL TRGKISQTDE 201 SAFEVGRNVA VTEGAVVFEN EYFQLLQYKP LTDKVHARPL LMVPPCINKY 251 YILDLQPESS LVRHVVEQGH TVFLVSWRNP DASMAGSTWD DYIEHAAIRA 301 IEVARDISGQ DKINVLGFCV GGTIVSTALA VLAARGEHPA ASVTLLTTLL 351 DFADTGILDV FVDEGHVQLR EATLGGGAGA PCALLRGLEL ANTFSFLRPN 401 DLVWNYVVDN YLKGNTPVPF DLLFWNGDAT NLPGPWYCWY LRHTYLQNEL 451 KVPGKLTVCG VPVDLASIDV PTYIYGSRED HIVPWTAAYA STALLANKLR 501 FVLGASGHIA GVINPPAKNK RSHWTNDALP ESPQQWLAGA IEHHGSWWPD 551 WTAWLAGQAG AKRAAPANYG NARYRAIEPA PGRYVKAKA PopB 1 FGWISAIASI IVGAIMVATG VGAAAGALMI AGGVMGVVSQ SVQQAAADGL 51 ISKEVMEKLG PALMGIEMAV ALLAAVVSFG GSAVGGLARL GAKIGGKAAE 101 MTASLASKVA DLGGKFGSLA GQSLSHSLKL GVQVSDLTLD VANGAAQATH 151 SGFQAKAANR QADVQESRAD LTTLQGVIER LKEELSRMLE AFQEIMERIF 201 AMLQAKGETL HNLSSRPAAI	I195-K234, Y250-R299, I301-R386, D401-R442, K451-498, F501-K518, S522-K562 PopB (40%): A98-K108, F114-K156, A169-R180, M188-R198, G207-I220
PhaC-PopBAg (MW: 101.2 kDa) PhaC 1 MATGKGAAAS TQEGKSQPFK VTPGPFDPAT WLEWSRQWQG TEGNGHAAAS 51 GIPGLDALAG VKIAPAQLGD IQQRYMKDFS ALWQAMAEGK AEATGPLHDR 101 RFAGDAWRTN LPYRFAAAFY LLNARALTEL ADAVEADAKT RQRIRFAISQ 151 WVDAMSPANF LATNPEAQRL LIESGGESLR AGVRNMMEDL TRGKISQTDE 201 SAFEVGRNVA VTEGAVVFEN EYFQLLQYKP LTDKVHARPL LMVPPCINKY 251 YILDLQPESS LVRHVVEQGH TVFLVSWRNP DASMAGSTWD DYIEHAAIRA 301 IEVARDISGQ DKINVLGFCV GGTIVSTALA VLAARGEHPA ASVTLLTTLL 351 DFADTGILDV FVDEGHVQLR EATLGGGAGA PCALLRGLEL ANTFSFLRPN 401 DLVWNYVVDN YLKGNTPVPF DLLFWNGDAT NLPGPWYCWY LRHTYLQNEL 451 KVPGKLTVCG VPVDLASIDV PTYIYGSRED HIVPWTAAYA STALLANKLR 501 FVLGASGHIA GVINPPAKNK RSHWTNDALP ESPQQWLAGA IEHHGSWWPD 551 WTAWLAGQAG AKRAAPANYG NARYRAIEPA PGRYVKAKA PopB 1 FGWISAIASI IVGAIMVATG VGAAAGALMI AGGVMGVVSQ SVQQAAADGL 51 ISKEVMEKLG PALMGIEMAV ALLAAVVSFG GSAVGGLARL GAKIGGKAAE 101 MTASLASKVA DLGGKFGSLA GQSLSHSLKL GVQVSDLTLD VANGAAQATH 151 SGFQAKAANR QADVQESRAD LTTLQGVIER LKEELSRMLE AFQEIMERIF 201 AMLQAKGETL HNLSSRPAAI Ag 1 SSHSKETEAR LTATEDAAAR AQARADEAYR KADEALGAAQ KAQQTADEAN 51 ERALRMLEKA SRKNATAEGR AINRRVENAT AEGRAINRRV ENATAEGRAIN 101 RRVENLTTTTV DDRRIATGKQ HLRRPGEEV	PhaC (70%): V21-R74, D78-K90, F115-T140, F146-R180, I195-K234, Y250-R299, D306-R386, G414-R442, L456-K498, F501-K518, R521-K562 PopB (34%): A98-K108, F114-K156, A169-R180, M188-R198 Ag (11%): R101-I116
Soluble proteins from *E. coli*	
Ag (MW: 17.1 kDa) 1 SSHSKETEAR LTATEDAAAR AQARADEAYR KADEALGAAQ KAQQTADEAN 51 ERALRMLEKA SRKNATAEGR AINRRVENAT AEGRAINRRV ENATAEGRAIN 101 RRVENLTTTTV DDRRIATGKQ HLRRPGEEV	Ag (39.7%): R10-A21, R30-A53, R101-I116

PopBAg (MW: 39.3 kDa)	
PopB 1 FGWISAIASI IVGAIMVATG VGAAAGALMI AGGVMGVVSQ SVQQAAADGL 51 ISKEVMEKLG PALMGIEMAV ALLAAVVSFG GSAVGGLARL GAKIGGKAAE 101 MTASLASKVA DLGGKFGSLA GQSLSHSLKL GVQVSDLTLD VANGAAQATH 151 SGFQAKAANR QADVQESRAD LTTLQGVIER LKEELSRMLE AFQEIMERIF 201 AMLQAKGETL HNLSSRPAAI	**P**opB (43%): A98-K108, F114-R180, M188-K206
Ag 1 SSHSKETEAR LTATEDAAAR AQARADEAYR KADEALGAAQ KAQQTADEAN 51 ERALRMLEKA SRKNATAEGR AINRRVENAT AEGRAINRRV ENATAEGRAIN 101 RRVENLTTTTV DDRRIATGKQ HLRRPGEEV	Ag (18%): R10-A21, R101-I116

*Confirmed sequences are in red colour.

APPENDIX III

Protein profile analysis of the whole-cell lysate and the isolated soluble proteins separated by SDS-PAGE and gel stained with Coomassie Blue. Several *E. coli* strains; ClearColi™ BL21 (DE3), BL21 (DE3), Star™ (DE3), Star™ (DE3) pLysS and Shuffle were used to produce and isolate PopBAg. Overexpression of the PopBAg was observed in pLysS, Star™ (DE3) pLysS and Shuffle. The soluble proteins were purified using the Zymo (Irvine, CA), His-Spin Protein Miniprep affinity purification (Section 2.8.4). The pET-16b_His_{10}-Ag, pET-16b_His_{10}-PopBAg and the His_{10}-PopBAg are indicated with red arrows.

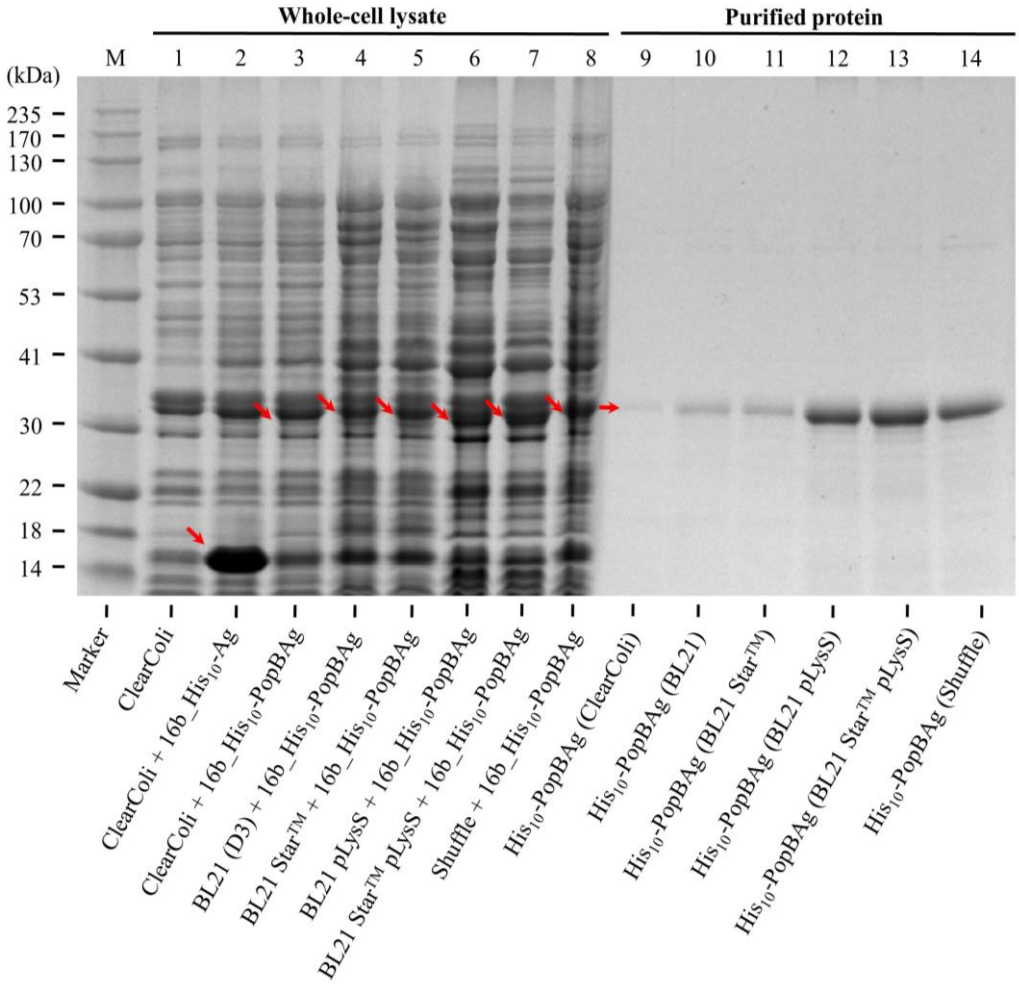

References

Abbas, A. K., Murphy, K. M., & Sher, A. (1996). Functional diversity of helper T lymphocytes. *Nature, 383*(6603), 787-793.

Aguilar, J., & Rodriguez, E. (2007). Vaccine adjuvants revisited. *Vaccine, 25*(19), 3752-3762.

Amara, A. A., & Bernd, H. (2003). Replacement of the catalytic nucleophile cysteine-296 by serine in class II polyhydroxyalkanoate synthase from *Pseudomonas aeruginosa*-mediated synthesis of a new polyester: identification of catalytic residues. *Biochemical Journal, 374*(2), 413-421.

Arnau, J., Lauritzen, C., Petersen, G. E., & Pedersen, J. (2006). Current strategies for the use of affinity tags and tag removal for the purification of recombinant proteins. *Protein Expression and Purification, 48*(1), 1-13.

Arnon, R. (2006). A novel approach to vaccine design-epitope-based vaccines. *The FEBS Journal, 273*, 33-34.

Bachmann, M. F., & Jennings, G. T. (2010). Vaccine delivery: a matter of size, geometry, kinetics and molecular patterns. *Nature Reviews Immunology, 10*(11), 787-796. doi:10.1038/nri2868

Banki, M. R., Gerngross, T. U., & Wood, D. W. (2005). Novel and economical purification of recombinant proteins: Intein-mediated protein purification using in vivo polyhydroxybutyrate (PHB) matrix association. *Protein Science, 14*(6), 1387-1395.

Baumann, U., Mansouri, E., & Von Specht, B.-U. (2004). Recombinant OprF–OprI as a vaccine against *Pseudomonas aeruginosa* infections. *Vaccine, 22*(7), 840-847.

Baxter, D. (2007). Active and passive immunity, vaccine types, excipients and licensing. *Occupational Medicine-Oxford, 57*(8), 552-556. doi:10.1093/occmed/kqm110

Blatchford, P. A., Scott, C., French, N., & Rehm, B. H. (2012). Immobilization of organophosphohydrolase OpdA from *Agrobacterium radiobacter* by overproduction at the surface of polyester inclusions inside engineered *Escherichia coli*. *Biotechnology and Bioengineering, 109*(5), 1101-1108.

Borlee, B. R., Goldman, A. D., Murakami, K., Samudrala, R., Wozniak, D. J., & Parsek, M. R. (2010). *Pseudomonas aeruginosa* uses a cyclic-di-GMP-regulated adhesin to reinforce the biofilm extracellular matrix. *Molecular Microbiology, 75*(4), 827-842.

Brandl, H., Gross, R. A., Lenz, R. W., & Fuller, R. C. (1988). *Pseudomonas oleovorans* as a source of poly (β-hydroxyalkanoates) for potential applications as biodegradable polyesters. *Applied and Environmental Microbiology, 54*(8), 1977-1982.

Braun, M., Jandus, C., Maurer, P., Hammann-Haenni, A., Schwarz, K., Bachmann, M. F., . . . Romero, P. (2012). Virus-like particles induce robust human T-helper cell responses. *European Journal of Immunology, 42*(2), 330-340.

Brennan, F. R., Jones, T. D., Gilleland, L. B., Bellaby, T., Xu, F., North, P. C., . . . Johnson, J. E. (1999). *Pseudomonas aeruginosa* outer-membrane protein F epitopes are highly immunogenic in mice when expressed on a plant virus. *Microbiology, 145*(1), 211-220.

Byrd, M. S., Sadovskaya, I., Vinogradov, E., Lu, H. P., Sprinkle, A. B., Richardson, S. H., . . . Wozniak, D. J. (2009). Genetic and biochemical analyses of the *Pseudomonas aeruginosa* Psl exopolysaccharide reveal overlapping roles for

polysaccharide synthesis enzymes in Psl and LPS production. *Molecular Microbiology, 73*(4), 622-638. doi:10.1111/j.1365-2958.2009.06795.x

Campisano, A., Overhage, J., & Rehm, B. H. (2008). The polyhydroxyalkanoate biosynthesis genes are differentially regulated in planktonic-and biofilm-grown *Pseudomonas aeruginosa*. *Journal of Biotechnology, 133*(4), 442-452.

Campodonico, V. L., Llosa, N. J., Grout, M., Doring, G., Maira-Litran, T., & Pier, G. B. (2010). Evaluation of flagella and flagellin of *Pseudomonas aeruginosa* as vaccines. *Infection and Immunity, 78*(2), 746-755. doi:10.1128/iai.00806-09

Chen, S., Parlane, N. A., Lee, J., Wedlock, D. N., Buddle, B. M., & Rehm, B. H. (2014). New skin test for detection of bovine tuberculosis on the basis of antigen-displaying polyester inclusions produced by recombinant *Escherichia coli*. *Applied and Environmental Microbiology, 80*(8), 2526-2535.

Choi, K.-H., Kumar, A., & Schweizer, H. P. (2006). A 10-min method for preparation of highly electrocompetent *Pseudomonas aeruginosa* cells: application for DNA fragment transfer between chromosomes and plasmid transformation. *Journal of Microbiological Methods, 64*(3), 391-397.

Colvin, K. M., Irie, Y., Tart, C. S., Urbano, R., Whitney, J. C., Ryder, C., . . . Parsek, M. R. (2012). The Pel and Psl polysaccharides provide *Pseudomonas aeruginosa* structural redundancy within the biofilm matrix. *Environmental Microbiology, 14*(8), 1913-1928.

Cotten, M., Baker, A., Saltik, M., Wagner, E., & Buschle, M. (1994). Lipopolysaccharide is a frequent contaminant of plasmid DNA preparations and can be toxic to primary cells in the presence of adenovirus. *Gene Therapy*, 239-246.

Courtney, J., Ennis, M., & Elborn, J. (2004). Cytokines and inflammatory mediators in cystic fibrosis. *Journal of Cystic Fibrosis, 3*(4), 223-231.

Crowe, S. R., Miller, S. C., & Woodland, D. L. (2006). Identification of protective and non-protective T cell epitopes in influenza. *Vaccine, 24*(4), 452-456.

Cui, Z., Han, D., Sun, X., Zhang, M., Feng, X., Sun, C., . . . Han, W. (2015). Mannose-modified chitosan microspheres enhance OprF-OprI-mediated protection of mice against *Pseudomonas aeruginosa* infection via induction of mucosal immunity. *Applied Microbiology and Biotechnology, 99*(2), 667-680.

Dadley-Moore, D. (2006). Learning from our successes. *Nature Reviews Immunology, 6*(4), 256-257.

Discola, K. F., Förster, A., Boulay, F., Simorre, J.-P., Attree, I., Dessen, A., & Job, V. (2014). Membrane and chaperone recognition by the major translocator protein PopB of the type III secretion system of *Pseudomonas aeruginosa*. *Journal of Biological Chemistry, 289*(6), 3591-3601.

Doering, G. (2010). Prevention of *Pseudomonas aeruginosa* infection in cystic fibrosis patients. *International Journal of Medical Microbiology, 300*(8), 573-577. doi:10.1016/j.ijmm.2010.08.010

Döring, G., Meisner, C., & Stern, M. (2007). A double-blind randomized placebo-controlled phase III study of a *Pseudomonas aeruginosa* flagella vaccine in cystic fibrosis patients. *Proceedings of the National Academy of Sciences, 104*(26), 11020-11025.

Doring, G., & Pier, G. B. (2008). Vaccines and immunotherapy against *Pseudomonas aeruginosa*. *Vaccine, 26*(8), 1011-1024. doi:10.1016/j.vaccine.2007.12.007

Douglas, M. W., Mulholland, K., Denyer, V., & Gottlieb, T. (2001). Multi-drug resistant *Pseudomonas aeruginosa* outbreak in a burns unit—an infection control study. *Burns, 27*(2), 131-135.

Draper, J., Du, J., Hooks, D., Lee, J., Parlane, N., & Rehm, B. (2013). Polyhydroxyalkanoate inclusions: polymer synthesis, self-assembly, and display technology. *Bionanotechnology biological self-assembly and its applications. Caister Academic Press, Norfolk*, 1-36.

Draper, J., & Rehm, B. (2012). Engineering bacteria to manufacture functionalized polyester beads. *Bioengineered, 3*(4), 203-208.

Engel, J., & Balachandran, P. (2009). Role of *Pseudomonas aeruginosa* type III effectors in disease. *Current Opinion in Microbiology, 12*(1), 61-66.

Esposito, D., & Chatterjee, D. K. (2006). Enhancement of soluble protein expression through the use of fusion tags. *Current Opinion in Biotechnology, 17*(4), 353-358.

Finkelman, F. D., Holmes, J., Katona, I. M., Urban Jr, J. F., Beckmann, M. P., Park, L. S., . . . Paul, W. E. (1990). Lymphokine control of in vivo immunoglobulin isotype selection. *Annual Review of Immunology, 8*(1), 303-333.

Flemming, H.-C., & Wingender, J. (2010). The biofilm matrix. *Nature Reviews Microbiology, 8*(9), 623-633.

Franklin, M. J., Nivens, D. E., Weadge, J. T., & Howell, P. L. (2011). Biosynthesis of the *Pseudomonas aeruginosa* extracellular polysaccharides, alginate, Pel, and Psl. *Frontiers in Microbiology, 2*.

Friedman, L., & Kolter, R. (2004a). Genes involved in matrix formation in *Pseudomonas aeruginosa* PA14 biofilms. *Molecular Microbiology, 51*(3), 675-690.

Friedman, L., & Kolter, R. (2004b). Two genetic loci produce distinct carbohydrate-rich structural components of the *Pseudomonas aeruginosa* biofilm matrix. *Journal of Bacteriology, 186*(14), 4457-4465.

Friedrich, B., Hogrefe, C., & Schlegel, H. (1981). Naturally occurring genetic transfer of hydrogen-oxidizing ability between strains of *Alcaligenes eutrophus*. *Journal of Bacteriology, 147*(1), 198-205.

Gerngross, T., & Martin, D. (1995). Enzyme-catalyzed synthesis of poly [(R)-(-)-3-hydroxybutyrate]: formation of macroscopic granules in vitro. *Proceedings of the National Academy of Sciences, 92*(14), 6279-6283.

Ghafoor, A., Hay, I. D., & Rehm, B. H. (2011). Role of exopolysaccharides in *Pseudomonas aeruginosa* biofilm formation and architecture. *Applied and Environmental Microbiology, 77*(15), 5238-5246.

Gibson, R. L., Burns, J. L., & Ramsey, B. W. (2003). Pathophysiology and management of pulmonary infections in cystic fibrosis. *American Journal of Respiratory and Critical Care Medicine, 168*(8), 918-951.

Gilleland, L. B., & Gilleland, H. (1995). Synthetic peptides representing two protective, linear B-cell epitopes of outer membrane protein F of *Pseudomonas aeruginosa* elicit whole-cell-reactive antibodies that are functionally pseudomonad specific. *Infection and Immunity, 63*(6), 2347-2351.

González-Miro, M., Rodríguez-Noda, L., Fariñas-Medina, M., García-Rivera, D., Vérez-Bencomo, V., & Rehm, B. H. (2017). Self-assembled particulate PsaA as vaccine against *Streptococcus pneumoniae* infection. *Heliyon, 3*(4), e00291.

Grage, K., Jahns, A. C., Parlane, N., Palanisamy, R., Rasiah, I. A., Atwood, J. A., & Rehm, B. H. (2009). Bacterial polyhydroxyalkanoate granules: biogenesis, structure, and potential use as nano-/micro-beads in biotechnological and biomedical applications. *Biomacromolecules, 10*(4), 660-669.

Hanahan, D. (1983). Studies on transformation of *Escherichia coli* with plasmids. *Journal of Molecular Biology, 166*(4), 557-580.

Hanefeld, U., Gardossi, L., & Magner, E. (2009). Understanding enzyme immobilisation. *Chemical Society Reviews, 38*(2), 453-468.

Harrington, L. E., Hatton, R. D., Mangan, P. R., Turner, H., Murphy, T. L., Murphy, K. M., & Weaver, C. T. (2005). Interleukin 17–producing CD4+ effector T cells develop via a lineage distinct from the T helper type 1 and 2 lineages. *Nature Immunology, 6*(11), 1123.

Hartl, D., Griese, M., Kappler, M., Zissel, G., Reinhardt, D., Rebhan, C., . . . Krauss-Etschmann, S. (2006). Pulmonary TH2 response in *Pseudomonas aeruginosa*–infected patients with cystic fibrosis. *Journal of Allergy and Clinical Immunology, 117*(1), 204-211.

Hauser, A. R. (2009). The type III secretion system of *Pseudomonas aeruginosa*: infection by injection. *Nature Reviews Microbiology, 7*(9), 654-665.

Hazer, B., & Steinbüchel, A. (2007). Increased diversification of polyhydroxyalkanoates by modification reactions for industrial and medical applications. *Applied Microbiology and Biotechnology, 74*(1), 1-12.

Hilleman, M. R. (2000). Vaccines in historic evolution and perspective: a narrative of vaccine discoveries. *Vaccine, 18*(15), 1436-1447.

Holder, I. A. (2004). *Pseudomonas* immunotherapy: a historical overview. *Vaccine, 22*(7), 831-839. doi:10.1016/j.vaccine.2003.11.028

Hooks, D. O., Blatchford, P. A., & Rehm, B. H. (2013). Bioengineering of bacterial polymer inclusions catalyzing the synthesis of N-acetylneuraminic acid. *Applied and Environmental Microbiology, 79*(9), 3116-3121.

Huang, D. B., Wu, J. J., & Tyring, S. K. (2004). A review of licensed viral vaccines, some of their safety concerns, and the advances in the development of investigational viral vaccines. *Journal of Infection, 49*(3), 179-209.

Hughes, E. E., Gilleland, L. B., & Gilleland, H. (1992). Synthetic peptides representing epitopes of outer membrane protein F of *Pseudomonas aeruginosa* that elicit antibodies reactive with whole cells of heterologous immunotype strains of *P. aeruginosa*. *Infection and Immunity, 60*(9), 3497-3503.

Jackson, K., Starkey, M., Kremer, S., Parsek, M., & Wozniak, D. (2004). Identification of psl, a locus encoding a potential exopolysaccharide that Is 612 essential for *Pseudomonas aeruginosa* PAO1 biofilm formation. *Journal of Bacteriology, 613*(186), 4466-4475.

Jahns, A. C., Haverkamp, R. G., & Rehm, B. H. (2008). Multifunctional inorganic-binding beads self-assembled inside engineered bacteria. *Bioconjugate Chemistry, 19*(10), 2072-2080.

Jahns, A. C., & Rehm, B. H. (2009). Tolerance of the *Ralstonia eutropha* class I polyhydroxyalkanoate synthase for translational fusions to its C terminus

reveals a new mode of functional display. *Applied and Environmental Microbiology, 75*(17), 5461-5466.

Jensen, P. Ø., Givskov, M., Bjarnsholt, T., & Moser, C. (2010). The immune system vs. *Pseudomonas aeruginosa* biofilms. *FEMS Immunology & Medical Microbiology, 59*(3), 292-305.

Kallerup, R. S., & Foged, C. (2015). Classification of vaccines *Subunit vaccine delivery* (pp. 15-29): Springer.

Keshavarz, T., & Roy, I. (2010). Polyhydroxyalkanoates: bioplastics with a green agenda. *Current Opinion in Microbiology, 13*(3), 321-326.

Knirel, Y. A. (1990). Polysaccharide antigens of *Pseudomonas aeruginosa*. *Critical Reviews in Microbiology, 17*(4), 273-304.

Koch, C. (2002). Early infection and progression of cystic fibrosis lung disease. *Pediatric Pulmonology, 34*(3), 232-236.

Koller, M., Salerno, A., Dias, M., Reiterer, A., & Braunegg, G. (2010). Modern biotechnological polymer synthesis: a review. *Food Technology and Biotechnology, 48*(3), 255-269.

Kolls, J. K., Kanaly, S. T., & Ramsay, A. J. (2003). Interleukin-17: an emerging role in lung inflammation. *American Journal of Respiratory Cell and Molecular Biology, 28*(1), 9-11.

Lavoie, E. G., Wangdi, T., & Kazmierczak, B. I. (2011). Innate immune responses to *Pseudomonas aeruginosa* infection. *Microbes and Infection, 13*(14), 1133-1145.

Lee, J., Parlane, N., Wedlock, D., & Rehm, B. (2017). Bioengineering a bacterial pathogen to assemble its own particulate vaccine capable of inducing cellular immunity. *Scientific Reports, 7*, 41607.

Legat, A., Gruber, C., Zangger, K., Wanner, G., & Stan-Lotter, H. (2010). Identification of polyhydroxyalkanoates in *Halococcus* and other haloarchaeal species. *Applied Microbiology and Biotechnology, 87*(3), 1119-1127.

Lemoigne, M. (1926). Products of dehydration and of polymerization of β-hydroxybutyric acid. *Bulletin De La Societe De Chimie Biologique, 8*, 770-782.

Liang, S., Zheng, D., Zhang, C., & Zacharias, M. (2009). Prediction of antigenic epitopes on protein surfaces by consensus scoring. *BMC Bioinformatics, 10*(1), 1.

Lindblad, E. B. (2004). Aluminium compounds for use in vaccines. *Immunology and Cell Biology, 82*(5), 497-505.

Liu, F., Li, W., Ridgway, D., Gu, T., & Shen, Z. (1998). Production of poly-β-hydroxybutyrate on molasses by recombinant *Escherichia coli*. *Biotechnology Letters, 20*(4), 345-348.

Ma, L., Conover, M., Lu, H., Parsek, M. R., Bayles, K., & Wozniak, D. J. (2009). Assembly and development of the Pseudomonas aeruginosa biofilm matrix. *PLoS Pathogens, 5*(3), e1000354.

Ma, L., Wang, J., Wang, S., Anderson, E. M., Lam, J. S., Parsek, M. R., & Wozniak, D. J. (2012). Synthesis of multiple *Pseudomonas aeruginosa* biofilm matrix exopolysaccharides is post-transcriptionally regulated. *Environmental Microbiology, 14*(8), 1995-2005. doi:10.1111/j.1462-2920.2012.02753.x

Madison, L. L., & Huisman, G. W. (1999). Metabolic engineering of poly (3-hydroxyalkanoates): from DNA to plastic. *Microbiology and Molecular Biology Reviews, 63*(1), 21-53.

Magalhães, P. O., Lopes, A. M., Mazzola, P. G., Rangel-Yagui, C., Penna, T., & Pessoa Jr, A. (2007). Methods of endotoxin removal from biological preparations: a review. *Journal of Pharmacy and Pharmaceutical Sciences, 10*(3), 388-404.

Mamat, U., Woodard, R. W., Wilke, K., Souvignier, C., Mead, D., Steinmetz, E., . . . Knox, C. (2013). Endotoxin-Free Protein Production-CleanColi™ Technology.

Martin, N. L., Rawling, E. G., Wong, R. S., Rosok, M., & Hancock, R. E. (1993). Conservation of surface epitopes in *Pseudomonas aeruginosa* outer membrane porin protein OprF. *FEMS Microbiology Letters, 113*(3), 261-266.

Martínez-Donato, G., Piniella, B., Aguilar, D., Olivera, S., Pérez, A., Castañedo, Y., . . . Burr, N. (2016). Protective T cell and antibody immune responses against hepatitis C virus achieved using a biopolyester-bead-based vaccine delivery system. *Clinical and Vaccine Immunology, 23*(4), 370-378.

Matthews, Q. L. (2010). Capsid-incorporation of antigens into adenovirus capsid proteins for a vaccine approach. *Molecular Pharmaceutics, 8*(1), 3-11.

Mayer, F., & Hoppert, M. (1997). Determination of the thickness of the boundary layer surrounding bacterial PHA inclusion bodies, and implications for models describing the molecular architecture of this layer. *Journal of Basic Microbiology, 37*(1), 45-52.

McAllister, F., Henry, A., Kreindler, J. L., Dubin, P. J., Ulrich, L., Steele, C., . . . Goldman, S. J. (2005). Role of IL-17A, IL-17F, and the IL-17 receptor in regulating growth-related oncogene-α and granulocyte colony-stimulating factor in bronchial epithelium: implications for airway inflammation in cystic fibrosis. *The Journal of Immunology, 175*(1), 404-412.

Mifune, J., Grage, K., & Rehm, B. H. (2009). Production of functionalized biopolyester granules by recombinant *Lactococcus lactis*. *Applied and Environmental Microbiology, 75*(14), 4668-4675.

Milacic, V., Bailey, B. A., O'Hagan, D., & Schwendeman, S. P. (2012). Injectable PLGA systems for delivery of vaccine antigens. *Long Acting Injections and Implants*, 429-458.

Mishra, M., Byrd, M. S., Sergeant, S., Azad, A. K., Parsek, M. R., McPhail, L., . . . Wozniak, D. J. (2012). *Pseudomonas aeruginosa* Psl polysaccharide reduces neutrophil phagocytosis and the oxidative response by limiting complement-mediated opsonization. *Cellular Microbiology, 14*(1), 95-106. doi:10.1111/j.1462-5822.2011.01704.x

Montor, W. R., Huang, J., Hu, Y., Hainsworth, E., Lynch, S., Kronish, J.-W., . . . LaBaer, J. (2009). Genome-wide study of *Pseudomonas aeruginosa* outer membrane protein immunogenicity using self-assembling protein microarrays. *Infection and Immunity, 77*(11), 4877-4886.

Moser, C., Jensen, P., Kobayashi, O., Hougen, H. P., Song, Z., Rygaard, J., & Kharazmi, A. (2002). Improved outcome of chronic *Pseudomonas aeruginosa* lung infection is associated with induction of a Th1-dominated cytokine response. *Clinical & Experimental Immunology, 127*(2), 206-213.

Moser, C., Kjaergaard, S., Pressler, T., Kharazmi, A., Koch, C., & Høiby, N. (2000). The immune response to chronic *Pseudomonas aeruginosa* lung infection in cystic fibrosis patients is predominantly of the Th2 type. *Apmis, 108*(5), 329-335.

Nossal, G. J. V. (2011). Vaccines of the future. *Vaccine, 29*, D111-D115. doi:10.1016/j.vaccine.2011.06.089

O'Hagan, D., Rahman, D., McGee, J., Jeffery, H., Davies, M., Williams, P., . . . Challacombe, S. (1991). Biodegradable microparticles as controlled release antigen delivery systems. *Immunology, 73*(2), 239.

O'Hagan, D., & Rappuoli, R. (2004). The safety of vaccines. *Drug Discovery Today, 9*(19), 846-854.

Ohama, M., Hiramatsu, K., Miyajima, Y., Kishi, K., Nasu, M., & Kadota, J.-i. (2006). Intratracheal immunization with pili protein protects against mortality associated with *Pseudomonas aeruginosa* pneumonia in mice. *FEMS Immunology & Medical Microbiology, 47*(1), 107-115.

Parlane, N. A., Grage, K., Lee, J. W., Buddle, B. M., Denis, M., & Rehm, B. H. (2011). Production of a particulate hepatitis C vaccine candidate by an engineered *Lactococcus lactis* strain. *Applied and Environmental Microbiology, 77*(24), 8516-8522.

Parlane, N. A., Grage, K., Mifune, J., Basaraba, R. J., Wedlock, D. N., Rehm, B. H., & Buddle, B. M. (2012). Vaccines displaying mycobacterial proteins on biopolyester beads stimulate cellular immunity and induce protection against tuberculosis. *Clinical and Vaccine Immunology, 19*(1), 37-44.

Parlane, N. A., Rehm, B. H., Wedlock, D. N., & Buddle, B. M. (2014). Novel particulate vaccines utilizing polyester nanoparticles (bio-beads) for protection against *Mycobacterium bovis* infection—A review. *Veterinary Immunology and Immunopathology, 158*(1), 8-13.

Parlane, N. A., Wedlock, D. N., Buddle, B. M., & Rehm, B. H. (2009). Bacterial polyester inclusions engineered to display vaccine candidate antigens for use as a novel class of safe and efficient vaccine delivery agents. *Applied and Environmental Microbiology, 75*(24), 7739-7744.

Peluso, L., De Luca, C., Bozza, S., Leonardi, A., Giovannini, G., Lavorgna, A., . . . Catania, M. R. (2010). Protection against *Pseudomonas aeruginosa* lung infection in mice by recombinant OprF-pulsed dendritic cell immunization. *BMC Microbiology, 10*(1), 9.

Peoples, O. P., & Sinskey, A. J. (1989). Poly-beta-hydroxybutyrate (PHB) biosynthesis in Alcaligenes eutrophus H16. Identification and characterization of the PHB polymerase gene (phbC). *Journal of Biological Chemistry, 264*(26), 15298-15303.

Peternel, Š., & Komel, R. (2011). Active protein aggregates produced in *Escherichia coli*. *International Journal of Molecular Sciences, 12*(11), 8275-8287.

Peters, V., & Rehm, B. H. (2005). In vivo monitoring of PHA granule formation using GFP-labeled PHA synthases. *FEMS Microbiology Letters, 248*(1), 93-100.

Peters, V., & Rehm, B. H. (2006). In vivo enzyme immobilization by use of engineered polyhydroxyalkanoate synthase. *Applied and Environmental Microbiology, 72*(3), 1777-1783.

Petrushina, I., Tran, M., Sadzikava, N., Ghochikyan, A., Vasilevko, V., Agadjanyan, M. G., & Cribbs, D. H. (2003). Importance of IgG2c isotype in the immune response to β-amyloid in amyloid precursor protein/transgenic mice. *Neuroscience Letters, 338*(1), 5-8.

Philip, S., Keshavarz, T., & Roy, I. (2007). Polyhydroxyalkanoates: biodegradable polymers with a range of applications. *Journal of Chemical Technology and Biotechnology, 82*(3), 233-247.

Phornphisutthimas, S., Thamchaipenet, A., & Panijpan, B. (2007). Conjugation in Escherichia coli. *Biochemistry and molecular biology education, 35*(6), 440-445.

Pollard, A. J., Perrett, K. P., & Beverley, P. C. (2009). Maintaining protection against invasive bacteria with protein-polysaccharide conjugate vaccines. *Nature Reviews Immunology, 9*(3), 212-220. doi:10.1038/nri2494

Priebe, G. P., & Goldberg, J. B. (2014). Vaccines for *Pseudomonas aeruginosa*: a long and winding road. *Expert Review of Vaccines, 13*(4), 507-519.

Priebe, G. P., Walsh, R. L., Cederroth, T. A., Kamei, A., Coutinho-Sledge, Y. S., Goldberg, J. B., & Pier, G. B. (2008). IL-17 is a critical component of vaccine-induced protection against lung infection by lipopolysaccharide-heterologous strains of *Pseudomonas aeruginosa*. *The Journal of Immunology, 181*(7), 4965-4975.

Qi, Q., & Rehm, B. H. (2001). Polyhydroxybutyrate biosynthesis in *Caulobacter crescentus*: molecular characterization of the polyhydroxybutyrate synthase. *Microbiology, 147*(12), 3353-3358.

Qiu, D., Damron, F. H., Mima, T., Schweizer, H. P., & Hongwei, D. Y. (2008). PBAD-based shuttle vectors for functional analysis of toxic and highly regulated genes in Pseudomonas and Burkholderia spp. and other bacteria. *Applied and Environmental Microbiology, 74*(23), 7422-7426.

Querec, T., Bennouna, S., Alkan, S. K., Laouar, Y., Gorden, K., Flavell, R., . . . Pulendran, B. (2006). Yellow fever vaccine YF-17D activates multiple dendritic cell subsets via TLR2, 7, 8, and 9 to stimulate polyvalent immunity. *Journal of Experimental Medicine, 203*(2), 413-424. doi:10.1084/jem.20051720

Ramsey, D. M., & Wozniak, D. J. (2005). Understanding the control of *Pseudomonas aeruginosa* alginate synthesis and the prospects for management of chronic infections in cystic fibrosis. *Molecular Microbiology, 56*(2), 309-322.

Rao, A. R., Laxova, A., Farrell, P. M., & Barbieri, J. T. (2009). Proteomic identification of OprL as a seromarker for initial diagnosis of *Pseudomonas aeruginosa* infection of patients with cystic fibrosis. *Journal of Clinical Microbiology, 47*(8), 2483-2488.

Rasiah, I. A., & Rehm, B. H. (2009). One-step production of immobilized α-amylase in recombinant *Escherichia coli*. *Applied and Environmental Microbiology, 75*(7), 2012-2016.

Rawling, E. G., Martin, N. L., & Hancock, R. (1995). Epitope mapping of the *Pseudomonas aeruginosa* major outer membrane porin protein OprF. *Infection and Immunity, 63*(1), 38-42.

Ray, V. A., Hill, P. J., Stover, K. C., Roy, S., Sen, C. K., Yu, L., . . . DiGiandomenico, A. (2017). Anti-Psl Targeting of *Pseudomonas aeruginosa* Biofilms for Neutrophil-Mediated Disruption. *Scientific Reports, 7*(1), 16065.

Rehm, B. (2003). Polyester synthases: natural catalysts for plastics. *Biochemical Journal, 376*(1), 15-33.

Rehm, B. (2006). Genetics and biochemistry of polyhydroxyalkanoate granule self-assembly: the key role of polyester synthases. *Biotechnology Letters, 28*(4), 207-213.

Rehm, B. (2007). Biogenesis of microbial polyhydroxyalkanoate granules: a platform technology for the production of tailor-made bioparticles. *Current Issues in Molecular Biology, 9*(1), 41.

Rehm, B. (2010). Bacterial polymers: biosynthesis, modifications and applications. *Nature Reviews Microbiology, 8*(8), 578-592.

Rehm, B., Antonio, R., Spiekermann, P., Amara, A., & Steinbüchel, A. (2002). Molecular characterization of the poly (3-hydroxybutyrate)(PHB) synthase from *Ralstonia eutropha*: in vitro evolution, site-specific mutagenesis and development of a PHB synthase protein model. *Biochimica et Biophysica Acta (BBA)-Protein Structure and Molecular Enzymology, 1594*(1), 178-190.

Rehm, B., Boheim, G., Tommassen, J., & Winkler, U. (1994). Overexpression of algE in *Escherichia coli*: subcellular localization, purification, and ion channel properties. *Journal of Bacteriology, 176*(18), 5639-5647.

Remminghorst, U., & Rehm, B. H. (2006). In vitro alginate polymerization and the functional role of Alg8 in alginate production by *Pseudomonas aeruginosa*. *Applied and Environmental Microbiology, 72*(1), 298-305.

Ren, Q., Guy, D., Kessler, B., & Witholt, B. (2000). Recovery of active medium-chain-length-poly-3-hydroxyalkanoate polymerase from inactive inclusion bodies using ion-exchange resin. *Biochemical Journal, 349*(2), 599-604.

Revets, H., Pynaert, G., Grooten, J., & De Baetselier, P. (2005). Lipoprotein I, a TLR2/4 ligand modulates Th2-driven allergic immune responses. *The Journal of Immunology, 174*(2), 1097-1103.

Reyes, P. R., Parlane, N. A., Wedlock, D. N., & Rehm, B. H. (2016). Immunogencity of antigens from *Mycobacterium tuberculosis* self-assembled as particulate vaccines. *International Journal of Medical Microbiology, 306*(8), 624-632.

Romagnani, S. (2000). T-cell subsets (Th1 versus Th2). *Annals of Allergy, Asthma & Immunology, 85*(1), 921-918.

Rosalia, R. A., Silva, A. L., Camps, M., Allam, A., Jiskoot, W., van der Burg, S. H., . . . Oostendorp, J. (2013). Efficient ex vivo induction of T cells with potent anti-tumor activity by protein antigen encapsulated in nanoparticles. *Cancer Immunology, Immunotherapy, 62*(7), 1161-1173.

Rosok, M. J., Stebbins, M., Connelly, K., Lostrom, M., & Siadak, A. (1990). Generation and characterization of murine antiflagellum monoclonal antibodies that are protective against lethal challenge with *Pseudomonas aeruginosa*. *Infection and Immunity, 58*(12), 3819-3828.

Roy-Burman, A., Savel, R. H., Racine, S., Swanson, B. L., Revadigar, N. S., Fujimoto, J., . . . Wiener-Kronish, J. P. (2001). Type III protein secretion is associated with death in lower respiratory and systemic *Pseudomonas aeruginosa* infections. *Journal of Infectious Diseases, 183*(12), 1767-1774.

Ruth, K., Grubelnik, A., Hartmann, R., Egli, T., Zinn, M., & Ren, Q. (2007). Efficient production of (*R*)-3-hydroxycarboxylic acids by biotechnological conversion of polyhydroxyalkanoates and their purification. *Biomacromolecules, 8*(1), 279-286.

Salata, O. V. (2004). Applications of nanoparticles in biology and medicine. *Journal of nanobiotechnology, 2*(1), 3.

Sambrook, J., Fritsch, E. F., & Maniatis, T. (1989). *Molecular cloning* (Vol. 2): Cold spring harbor laboratory press New York.

Schlegel, H., Kaltwasser, H., & Gottschalk, G. (1961). A submersion method for culture of hydrogen-oxidizing bacteria: growth physiological studies. *Archives of Microbiology, 38,* 209-222.

Sharma, A., Krause, A., & Worgall, S. (2011). Recent developments for Pseudomonas vaccines. *Human Vaccines, 7*(10), 999-1011. doi:10.4161/hv.7.10.16369

Singh, M., Kazzaz, J., Ugozzoli, M., Malyala, P., Chesko, J., & O'Hagan, D. T. (2006). Polylactide-co-glycolide microparticles with surface adsorbed antigens as vaccine delivery systems. *Current Drug Delivery, 3*(1), 115-120.

Singh, M., & O'Hagan, D. (1999). Advances in vaccine adjuvants. *Nature Biotechnology, 17*(11), 1075.

Skeiky, Y. A. W., & Sadoff, J. C. (2006). Advances in tuberculosis vaccine strategies. *Nature Reviews Microbiology, 4*(6), 469-476.

Spiekermann, P., Rehm, B. H., Kalscheuer, R., Baumeister, D., & Steinbüchel, A. (1999). A sensitive, viable-colony staining method using Nile red for direct screening of bacteria that accumulate polyhydroxyalkanoic acids and other lipid storage compounds. *Archives of Microbiology, 171*(2), 73-80.

Steinman, L. (2007). A brief history of T H 17, the first major revision in the T H 1/T H 2 hypothesis of T cell–mediated tissue damage. *Nature Medicine, 13*(2), 139.

Steinmann, B., Christmann, A., Heiseler, T., Fritz, J., & Kolmar, H. (2010). In vivo enzyme immobilization by inclusion body display. *Applied and Environmental Microbiology, 76*(16), 5563-5569.

Stubbe, J., & Tian, J. (2003). Polyhydroxyalkanoate (PHA) homeostasis: the role of the PHA synthase. *Natural Product Reports, 20*(5), 445-457.

Sudesh, K., & Iwata, T. (2008). Sustainability of biobased and biodegradable plastics. *CLEAN–Soil, Air, Water, 36*(5-6), 433-442.

Taguchi, S., & Doi, Y. (2004). Evolution of polyhydroxyalkanoate (PHA) production system by "enzyme evolution": successful case studies of directed evolution. *Macromolecular Bioscience, 4*(3), 145-156.

Tan, H.-L., Regamey, N., Brown, S., Bush, A., Lloyd, C. M., & Davies, J. C. (2011). The Th17 pathway in cystic fibrosis lung disease. *American Journal of Respiratory and Critical Care Medicine, 184*(2), 252-258.

Tart, A. H., Blanks, M. J., & Wozniak, D. J. (2006). The AlgT-dependent transcriptional regulator AmrZ (AlgZ) inhibits flagellum biosynthesis in mucoid, nonmotile *Pseudomonas aeruginosa* cystic fibrosis isolates. *Journal of Bacteriology, 188*(18), 6483-6489.

Tenover, F. C. (2006). Mechanisms of antimicrobial resistance in bacteria. *The American Journal of Medicine, 119*(6), S3-S10.

Thomson, N., Summers, D., & Sivaniah, E. (2010). Synthesis, properties and uses of bacterial storage lipid granules as naturally occurring nanoparticles. *Soft Matter, 6*(17), 4045-4057.

Tian, J., Sinskey, A. J., & Stubbe, J. (2005). Kinetic studies of polyhydroxybutyrate granule formation in *Wautersia eutropha* H16 by transmission electron microscopy. *Journal of Bacteriology, 187*(11), 3814-3824.

Van Duin, D., Medzhitov, R., & Shaw, A. C. (2006). Triggering TLR signaling in vaccination. *Trends in Immunology, 27*(1), 49-55.

Vance, R. E., Rietsch, A., & Mekalanos, J. J. (2005). Role of the type III secreted exoenzymes S, T, and Y in systemic spread of *Pseudomonas aeruginosa* PAO1 in vivo. *Infection and Immunity, 73*(3), 1706-1713.

Vincent, J.-L., Rello, J., Marshall, J., Silva, E., Anzueto, A., Martin, C. D., . . . Sakr, Y. (2009). International study of the prevalence and outcomes of infection in intensive care units. *Jama, 302*(21), 2323-2329.

Vincent, J.-L., Sakr, Y., Sprung, C. L., Ranieri, V. M., Reinhart, K., Gerlach, H., . . . Payen, D. (2006). Sepsis in European intensive care units: results of the SOAP study. *Critical Care Medicine, 34*(2), 344.

Von Specht, B., Gabelsberger, J., Knapp, B., Hundt, E., Schmidt-Pilger, H., Bauernsachs, S., . . . Domdey, H. (2000). Immunogenic efficacy of differently produced recombinant vaccines candidates against *Pseudomonas aeruginosa* infections. *Journal of Biotechnology, 83*(1), 3-12.

Waugh, D. S. (2005). Making the most of affinity tags. *Trends in Biotechnology, 23*(6), 316-320.

Westritschnig, K., Hochreiter, R., Wallner, G., Firbas, C., Schwameis, M., & Jilma, B. (2014). A randomized, placebo-controlled phase I study assessing the safety and immunogenicity of a *Pseudomonas aeruginosa* hybrid outer membrane protein OprF/I vaccine (IC43) in healthy volunteers. *Human Vaccines & Immunotherapeutics, 10*(1), 170-183.

Wolfgang, M. C., Jyot, J., Goodman, A. L., Ramphal, R., & Lory, S. (2004). *Pseudomonas aeruginosa* regulates flagellin expression as part of a global response to airway fluid from cystic fibrosis patients. *Proceedings of the National Academy of Sciences of the United States of America, 101*(17), 6664-6668.

Woodard, R. W., Meredith, T. C., & Aggarwal, P. (2007). Viable non-toxic gram-negative bacteria: Google Patents.

World Health Organisation. (2017, February 27). List of bacteria for which new antibiotics are urgently needed. Retrieved from http://www.who.int/news-room/detail/27-02-2017-who-publishes-list-of-bacteria-for-which-new-antibiotics-are-urgently-needed.

Wu, W., Huang, J., Duan, B., Traficante, D. C., Hong, H., Risech, M., . . . Priebe, G. P. (2012). Th17-stimulating Protein Vaccines Confer Protection against *Pseudomonas aeruginosa* Pneumonia. *American Journal of Respiratory & Critical Care Medicine, 186*(5), 420-427 428p. doi:10.1164/rccm.201202-0182OC

Xiang, S. D., Scholzen, A., Minigo, G., David, C., Apostolopoulos, V., Mottram, P. L., & Plebanski, M. (2006). Pathogen recognition and development of particulate vaccines: does size matter? *Methods, 40*(1), 1-9.

Ye, P., Garvey, P. B., Zhang, P., Nelson, S., Bagby, G., Summer, W. R., . . . Kolls, J. K. (2001). Interleukin-17 and lung host defense against *Klebsiella pneumoniae* infection. *American Journal of Respiratory Cell and Molecular Biology, 25*(3), 335-340.

Young, L. S., Meyer, R. D., & Armstrong, D. (1973). *Pseudomonas aeruginosa* vaccine in cancer patients. *Annals of Internal Medicine, 79*(4), 518-527.